(CR-115677)

N72-28881

C-1

# PARTICLES AND FIELDS SUBSATELLITE PROGRAM

FINAL REPORT

FEBRUARY 1972

(NASA-CR-115677) PARTICLES AND FIELDS SUBSATELLITE PROGRAM Final Report H.J. Horn (TRW Systems Group) Feb. 1972 175 p
CSCL 22C

N72-28881

Unclas
G3/31 35648


TRW
SYSTEMS GROUP
ONE SPACE PARK • REDONDO BEACH, CALIFORNIA

8220.57-1-68
Exh. C, Par. 3.1.6.2
Sales Number: 16763

# PARTICLES AND FIELDS SUBSATELLITE PROGRAM

## FINAL REPORT

FEBRUARY 1972

Prepared by TRW Systems for:
NATIONAL AERONAUTICS AND SPACE ADMINISTRATION
MANNED SPACECRAFT CENTER
Under Contract NAS 9-10800

Prepared by Harry J. Horn
Harry J. Horn

Approved by Thomas H. Pedersen
Thomas H. Pedersen
P&F Project Manager

8220.57-1-68

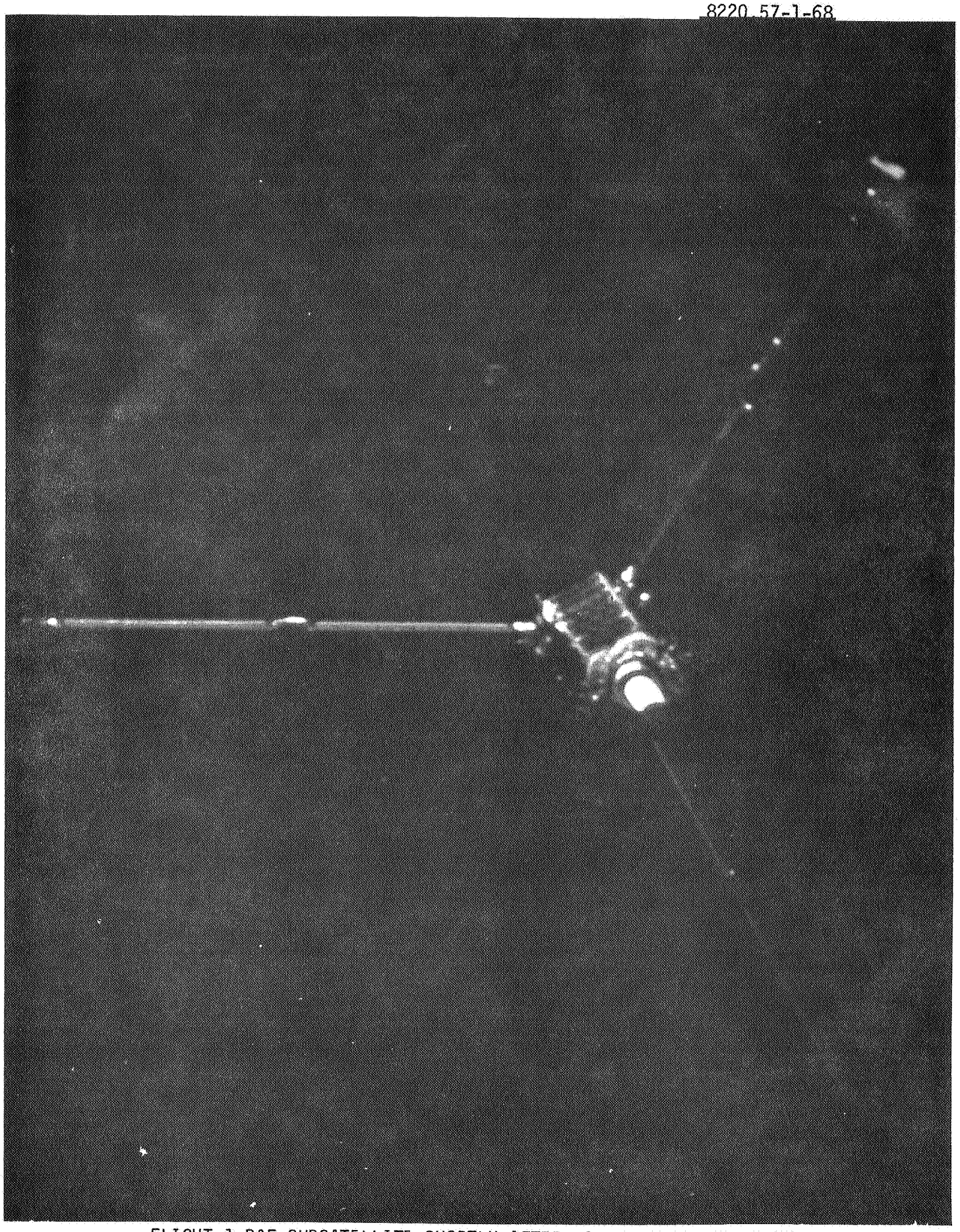

FLIGHT 1 P&F SUBSATELLITE SHORTLY AFTER LAUNCH FROM APOLLO 15

TABLE OF CONTENTS

# 1. INTRODUCTION

This final report for the Particles & Fields Subsatellite Program is prepared and submitted in accordance with Contract NAS 9-10800. Exhibit C, Paragraph 3.1.6.2, and Document Summary Table Item #9. The basic purpose of the program is to provide three subsatellites with one for launch with Apollo 15, and one for launch with Apollo 16. At this time all three subsatellites have been completed and the Flight #1 subsatellite has been successfully placed in orbit from the Apollo 15 CSM. The Flight 2 subsatellite is scheduled for launch with the Apollo 16 mission on April 16, 1972.

## 2. SYSTEM DESCRIPTION

The Particles and Fields Lunar Subsatellite and its mission are briefly described on the following pages. This is done primarily through the use of pictorial illustrations.

The basic P&F mission is to investigate two fundamental problems of space physics: the formation and dynamics of the Earth's magnetosphere, and the boundary layer of the solar wind as it flows over the Moon. The spacecraft system provides a means of making measurements of energetic particles and magnetic fields while in lunar orbit utilizing the moon as a large absorber. The P&F Subsatellite also provides the additional capability of making precise phase-locked two way doppler measurements, through the lunar orbiting subsatellite. This can be done over an extended period of time and without velocity correction disturbances. Analysis of this doppler data permits mapping of the Moon's gravitational field and development of the lunar mass model.

Figure 1 illustrates the mission concept by showing the Earth's magnetic field at the Moon, with an orbiting P&F Satellite, passing through the magnetotail. The satellite stores data as it passes behind the Moon and transmits this data to a NASA Earth station when it is in view of the station.

Figure 2 pictures the subsatellite in orbit just after separation from the CSM and after the booms have deployed.

Figure 3 shows the spacecraft in lunar orbit while it is communicating with an Earth station. Communication includes dumping of stored scientific data from the satellite's digital memory and receipt of commands for spacecraft control. The satellite is shown with its spin-axis and dipole pattern antennas approximately normal to the ecliptic. This attitude is required for orientation of the magnetometer, and for most favorable RF linkage with ground stations. The spin-axis is aligned by selectively orientating the Apollo vehicle at the time of separation.

Figure 4 pictures the subsatellite in lunar orbit performing its mission.

Figure 5 is a drawing of the satellite while mated to the launch assembly and to the deployment mechanism which pre-positions the satellite to the CSM mold line along guide rails just prior to separation.

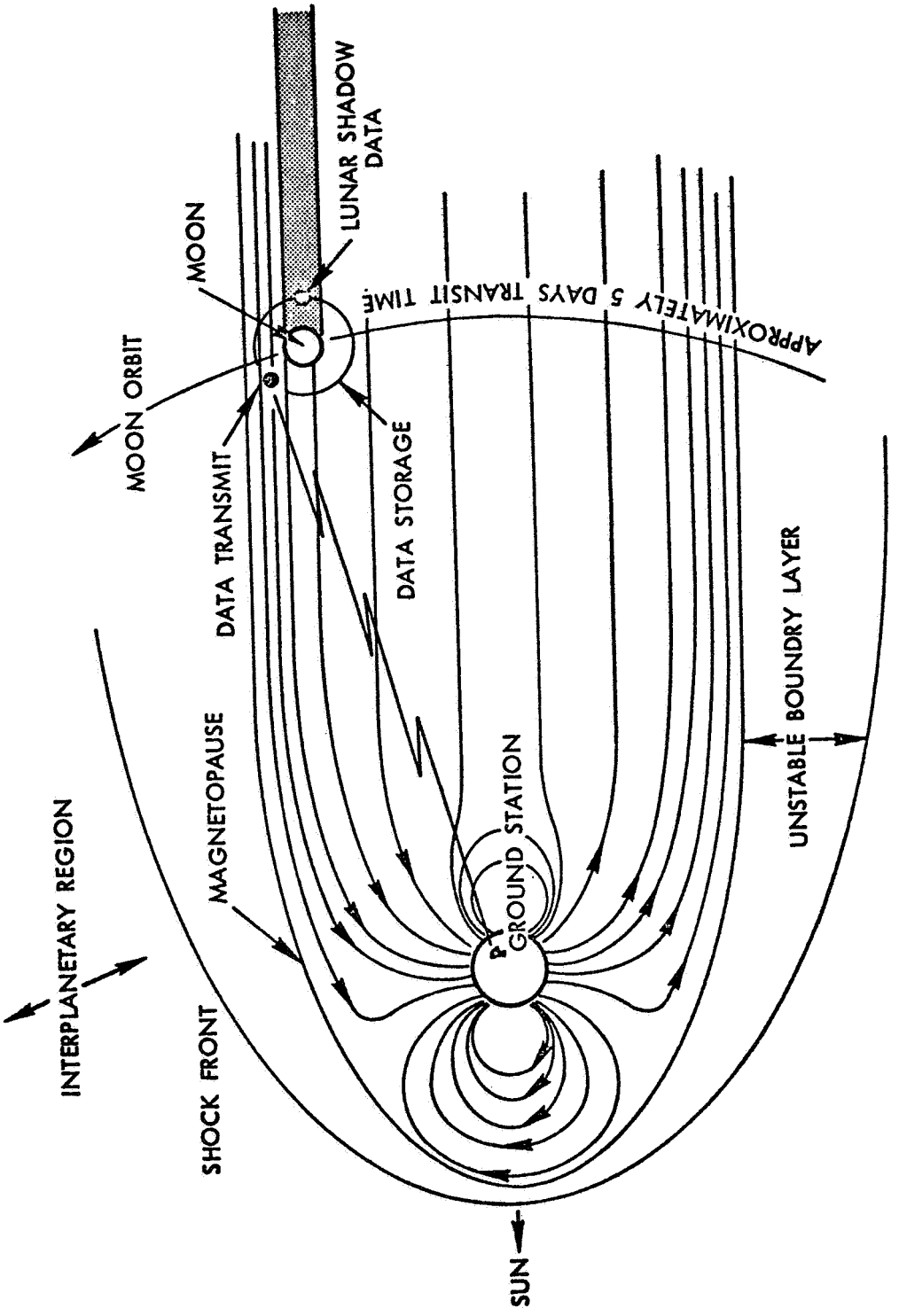


Figure 1. Mission Concept

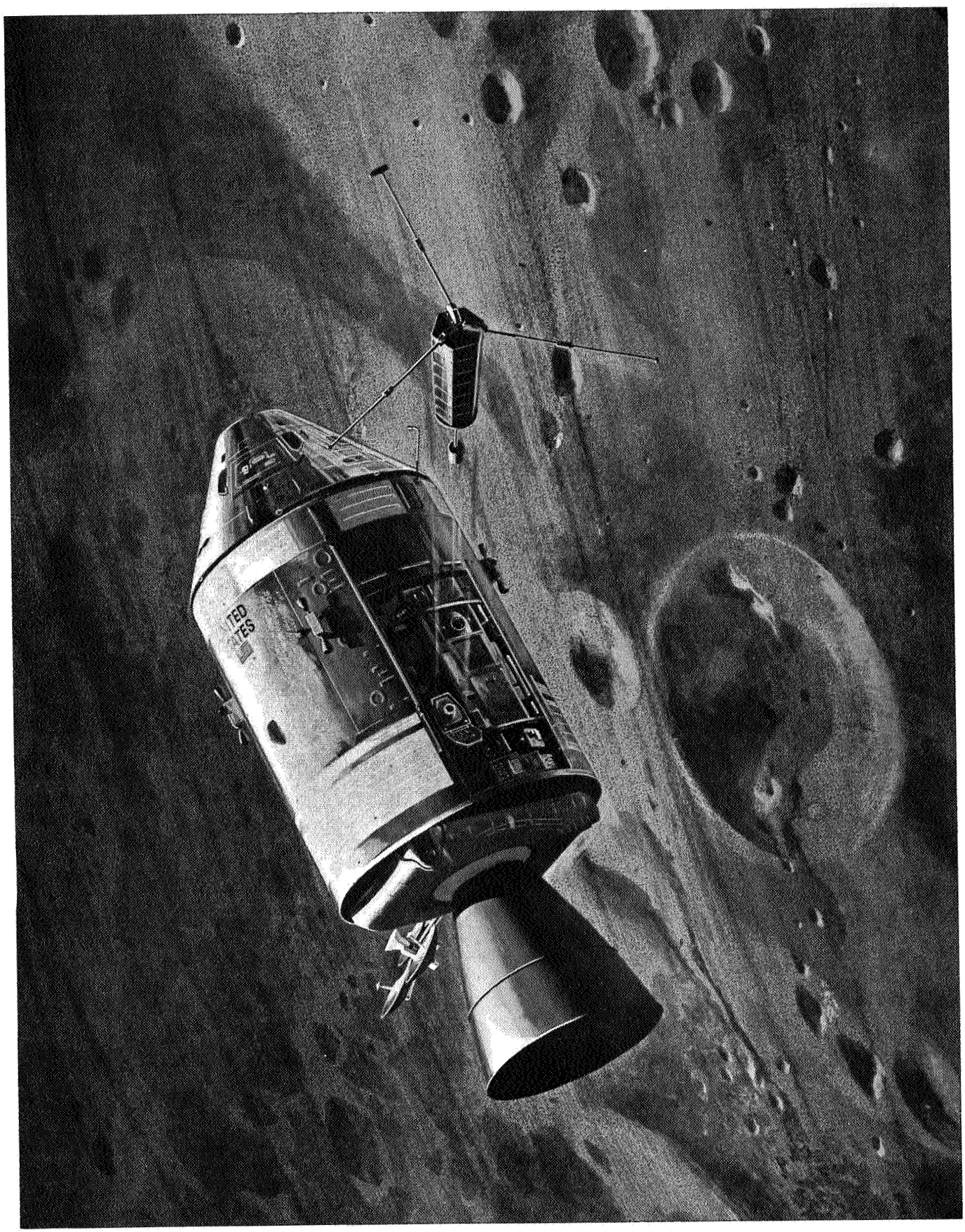

FIGURE 2 SUBSATELLITE BEING EJECTED INTO LUNAR ORBIT FROM APOLLO 16/16 CSM

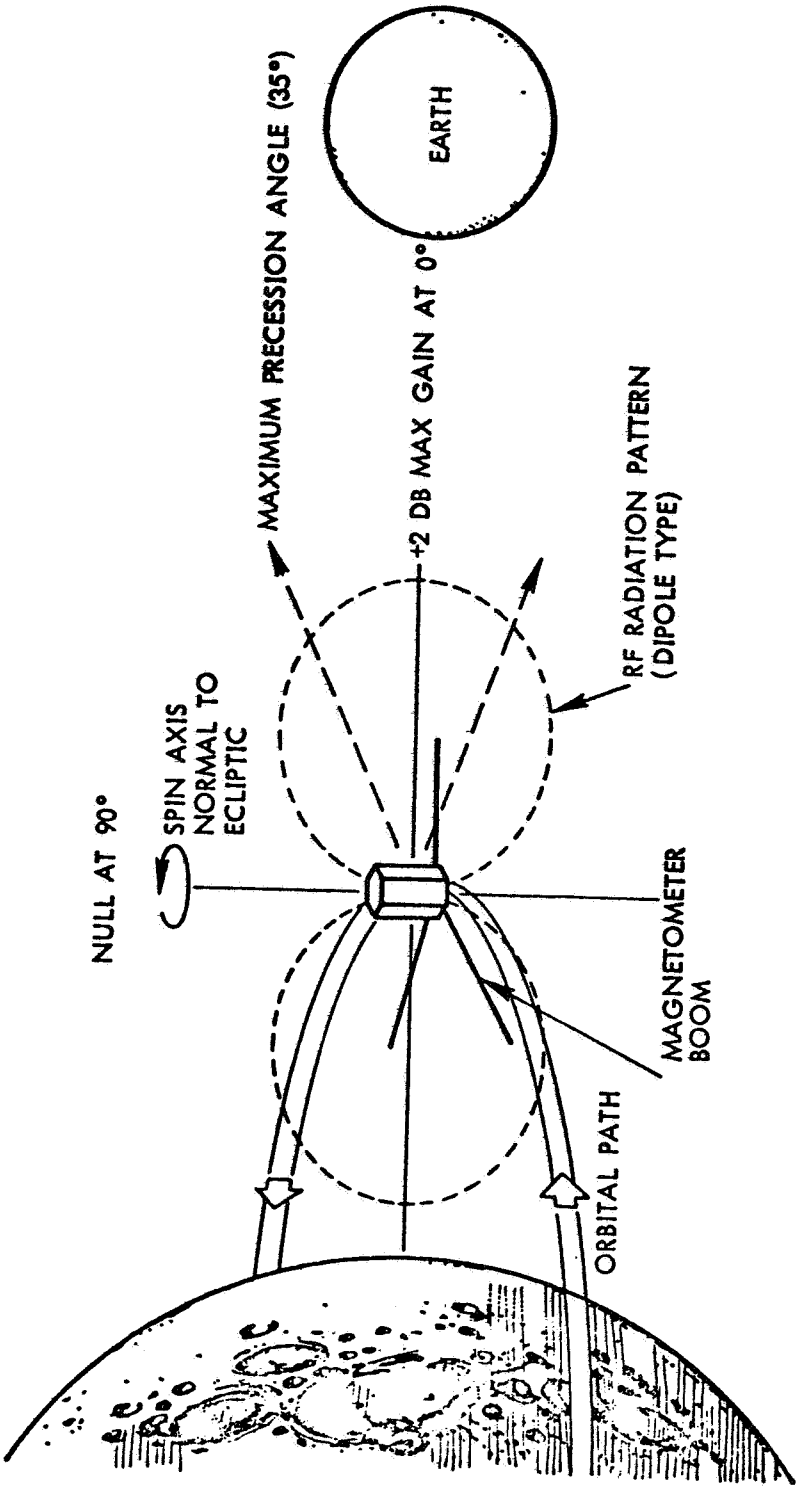


Figure. 3 . P&F Satellite In Lunar Orbit

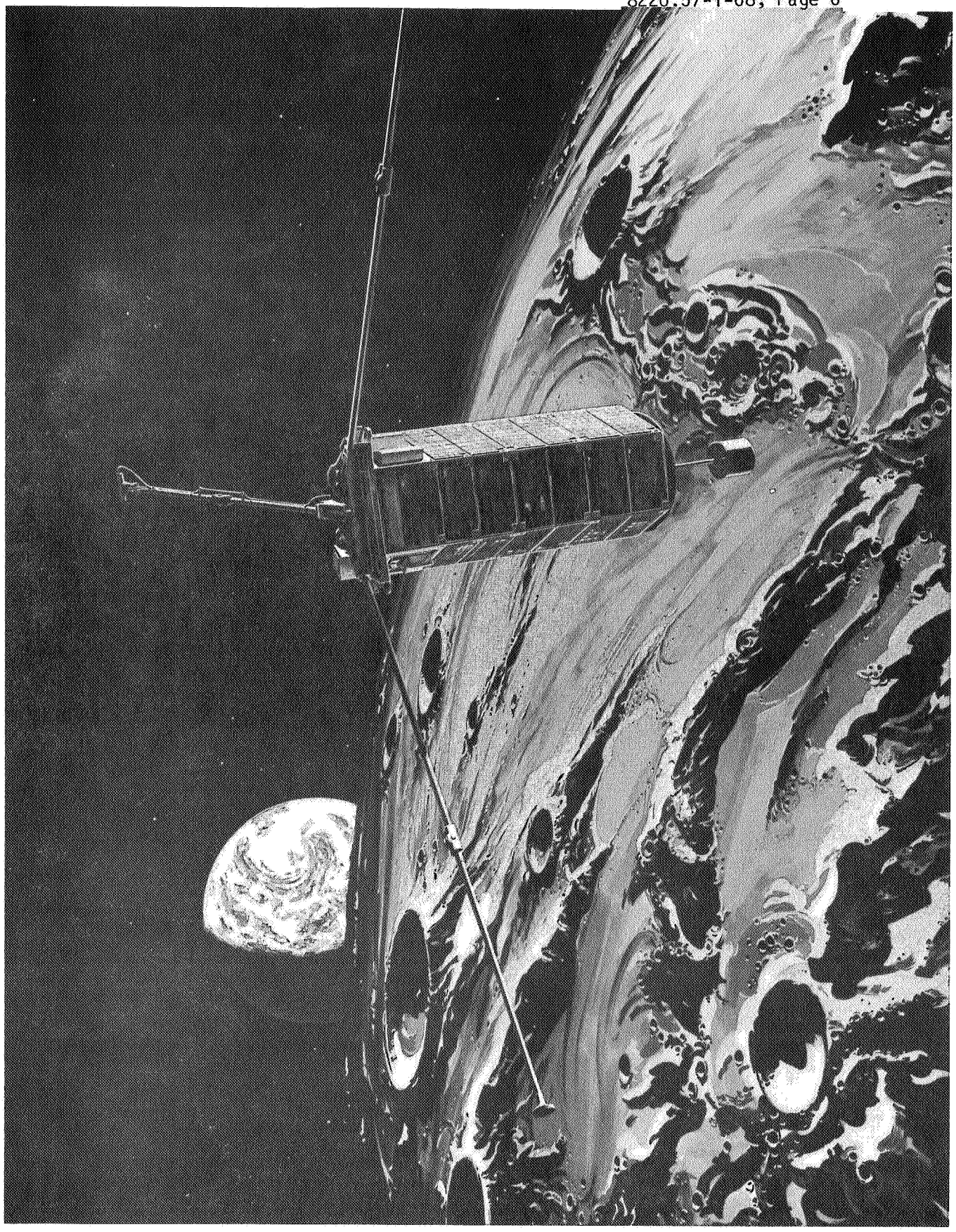

FIGURE 4 P & F SUBSATELLITE IN LUNAR ORBIT

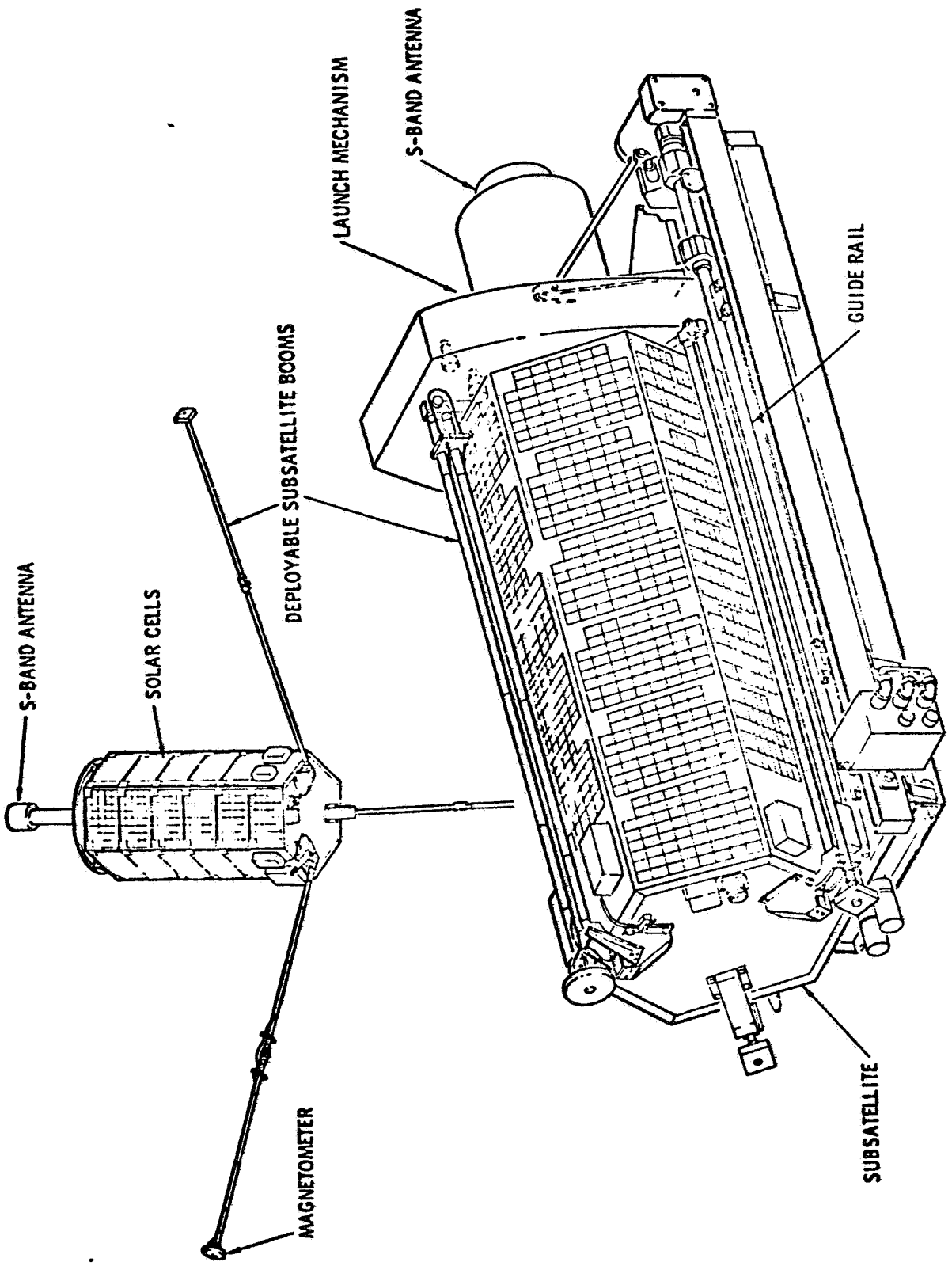


FIGURE 5 SUBSATELLITE WITH LAUNCH MECHANISM

Figure 6 is a photograph of the Flight #1 P&F Subsatellite and its electrical ground support equipment.

Figure 7 is a photograph of the Flight #1 P&F Subsatellite with two solar panels removed. It shows the interior configuration of the subsatellite and includes labels to identify the individual boxes.

Figure 8 shows the subsatellite location while stowed in the Apollo Scientific Instrument Module (SIM). In this configuration it is contained within a protective enclosure.

The photographs of Figure 9 illustrate the prepositioning operation which is performed just prior to separation. The equipment shown is the High Fidelity Mock-up of P&F Subsatellite in the NASA/MSC Apollo 15 SIM Bay Trainer.

Figure 10 is a photograph of the P&F system Mechanical GSE in use. The subsatellite is attached at both ends to the Installation Handling Fixture (GSE item) which is being used in its horizontal configuration. This fixture is providing the means of attaching the subsatellite to a lifting device and a hydra-set. The satellite is being positioned horizontally for attachment to the Rotation Fixture (GSE item). The Rotation Fixture has been rotated to its 90° configuration. The subsatellite has just been moved from the vibration table.

Figure 11 is a simplified block diagram of the satellite system. The basic subsystems are the Particles Experiment Subsystem (PES), Fields Experiment Subsystem (FES), Communications and Phase-Lock Tracking System, Data Handling and Storage, Sun Sensor and Sectoring Logic, Electrical Power, and Structural and Launch Platform.

Table 1 provides a summary of system features.

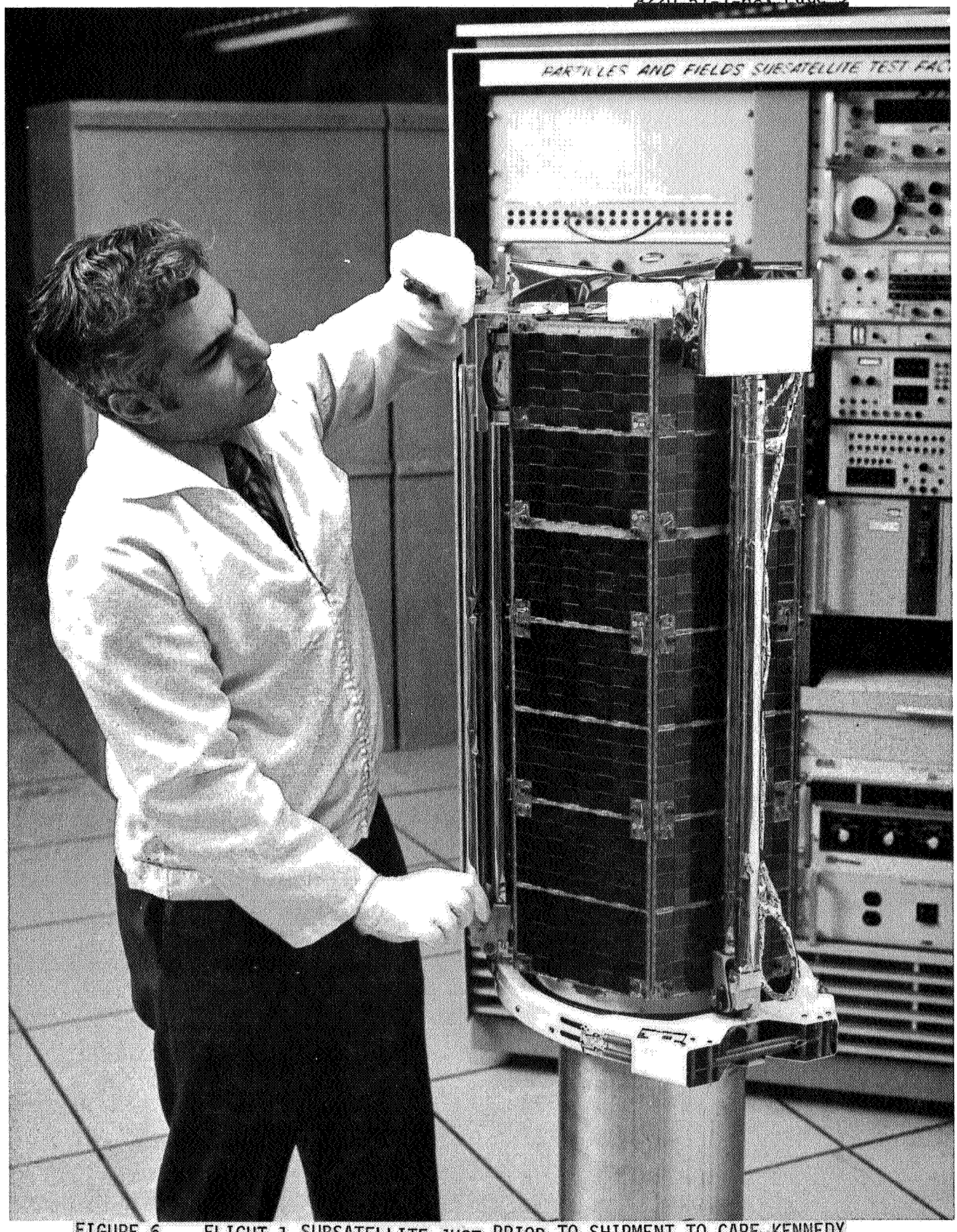


FIGURE 6 FLIGHT 1 SUBSATELLITE JUST PRIOR TO SHIPMENT TO CAPE KENNEDY

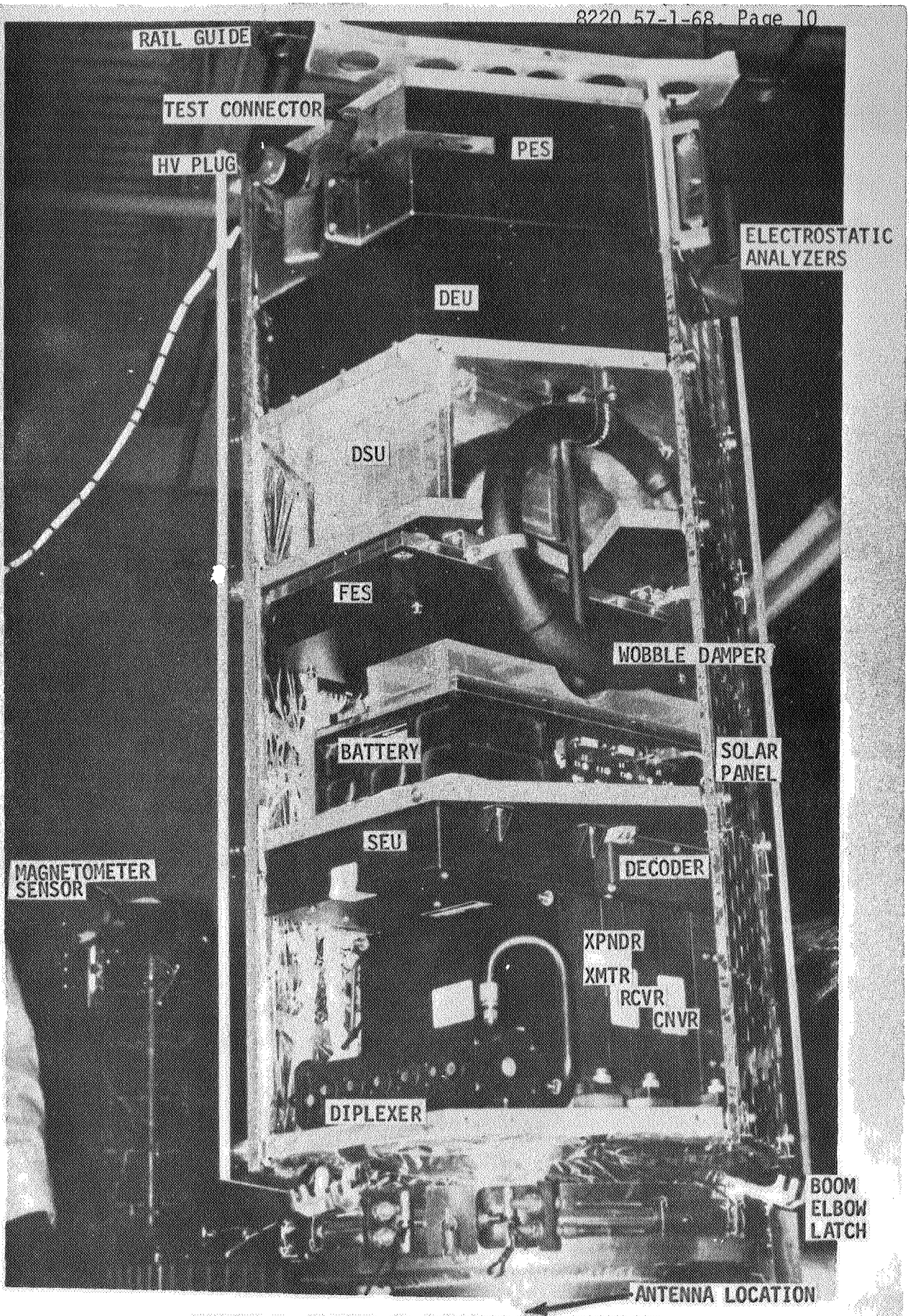


FIGURE 7 FLIGHT #1 SUBSATELLITE INTERIOR CONFIGURATION

FIGURE 8 APOLLO 15/16 EXPERIMENT CONFIGURATION IN SIM BAY

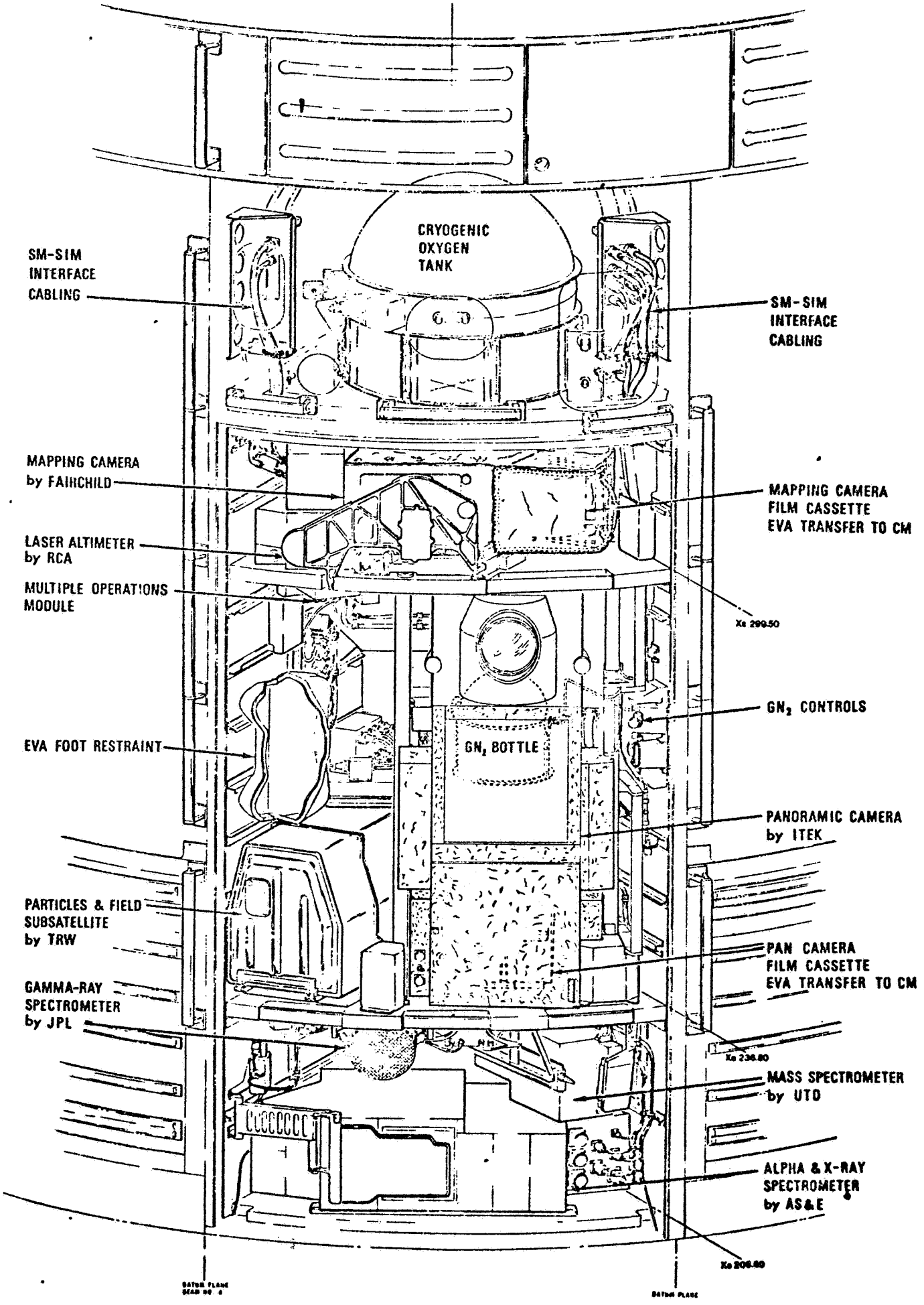

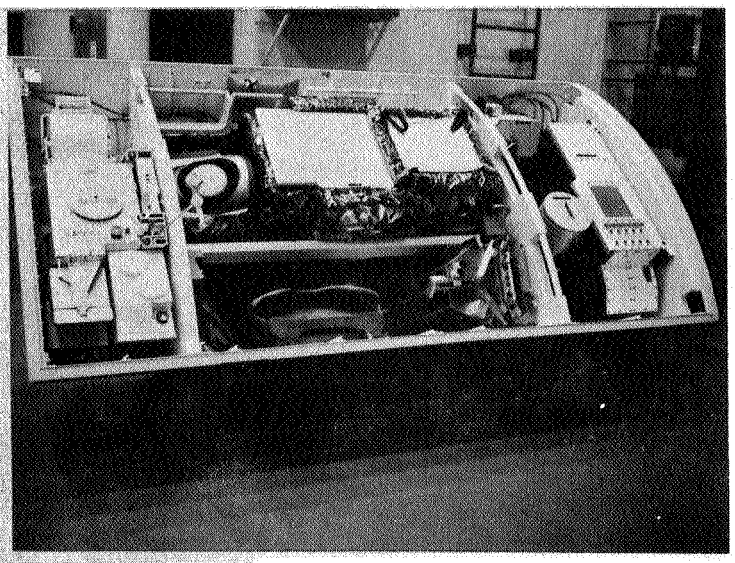

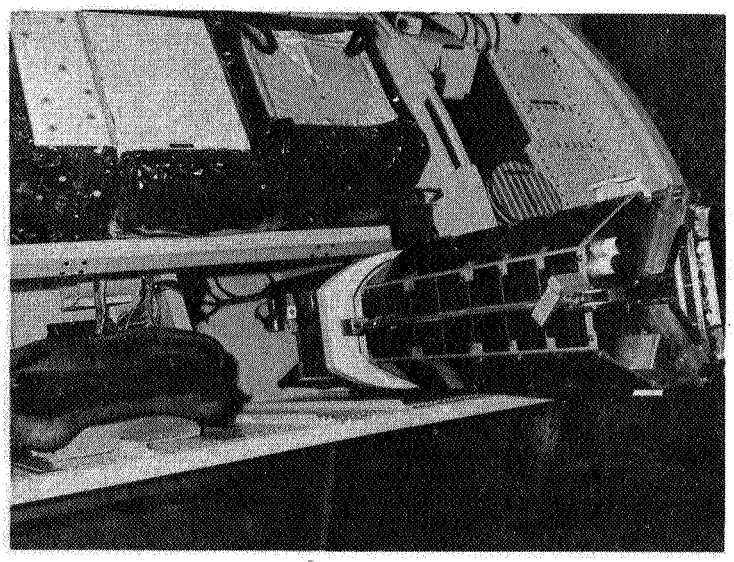

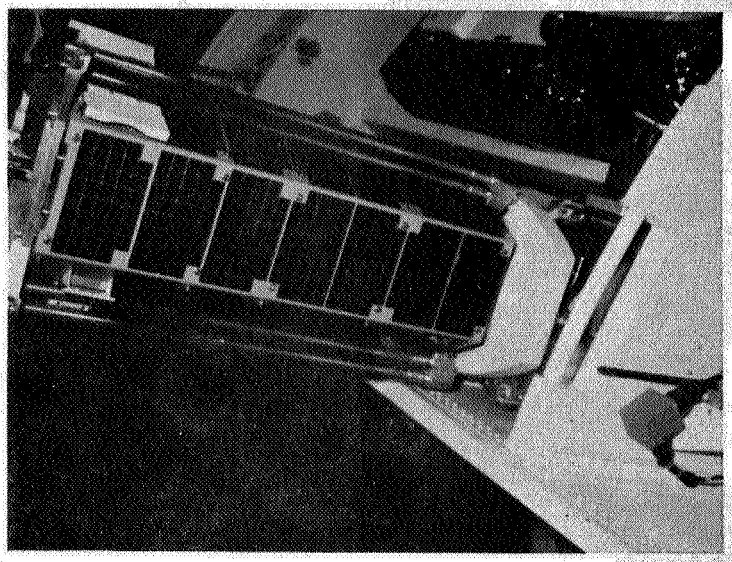

PARTICLES & FIELDS SUBSATELLITE
HIGH FIDELITY MOCK-UP
IN NASA/MSC APOLLO 15 SIM BAY TRAINER

FIGURE 9

FIGURE 10 FLIGHT 1 SUBSATELLITE

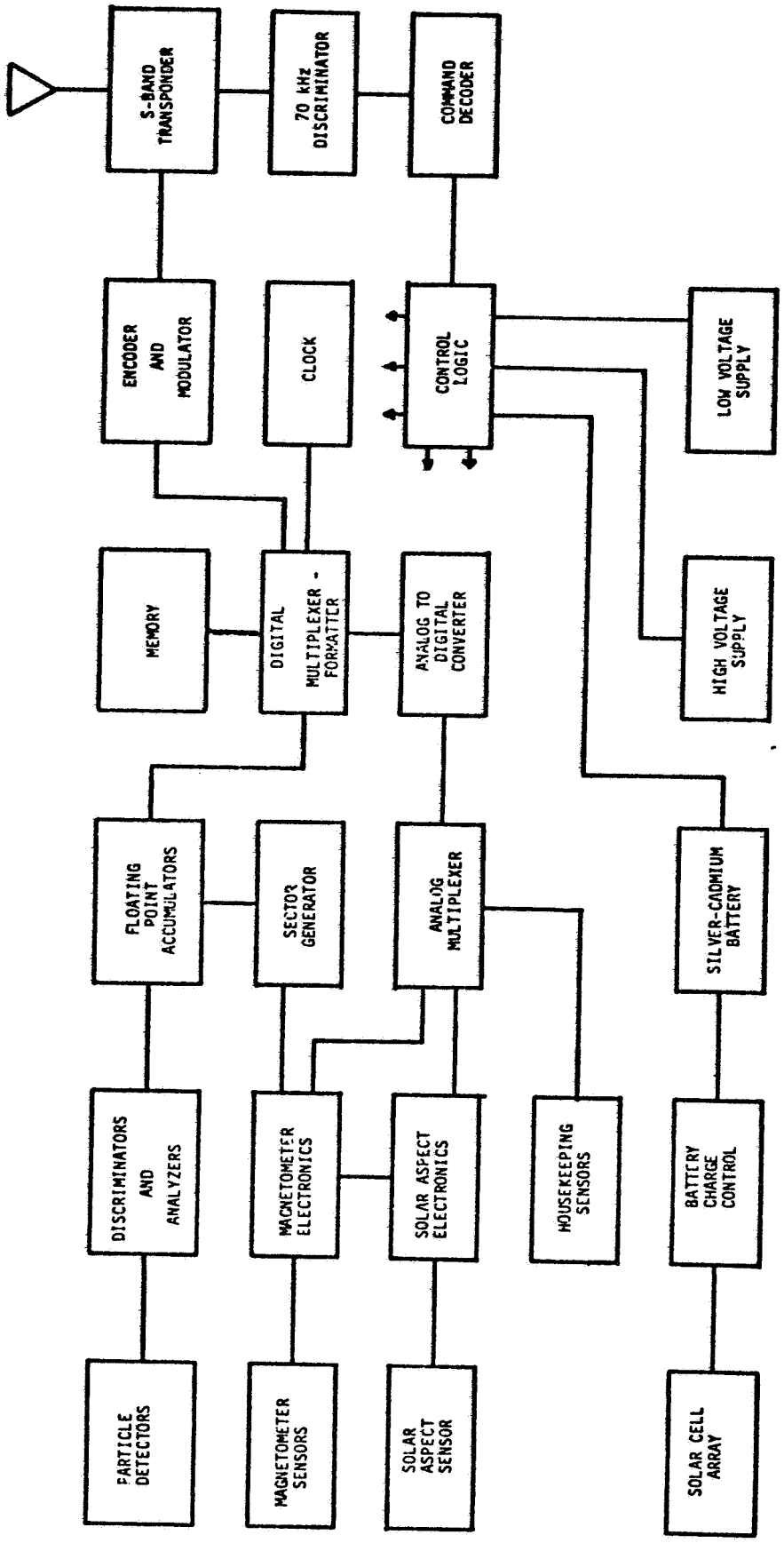


FIGURE 11 S-Band P&F Satellite System Block Diagram

TABLE I. S-BAND PARTICLES AND FIELDS SUBSATELLITE
SUMMARY OF FEATURES

| | |
|---|---|
| **General** | |
| Spacecraft Size | Hexagonal prism, 14-inch diagonal by 30 inches long |
| Spacecraft Weight | 81 pounds |
| Total Launch Weight | 94 pounds |
| Orbit | Lunar (Apollo) |
| Orbit Period | 119 min, 61% sunlit |
| Method of Launch | Apollo SIM |
| Attitude Stabilization | Spin at 12 rpm, normal to ecliptic plane |
| **Payload** | |
| Basic Measurements | Particles and magnetic fields, Doppler |
| Instruments | Solar state detectors<br>Electrostatic analyzers<br>Fluxgate magnetometer<br>Coherent S-Band Transponder |
| **Communication** | |
| Transponder | 240/221 phase-locked turnaround ratio |
| Downlink Frequency | 2282.5 MHz or 240/221 x Uplink |
| Radiated Power | 1.0 watt |
| Transmitted Bit Rate | 128 bps |
| Modulation | PCM/FSK/PM square wave subcarrier (NRZ-M) |
| Telemetry Data Subcarrier Frequency | 32,768 Hz |
| Uplink Frequency | S-Band (2101.8 MHz) |
| Command Format | MSFN Digital |
| Command Subcarrier Frequency | 70 KHz |
| **Data Handling** | |
| Data Storage | Core memory |
| Storage Capacity | 49,152 bits |
| Read-In Rate | 8 or 16 bps |
| Read-Out Rage | 128 bps |
| Data Dump Period | 8 minutes 32 seconds |
| **Electrical Power** | |
| Solar Cell Array Output | 24 watts at 17 volts |
| Battery (AgCd) | 11-Cell, 10 AH |

## 3. CHRONOLOGY OF KEY EVENTS

MAY 1970

A. S/C Hardware Contract Signed
B. TRW PDR - May 14, 15
C. ATC, Time Zero Subcontracts signed.
D. Zero Gravity Trainer launch platform delivered.
E. Delivery of Q.A., Rel., Safety, CADM, EMC, & Mag. Cleanliness Plans

JUNE 1970

A. ATC - PDR on June 4, 5
B. Time Zero PDR on June 18
C. Delivery of Zero Gravity Trainer Subsatellite
D. Test firing of NASA supplied pyro cartridges.

JULY 1970

A. TRW CDR - July 14, 15.
B. Fields Experiment CDR - July 29

AUGUST 1970

A. Particles Experiment CDR at ATC - August 4, 5
B. Successful breadboard command decoder compatibility test at MSC, August 28.

SEPTEMBER 1970

A. Mass Model Vibration tests successfully completed.
B. Final EMC analysis completed.

OCTOBER 1970

A. Mass Model deployment test complete.
B. Thermal design & analysis of orbit performance completed.
C. Qual, Flight 1, Flight 2, Launch Platform hardware complete, Qual Structure complete.

KEY EVENTS (Continued)

NOVEMBER 1970

A. Spacecraft System breadboard tests completed.
B. Mass Model Separation test completed.
C. Flight 1, Flight 2 structures complete.
D. High Fi mockup deliveried to MSC.
E. Qualification Decoder, Qual Antenna passed Qual tests.
F. BC/S passed acceptance tests.

DECEMBER 1970

A. Successful completion of MSFN compatibility tests with qual subsatellite at Houston - December 30.
B. Qual DSU completed Qualification Tests
C. Qual DEU completed Qualification Tests
D. Qual Transponder completed Qualification Tests
E. Qual SEU completed Qualification Tests
F. Flight 1 SEU completed Acceptance Tests

JANUARY 1971

A. Successful completion of MSFN compatibility test with qual subsatellite at KSC - January 6.

B. Flight 1, Flight 2 Decoder completed Acceptance Tests
C. Flight 1, Flight 2 DSU completed Acceptance Tests
D. Flight 1 Transponder completed Acceptance Tests*
E. Flight 1, Flight 2 Antenna completed Acceptance Tests
F. Qual, Flight 1, Flight 2 Solar Panels completed Acceptance Tests.

FEBRUARY 1971

A. Qual, Flight 1 Subsatellite outgassing bake complete.
B. Qual, Flight 1, Flight 2 Sun Sensors completed Acceptance Tests
C. Qual Battery completed Qualification tests **
D. Flight 2 SEU completed Acceptance Tests.

* Flight 1 transponder retested in March 71.
** A second qual battery was built and requalified.

KEY EVENTS (Continued)

MARCH 1971

A. Qual Spacecraft Phase One Acceptance Review (except PES), March 8 - March 12.
B. Flight 1 Transponder retest acceptance completed.
C. Qual FES (001) passed Qualification Tests.
D. Flight 2 DEU (003) completed Acceptance TEsts.

APRIL 1971

A. Flight 1 Spacecraft Phase One Acceptance Review (except PES), April 6, 7.
B. Qual, Flight 1 Spacecraft Test program initiated with inoperative high voltage systems (Qual PES engineering model, Flight 1 PES2-2).
C. Flight 2 Transponder completed Acceptance Tests. FES 003 passed "super" Qualification Tests.
D. Flight 2 FES (S/N 003) installed in Qual Spacecraft.
E. Qual FES (S/N 001) installed in Flight 1 Spacecraft.
F. Flight 1 Battery (005) completed Acceptance Tests.

MAY 1971

A. Qual PES completed Qual program with high voltage operational.
B. Flight 1 PES 2-3 completed acceptance program with high voltage operational.
C. Particles Experiment (PES) acceptance review - May 7.
D. Flight 1 Spacecraft completes Acceptance program with high voltage operational (PES 2-3).
E. Qual Spacecraft completes qualification program.
F Flight 1 Spacecraft Phase Two acceptance review - May 26.
G. Flight 1 Spacecraft shipped to KSC - May 29.
H. Resdesigned battery (006) qual tests completed.

JUNE - JULY 1971

A. Flight 2 (002) FES completed Acceptance Tests.
B. Flight 2 (003) Battery completed Acceptance Test.
C. Flight 2 PES (2-4) completed Acceptance Tests.
D. Qual Spacecraft Phase Two Acceptance Review - June 21
E. Flight 2 Spacecraft Phase One Acceptance Review - June 21
F. PES Flight 2 acceptance review - June 29.

KEY EVENTS (Continued)

JUNE - JULY 1971 (Continued)

G. Final Battery Charge completed on Flight 1 Spacecraft on pad at Cape Kennedy, July 16, 1971.

H Flight Two Spacecraft completed Acceptance Test Program.

I. Flight Two Spacecraft Phase Two Acceptance Review - July 21, 22.

J Flight Two Spacecraft put into storage - July 23.

SEPTEMBER - OCTOBER 1971

A. PES 2-4 removed from Flight 2 Spacecraft for repair.

B. DEU modified to incorporate "low count"fix.

C. FES modified to double magnetometer gain.

NOVEMBER 1971

A PES 2-4 reinstalled in Flight 2 spacecraft.

B. Thermal tape added to PES.

C. Flight two spacecraft phase two reacceptance review - November 4, 1971.

D. 7x12 vacuum chamber failure seriously damages Flight 2 S/C - Nov. 15, 1971.

E. Flight 2 spacecraft completely disassembled for repair. PES 2-4 to be replaced with PES 2-2. DEU repaired, CDU repaired. All other units given confidence unit tests.

DECEMBER 1971

A. PES 2-2 installed in Flight 2 spacecraft.

B. Flight 2 spacecraft rebuilt and functionally tested.

JANUARY 1972

A. High voltage fails during Flight 2 spacecraft thermal vacuum.

B. Repaired PES 2-4 installed in Flight 2 spacecraft.

FEBRUARY 1972

A. Flight two completes acceptance tests.

B. Flight two unit Phase II reacceptance review - February 1-3 1972.

C. Partial failure of Flight 1 spacecraft in orbit - February 3, 1972.

D. Flight two spacecraft shipped to KSC - February 6, 1972

4. HARDWARE DELIVERY ACCOMPLISHMENTS

Hardware delivery accomplishments are tabulated below by Contract Item number. The Zero-G Training Unit Subsatellite was added via Contract Change Authorization #1.

| Item No. | Contract Reference | Item | Required Delivery Date | Actual Delivery Date |
|---|---|---|---|---|
| 1 | Exhibit "A" Par. 3.3 | Zero-G Training Unit Launch Platform Unit | 5-13-70 | 5-21-70 |
| NN | Exhibit "A" Par. 3.3 | Zero-G Training Unit Subsatellite | 6-8-70 | 6-8-70 |
| 2 | Exhibit "A" Par. 3.2 | Hi-Fidelity Mock-up of the Subsatellite including Launch Platform | 9-15-70 | 9-18-70 |
| 3 | Exhibit "A" Par. 3.1 | Flight Launch Platform No. 1 | 1-15-71 | 5-28-71 |
| 4 | Exhibit "A" Par. 3.1 | Flight Subsatellite No. 1 | 5-7-71 | 5-28-71 |
| 5 | Exhibit "A" Par. 3.1 | Flight Subsatellite No. 2 Including Launch Platform | 2-6-72 | 2-6-72 |
| 6 | Exhibit "A" Par. 3.1 | Flight Subsatellite No. 3 Including Launch Platform (To be used in Qualification Testing) | 5-28-71 | 6-24-71 |
| 7 | Exhibit "A" Par. 3.4 | Ground Support Equipment | 4-23-71 | 5-28-71 |
| 8 | Exhibit "A" Par. 3.5 | Test Equipment | At Contract Completion | Not Yet Done |
| 9 | | Development Test Model (Residual) | At Contract Completion | Not Yet Done |

5. DOCUMENTATION ACHIEVEMENT

Achievement of contractual documentation requirements are described in this section of the final report, and are presented in the same order as listed in the Contract Documentation Summary Table, Exhibit C, by Item Number.

ITEM NO.

1&2 All P & F Subsatellite Program Contract End Item (CEI) specifications together with required and actual submittal dates, and latest issue information, are listed below. The Mechanical GSE CEI specification was requested at a later date by MSC, to replace EQ1-398A and to incorporate additional equipment, and had no specific required submittal date. The first and final Mechanical GSE specification submittal was on 5 March 1971.

CONTRACT END ITEM SPECIFICATIONS

| Document No. | CEI Specification | Req'd Submittal | | Req'd Submittal | |
|---|---|---|---|---|---|
| | | Prelim | Final | Prelim | Final |
| SY1-36C/SCN-8 | P & F Subsatellite System | 5/4/70 | 6/30/70 | 5/14/70 | 6/11/70 |
| EQ1-398A | Insertion Fixture (Superceded by EQ1-408) | 5/4/70 | 6/30/70 | 5/14/70 | 7/13/70 |
| EQ1-408NC | Mechanical GSE | no required dates | | 3/5/71 | 3/5/71 |
| EQ3-387D | Battery Charger/Simulator | 5/4/70 | 6/30/70 | 5/14/70 | 6/11/70 |
| EQ15-2A | High Fidelity Mockup | 5/4/70 | 6/30/70 | 5/14/70 | 7/13/70 |
| EQ15-3A | Zero Gravity Trainer | 5/4/70 | 6/30/70 | 5/14/70 | 7/13/70 |

3 Engineering Change Proposals (ECPs) are called out in the Contract on an "as required" basis. All ECP's to date, together with their submittal dates, are listed on the attached ECP table.

4 Specification Change Notices (SCN's) are called out in the Contract on an "as required" basis, with both preliminary and final submittals listed on the attached SCN table.

5 Specification Change Logs are called for in the Contract on an "as required" basis. These have been submitted as part of each preliminary and final SCN, and are included in each affected specification immediately after the title page.

# ECP INDEX

| ECP # | DATE | TITLE |
|---|---|---|
| 001 | 8/26/70 | Sunshades for Analyzers |
| 002 | 8/27/70 | Attitude Determination System |
| 002A | 9/3/70 | Attitude Determination System, Rev. A |
| 003 | 8/7/70 | Antenna Phase Measurements |
| 004 | 8/21/70 | Subsatellite Changes |
| 005 | 9/22/70 | Antenna Hat & Radome |
| 006 | 9/22/70 | Automatic Transmitter Turnoff |
| 007 | 2/6/71 | ADDITIONAL LAUNCH SUPPORT FOR LAUNCH #1 |
| 008 | 2/25/71 | Subsatellite Test Tape |
| 009 | 10/23/70 | Expanded Test Program |
| 010 | 3/2/71 | Subsatellite Changes |
| 011 | 1/26/71 | Product Assurance Changes |
| 012 | 12/9/70 | MSFN Compatibility Tests |
| 013 | 1/28/71 | Zero Gamma & ADC Reference Voltages |
| 014 | 3/9/71 | Mission Study Support to NAR |
| 015 | 7/2/71 | SUSTAINING OPERATION SUPPORT |
| 016 | 2/26/71 | Magnetometer Changes |
| 016MOD | 3/11/71 | Magnetometer Changes |
| 017 | 8/27/71 | F2 LAUNCH SUPPORT |
| 018 | 6/9/71 | Particles Analyzer Calibrtion at Berkeley |
| 019 | 4/19/71 | Boom Damper Modification |
| 020 | 4/22/71 | Battery Internal Design Change |
| 021 | 4/19/71 | Magnetometer Thermal Env. Mod. |
| 022 | 4/19/71 | Subsatellite Thermal Changes |
| 022A | 5/13/71 | Subsatellite Thermal Changes |
| 023 | 4/29/71 | BC/S Changes |
| 024 | 5/12/71 | Battery Electronics Cover |
| 025 | 5/20/71 | FES Internal Electronics MOD |
| 026 | 5/22/71 | PES Reliability Logic Change |
| 027 | 6/4/71 | PES High Voltage Power Supply Parts |
| 028 | 6/21/71 | Flight 2 S/C Extended Solar Thermal Vacuum Test |
| 029 | ------- | Not Used |
| 030 | 7/16/71 | Additional KSC Operations for Flight 1 |
| 031 | 6/21/71 | PES HV Power Supply Parts (704 Module) |
| 032 | 9/1/71 | DEU Accumulator Design Modifications |
| 033 | 9/24/71 | Magnetometer Gain Changes |
| 034 | 10/4/71 | Subsatellite Thermal Redesign for Lwr. Temp.Solid State Telescopes |
| 035 | 10/19/71 | Additional F2 Subsatellite Vit & T/ V Tests |
| 036 | 10/15/71 | Attitude Determination of the Flight 2 P&F S/S |
| 037 | 3/22/72 | In Orbit Performance Analysis |
| 038 | 3/21/72 | PROGRAM EXTENSION IN SUPPORT OF APOLLO 16 LAUNCH SLIP |
| 039 | 3/23/72 | Flight 2 S/S Final Trim Weight Shape (NO COST) |

| SCN | SUBMITTAL DATE | | MSC APPROVAL |
|---|---|---|---|
| | Prelim. | Final | Date |
| SCN-1/EV3-12A (Acc. Test Spec) | 3/5/71 | 6/25/71 | 3/19/71 (-37) |
| SCN-1/EV3-9A (Qual. Test Spec) | 3/5/71 | 6/25/71 | 3/19/71 (-37) |
| SCN-1/16763-18B (Cert. Plan) | 3/5/71 | 6/25/71 | 3/19/71 (-37) |
| SCN-1/16763-42A (P&I Spec) | 3/5/71 | 5/21/71 | 3/19/71 (-37) |
| SCN-2/EV3-12A (Acc. Test Spec) | 4/30/71 | - | Revision Req'd |
| SCN-2/16763-18B (Cert. Plan) | 4/30/71 | - | Revision Req'd |
| SCN-1/SY1-36C (ECP-001) | 4/30/71 | 5/21/71 | 5/14/71 (-65) |
| SCN-2/SY1-36C (ECP-002) | 4/30/71 | 5/21/71 | 5/14/71 (-65) |
| SCN-3/SY1-36C (ECP-016) | 4/30/71 | 5/21/71 | 5/14/71 (-65) |
| SCN-2/16763-42A (P&I Spec) | 5/3/71 | 5/21/71 | 5/14/71 (-64) |
| SCN-4/SY1-36C (ECP-004) | 5/4/71 | 5/21/71 | 5/14/71 (-65) |
| SCN-2A/EV3-12A | 5/12/71 | 5/26/71 | 5/25/71 (-75) |
| SCN-2A/16763-18B | 5/14/71 | 6/25/71 | 5/21/71 (-70) |
| SCN-2/EV3-9A | 5/18/71 | 5/26/71 | 5/25/71 (-74) |
| SCN-5/SY1-36C (Temp) | 5/25/71 | 7/12/71 | 5/27/71 (-80) |
| SCN-3/16763-18B (Cert Plan) | 5/26/71 | 6/25/71 | 5/27/71 (-81) |
| SCN-6/SY1-36C (Update SSD Geom. Factor) | 6/9/71 | 7/8/71 | 6/27/71 (-91) |
| SCN-4/16763-18B (Cert Plan) | 6/9/71 | 7/8/71 | 6/27/71 (-91) |
| SCN-3/EV3-9A (Super Qual for FES) | 6/11/71 | 7/8/71 | 6/27/71 (-91) |
| SCN-7/SY1-36C (Mag. Repeatability Deleted) | 6/25/71 | 7/12/71 | 7/2/71 (-94) |
| SCN-3/EV3-12B (extended STV for F2) | 6/28/71 | 7/20/71 | 7/13/71 (-97) |
| SCN-1/16763-40B (Meas. List) | 7/20/71 | 8/13/71 | 7/27/71 (-L90) |
| SCN-8/SY1-36C (Doc. Rev. Ltrs.) | 7/20/71 | 8/13/71 | 7/27/71 (-L90) |

Item
No.

6 Engineering drawings were submitted in the form of 35mm microfilm aperture cards as directed in MSC TWX EE17/70-122. A complete listing of the drawings was provided to both NASA MSC and KSC in "Tab" runs in the Acceptance Data Packages. Transmittal lists and periodic summary lists of drawing submittals were also made. There are approximately 800 drawings presented in approximately 1300 microfilm cards. Scientific Instrumentation drawings by ATC and Time-Zero (to the piece part level) were sent to NASA in paper print form.

7 Monthly progress reports started with the month of May, 1970 and continued through the month of June/July 1971. This last report covered the month of June plus that portion of July until the 23rd, at which time the formal acceptance testing of Flight #2, and the last acceptance review were completed, and the level of program effort was substantially reduced to approximately a sustaining level. The scientific instrumentation reports covering ATC and Time-Zero activities were included in the basic report until and including the September 1970 report; for subsequent months the ATC and Time-Zero reports were sent directly to MSC, as requested in MSC TWX #EE17/70-122. Submittals were required on the 15th of the month following the reporting period. As the program progressed and the documentation load became very heavy, program progress reports were assigned very low priority because of the heavy schedule pressures and many on-site meetings held at TRW by NASA, which reduced the need for prompt progress report delivery.

8 Monthly financial management reports started with the report due 22 June 1970, and continued through the report due 22 September 1971. These were submitted on NASA 533 forms and included quarterly reports. Submittals were required on the 22nd of the month following the reporting month, and were typically made on or close to that date.

9 Preliminary and final versions of the final report were required. The preliminary submittal was required on 1 October 1971 and was made on 29 October 1971 . This report is the final version.

10 Review minutes were required in two parts, A and B, with Part B covering review meeting action item disposition. Part B minutes were required one month after each review and these were supplied for the first 3 reviews, namely the PDR, June review, and CDR. Thereafter MSC requested that subsequent Part B submittals be replaced by submitting each issue of the more frequently updated informal TRW Action Item Log which was done during the remainder of the program. Part A minutes were submitted shortly after the meetings to the MSC Experiment Manager for preliminary review. Formal submittals were made following incorporation of his suggested changes. Reviews were held each month from May 1970 through January 1971 and Part A minutes were submitted for each.

Item No.

11 Reports were required and submitted following each Acceptance Review as listed below.

| Date | Acceptance Review |
|---|---|
| 3/8-12/71 | Qualification Unit Phase One C.A.R. |
| 4/6-7/71 | Flight #1 Phase One C.A.R. |
| 5/7/71 | PES Flight #1 C.A.R. |
| 5/26-28/71 | Flight #1 Phase Two C.A.R. |
| 6/21-24/71 | Flight #2 Phase One and Qualification Unit Phase Two C.A.R. |
| 6/29-30/71 | PES Flight #2 C.A.R. |
| 7/21-22/71 | Flight #2 Phase Two C.A.R. |
| 11/4/71 | Flight #2 Phase Two Re-Acceptance |
| 2/1-3/72 | Flight #2 Re-Acceptance |

12 Acceptance data packages were submitted for all units (subsystems) and spacecraft each at the applicable acceptance review. Corrections or changes were identified during the reviews and subsequently incorporated. Data packages are listed on an attached table together with the submittal dates for the corrected packages.

13 Material review records were submitted at the acceptance reviews as required as part of the applicable data packages (see Acceptance Data Package Summary List).

14 The Failure Mode & Effects Analysis (FMEA) submittal was originally required on 5/4/70 but this was changed by MSC direction to be 6/30/70. Actual first submittal was made 7/1/70. The final issue is a B revision.

15 Failure reports were made on NASA/MSC Failure Investigation Action Report (FIAR) forms. FIAR's were submitted both individually at the time of each failure, and as part of the applicable acceptance data package. Reports were required 24 hours after failure. In general failure reports were telephoned to MSC within 24 hours and this was followed by an initial submittal of the FIAR form. To date 109 FIAR's have been submitted and these are listed on pages 36, 37 and 38.

TRW

## P & F DATA PACKAGE STATUS

| NAME | QUAL. S/N | QUAL. #BKS. | QUAL. MSC | FLT. 1 S/N | FLT. 1 #BKS. | FLT. 1 MSC | FLT. 2 S/N | FLT. 2 #BKS. | FLT. 2 MSC | REMARKS |
|---|---|---|---|---|---|---|---|---|---|---|
| ANTENNA | 003 | (1) | C | 002 | (1) | C | 001 | (1) | J/B/C | |
| BATTERY | 001 | (1) | B | 005 | (1) | C | 003 | (1) | J | S/N 005 BKS. (1) |
| C.D.U. | 001 | (1) | B | 002 | (1) | C | 003 | (1) | J | |
| CONVERTER | 001 | (1) | B | 002 | (1) | C | 003 | (1) | J | |
| D.E.U. | 001 | (1) | B | 003 | (1) | D | 002 | (1) | J/C/I | |
| DIPLEXER | 011 | (1) | B | 012 | (1) | C | 013 | (1) | J | |
| D.S.U. | 001 | (1) | B | 002 | (1) | C | 003 | (1) | J | |
| MAGNETOMETER (FES) | 003 | (3) | E | 001 | (3) | C | 002 | (1) | J | |
| PARTICLES (PES) | 2-2 | (3) | E | 2-3 | (3) | D | 2-4 | (2) | J | |
| RECEIVER | 001 | (1) | B | 002 | (1) | C | 003 | (1) | J | |
| S.E.U. | 001 | (1) | B | 002 | (1) | C | 003 | (1) | J | |
| SOLAR ARRAY | 003 | (1) | J | 002 | (1) | A | 001 | (1) | A/G | |
| S/S-LANCH. STRUCTOR | 001 | (1) | A | 002 | (1) | A | 003 | (1) | J | |
| SUN SENSOR | 003 | (1) | B | 001 | (1) | C | 004 | (1) | J | |
| TRANSMITTER | 001 | (1) | B | 002 | (1) | C | 003 | (1) | J | |
| TRANSPONDER | 001 | (1) | B | 002 | (2) | C | 003 | (1) | J | |
| P&F S/S DATA PKG. | 001 | (7) | D/H/F | 002 | (6) | D | 003 | (11) | | |

(A) Delivered at Acceptance Review 3/12/71
(B) Sent Air Express to F. Troutman 4/02/71
(C) Sent Air Express to F. Troutman 5/03/71
(D) Sent Air Express to J. Johnson 6/04/71
(E) Hand Carried by J. Gardner to MSC 6/10/71
(F) Sent Air Express to F. Troutman 6/13/71
(G) Book 1 - Originally Assigned to Qual.
(H) Preliminary Delivery of 3 Books, Final Delivery was 4 Books.
(I) Book 1 - Originally Assigned to Flt. 1
(J) Sent Air Express to F. Troutman 7/15/71

| Item No. | |
|---|---|
| 16 | Failure Analysis Reports (FAR's) were submitted as required as part of update FIAR's (see FIAR Summary List). |
| 17 | Corrective Action Reports were submitted as part of the final FIAR forms (see FIAR Summary List). |
| 18 | Certification Plan submittal was required on 6/4/70 with actual first submittal on 6/24/71. The latest is Revision B with SCN-4. |
| 19 | Development Test Plan submittal was required on 6/4/70 with actual first submittal on 6/15/70. The latest issue is Revision B. |
| 20 | Qualification Test Specification submittal was required 2 months prior to test. Actual first submittal was on 9/15/70. The latest issue is Revision B with SCN-3. |
| 21 | Acceptance Test Specification submittal was required 2 months prior to test. Actual first submittal was on 9/15/70. The latest issue is Revision B with SCN-3. |
| 22&23 | Preinstallation Acceptance Test Specifications and Integration and Prelaunch Test Requirements Package required submittals for these items were 9/15/70 but this was delayed by agreement with MSC (refer to customer review meeting minutes). Following subsequent TRW documentation support activities it was agreed with Mr. Jack Johnson the MSC Experiment Manager that the requirements for Items 22 and 23 had been fulfilled by TRW letters #8230.14-52 and 8230.14-50, both of 7 December 1970. These provided detailed inputs and corrections to Mr. Richard Bohlman of NASA/KSC on the NASA P & F Subsatellite Pre-launch Checkout document #TCP-KL-6007-LM10, dated 27 November 1970, prepared by Grumman Aerospace Corporation, and to Mr. George Doland of NASA/MSC on the NASA P & F Subsatellite/MSFN Systems Compatibility and Performance Test Procedure #HASD No. OB3069, dated 18 November 1970, prepared by Lockheed Electronics Company. |
| 24&25 | Qualification & Acceptance Test Procedures submittals were required 2 weeks prior to test (qual), and 1 month prior to test (acceptance). The contract initially required only end item level procedures but submittal of unit level procedures was added later. Early versions of the more important procedures were submitted to MSC in printed paper form for early review, then again when any changes had been incorporated. Subsequently they were submitted as 35 mm microfilm aperture cards and updated as revisions were made. The procedures were also submitted to MSC as part of the acceptance data packages. Procedures are listed on the attached unit level and spacecraft level procedure summary lists. Procedures by the major subcontractor ATC and Time-Zero |

submitted in printed form, and are also in the acceptance data packages. ATC and Time-Zero procedures are listed below:

ATC

a) ATC PES Acceptance Test Procedure, TP 1141-014
b) ATC Subassembly 13 Telescope Electronics Precalibration Measurments Test Procedure, TP 1141-014

TIME-ZERO

a) T-Z Acceptance Test Procedure, Apollo Subsatellite Magnetometer, S 10070019
b) T-Z Calibration Procedure, Apollo Subsatellite Magnetometer, S 10070026

26 Preinstallation Acceptance Test Procedures requirement was satisfied by the work described under Items 22 and 23 above.

27 Scientific Instrumentation Calibration Procedures submittes were required 2 weeks prior to calibration. These are as follows:

a) Foil Calibration Procedure, Parylene N, TP 1141-016
b) Telescope Subassemblies 11 and 12, TP 1141-11 & 12
c) Curved Plate Analyzer Subassemblies 1, 2, 3 & 4
d) Telescope Noise Counting Rate Adjustment, TP 1141-017
e) Particles Subsystem Calibration, TP 1141-013

28 No item 28 was given in the Contract

29 Qualification Test Reports were to be submitted by 5/15/71 and were submitted as part of the acceptance data packages (refer to the acceptance data package summary list).

30 Calibration Data Reports submittals were required at the phase two acceptance reviews. Submittals were as follows:

| | Submittal Date |
|---|---|
| Flight #1 Subsatellite Calibration Data Report, 16763-30-01 (latest revision is Rev. B) | 5/26/71 |
| Qualification Unit Calibration Data Report, 16763-30-03 (latest revision is NC) | 6/16/71 |
| Flight #2 Subsatellite Calibration Report, 16763-30-02 (latest revision is Rev. B) | 7/29/71 |

31 Experiment Support Requirements submittal was required to be made at the CDR, and actual submittal was at the CDR.

32 Spares Requirements was mutually agreed with MSC as not applicable to the Subsatellite program.

33-39 Submittal of documentation items 33 through 39 was required to be 5/4/70. However contract go-ahead was not obtained until 5/15/70, therefore submittals were made at that time, as listed below:

| | DOCUMENT (Latest Revision) | REQUIRED SUBMITTAL DATE | ACTUAL DATE |
|---|---|---|---|
| 33 | Quality Assurance Plan (Rev. B) | 5/4/70 | 5/15/70 |
| 34 | Reliability Plan (Rev. C) | 5/4/70 | 5/15/70 |
| 35 | Configuration Management Plan (NC) | 5/4/70 | 5/15/70 |
| 36 | System Safety Plan (NC) | 5/4/70 | 5/15/70 |
| 37 | EMC Control Plan (NC) | 5/4/70 | 5/15/70 |
| 38 | Magnetic Cleanliness Plan (NC) | 5/4/70 | 5/15/70 |
| 39 | Development Schedule (NC) | 5/4/70 | 5/15/70 |
| 40 | Measurement List (Rev. B, SCN-1) | 7/14 (CDR) | 7/14/70 |
| 41 | Command List (Rev. B) | 7/14 (CDR) | 5/15/70 |
| 42 | Subsatellite/MSFN P&I Specification (REV. A SCN-2) | 7/14 (CDR) | 7/14/70 |

43 Operational Data Book requirement is considered to have been satisfied by the considerable support provided to NASA MSC, particularly to Flight Operations Directorate (FOD), in the form of supply of input material, review and correction of material, meetings, and telephone discussions by both the TRW Redondo Beach personnel and by the TRW resident representative at MSC, during preparation of the MSC documents P&F Subsatellite Systems Handbook, Console Handbook, and others.

44 Parts and Materials List submittal was required on 6/30/70, and was made on that date. The latest issue is Revision C.

No #. Others important whose submittal was not initially required but was added later included the subsystem equipment specifications as listed below (latest issue is show):

Subsystem Level Equipment Specifications

| | |
|---|---|
| EQ3-290 NC | Battery Assembly, P&F |
| EQ4-892 D | Particles Experiment Subsystem, P&F |
| EQ4-893 D | Fields Experiment Subsystem, P&F |
| EQ4-918 NC | Command Decoder, P&F |
| EQ4-919/SCN-1 | Digital Electronics Unit (DEU), P&F |
| EQ4-945 B | Diplexer, P&F |
| EQ4-955 NC | Data Storage Unit (DSU), P&F |
| EQ4-957NC/SCN-1 | Sun Sensor Unit, P&F |
| EQ4-959 NC | Spacecraft Electronics Unit (SEU), P&F |
| EQ4-960 NC | Antenna Assembly, P&F |
| EQ4-973NC/SCN-2 | Transponder Converter, P&F |
| SS6-33NC | S-Band Transponder, P&F |

# P&F UNIT LEVEL TEST PROCEDURES AVAILABLE IN MICROFILM FILE

| | |
|---|---|
| HC-00K-01/D1 | P and F Subsatellite Assembly Magnetic Properties Procedure |
| HC-01Q-01/NC | Ordnance Qualification/Lot Acceptance Test Procedure |
| HC-06A-01/A5 | Command Decoder Acceptance Test Procedures |
| HC-06A-02/B3 | DEU Unit Acceptance Test Procedure, A7 |
| HC-06A-03/A | DSU Unit Acceptance Test Procedure, A4 |
| HC-06A-04/A2 | S-Band Receiver Acceptance Test Procedure |
| HC-06A-05/A1 | S-Band Transmitter Acceptance Test Procedure |
| HC-06A-06/A4 | S-Band Transponder Acceptance Test Procedure |
| HC-06C-01/A2 | Command Decoder Functional Test Procedure (Plus Attachment I & Attachment II) |
| HC-06C-02/A3 | DEU Functional Test Procedure |
| HC-06C-03/A2 | DSU Functional Test Procedure |
| HC-06C-04/NC | Command Decoder Functional Board Test |
| HC-06C-05/NC | Functional Test Procedure for the Hat Assembly |
| HC-06Q-01/A2 | Command Decoder Qualification Test Procedure |
| HC-06Q-02/A7 | DEU Unit Qualification Procedure |
| HC-06Q-03/A4 | DSU Unit Qualification Test Procedure |
| HC-06Q-04/A1 | S-Band Transponder Qual Test Procedure |
| HC-06T-01/A1 | Functional Test Procedure for the OMNI Dipole Array Antenna |
| HC-09A-01/A5 | Battery Charger/Simulator Acceptance Test Procedure, P&F |
| HC-09H-01/A1 | S-Band Transmitter Calibration Procedure |
| HC-09H-02/A1 | S-Band Test Transmitter Calibration Procedure |
| HC-09Q-01/A | Battery Charger Simulator EMI Qualification Test Procedure 16 |
| HC-12A-03/A | SEU Acceptance Test Procedure, A1 |
| HC-12C-01/A7 | SEU Functional Test Procedure |
| HC-12C-02/A2 | Transponder Converter Electrical Test Procedure |
| HC-12H-01/A1 | DEU Tester Calibration Procedure |
| HC-12H-02/A1 | Calibration Procedure Resistive Load Bank, Converter |
| HC-12Q-03/A | SEU Qual Test Procedure, A1 |
| HC-12T-01/A2 | SEU Component Select-In-Test Procedure |
| HC-14A-01/A1 | Acceptance Test Procedure, Battery Assembly |
| HC-14B-01/A1 | Activation and Formation Procedure, 10 AH Cell |
| HC-14C-01/A* | Solar Panel Functional Bench Test |
| HC-14C-02/C | Functional Bench Test Procedure, Battery Assembly |
| HC-14F-01/A | Battery Fabrication Test Procedure, A3 |
| HC-14K-01/NC | Solar Array Panel Magnetic Properties Procedure |
| HC-14K-02/NC | P&F Magnetic Properties Procedure, Solar Array |
| HC-14Q-01/B1 | Battery Qualification Test Procedure |
| HC-14R-01/NC | |
| HC-14R-02/A | Cost Acceptance and Selection, A1 |
| HC-16A-01/C1 | Magnetic Fields Experiment Acceptance Test Procedure |
| HC-16A-02/A2 | Particles Experiment Subsystem (PES) Acceptance Test Procedure |
| HC-16Q-01/B1 | Magnetic Fields Experiment Qualification Test Procedure |
| HC-16Q-02/NC | Particles Experiment Subsystem (PES) Qualification Test Procedure |
| HC-17A-01/A1 | Sun Sensor Acceptance Test Procedure |
| HC-17C-01/B | Sun Sensor Electronics Board Functional TP |
| HC-17C-02/A1 | Sun Sensor Unit Functional Test Procedure |
| HC-17H-01/A2 | Sun Sensor Optical Alignment Procedure |
| HC-17Q-01/A2 | Sun Sensor Qualification Test Procedure |
| HC-19H-01/NC | SEU Test Set Calibration Procedure |

P&F SPACECRAFT LEVEL TEST PROCEDURES
LATEST ISSUE LIST

| PROCEDURE NUMBER | TITLE |
|---|---|
| HC-21A-01/D2 | SUBSATELLITE ACCEPTANCE VIBRATION |
| HC-21K-01/B4 | MAGNETIC CLEANLINESS MEASUREMENTS |
| HC-21M-01/A2 | MECHANICAL ASSEMBLY & DISASSEMBLY |
| HC-21M-02/A1 | LAUNCHER/SUBSATELLITE RIGGING |
| HC-21M-03 | HOISTING & HANDLING |
| HC-21M-04/A | STORAGE PROCEDURE |
| HC-21Q-01/C2 | SUBSATELLITE QUALIFICATION VIBRATION |
| HC-21S-01/C9 | INTEGRATION & FUNCTIONAL TEST |
| HC-21S-02/NC | BOOM ALIGNMENT |
| HC-21S-03/B2 | MASS PROPERTIES MEASUREMENT |
| HC-21S-04/F4 | INTEGRATED SYSTEMS TEST |
| HC-21S-05/C2 | SUBSATELLITE LIMITED FUNCTIONAL |
| HC-21S-06/C4 | SOLAR THERMAL VACUUM |
| HC-21S-07 | THERMAL VACUUM (FLT2 IN 7x12 CHAMBER) |
| HC-21S-08/B1 | SOLAR THERMAL VACUUM (FLT 2 IN 30 FT CHAMBER) |
| HC-21T-01 | LEAKAGE RESISTANCE TEST FOR HARNESS |
| HC-21T-02 | BATTERY CHARGING & DISCH (IN SIM) |
| HC-21T-03 | BATTERY CHARGING & DISCH (NOT IN SIM) |

## 6. TECHNICAL PROBLEMS ENCOUNTERED

Technical problems which were encountered during the P & F program together with their solutions are detailed and reported to the MSC on Failure Investigation Action Reports (FIAR's). These are tabulated herein on an attached table. The problems considered to be the most serious are listed below and subsequently described in some detail.

### Most Serious Technical Problems

PES High Voltage Problem
Spacecraft Thermal Design
Boom Failure
Boom Damper Leakage
Battery Case Redesign
Diode, Replacement

### PES HIGH VOLTAGE PROBLEM

The most serious technical problem in the P & F Subsatellite program involved arc-overs in the Particles Experiment Subsystem (PES) high voltage supply. This problem was first encountered during the thermal/vacumm portion of the PES unit level qualification testing. It occurred on March 1 just after receipt of the PES S/N 1-1 at TRW from the subcontractors ATC, and was detected when the high voltage dropped to approximately one-half of spec value. Subsequent investigation showed this to be a design problem associated with the potting compound. The 707 High Voltage module was a completely potted unit which suffered voids and cracking of the potting compound opening paths for corona/arcing of the high voltage to ground when the unit was exposed to low temperature and hard vacuum. In the temperature excursion from the curing temperature of 200°F to room temperature, a 2% bulk shrinkage of the C60 material occurs. Subsequent shrinkage occurs during the excursions to 35°F during test. This same shrinkage occurred in other ATC high voltage module applications which had been used successfully on other programs but was not as critical because a substantially smaller volume of this material was used.

Because of the severe schedule pressures which by this time existed in the program, a multiple approach to the problem was undertaken involving a number of potential fixes. The eventual solution to the problem was elimination of the potting material and substitution of conformal coating. The solution additionally incorporated mechanical strengthening of the unit through the use of spot bonding of components which became necessary because of the elimination of the full potting. Solution of this problem required large expenditures of money, extreme compression of the overall spacecraft level test program, and a considerable period of time with delivery of the 1st successful PES on May 7. Two large TRW thermal/vacuum chambers were relocated to ATC for 24 hour usage during the period, and involvement of high voltage experts from TRW and other organizations.

## SPACECRAFT THERMAL DESIGN

The initial engineering solar thermal vacuum tests on the qualification subsatellite indicated in-orbit subsatellite temperatures significantly colder than earlier predictions indicated, and also indicated excessive temperature drop during the 3 1/2 hour eclipse. This proved to be a stubborn problem to solve and required considerable time and effort. The solution consisted of many design changes which increased the general temperature level of the subsatellite and reduced the rate of temperature drop by isolation of the spacecraft interior from the exterior surface. The detail design changes were as follows.

1. Transponder stand-offs changed from aluminum to fiberglass.

2. Heat sink and thermal insulator with washer stand-offs added under Fields Experiment Subsystem Electronics package.

3. Removed white paint from platform #5, the boom brackets, analyzer sun shades, and connector backet, and thermally insulated the platform and mounted equipment with a multi-layer kapton insulating blanket.

4. Aluminum foil tape was added to the outside of the entire DSU and its mating platform and the side of the #3 platform facing the DSU, the cable clamps on the magnetometer boom, the exposed surfaces of the particles experiment, the outside of the sun shades and platform #1 between the antenna and base ring.

5. Fiberglass washers added between the solar array inserts and the equipment platform, and under the bolt heads attaching the solar array.

6. Added a multi-layer mylar blanket to platform #1, covering the inside of the base ring and to the outside of the fiberglass booms. Added a single layer of aluminized mylar covering to the inside of the solar panels.

7. Added a multi-layer kapton insulation blanket wrap to the central portion of the NR-interfacing rail bracket; the exposed rail ends were also covered with aluminized mylar tape.

8. The inside of the particle experiment sun shades were painted black. Also added fiberglass stand-off washers between the sun shades and the curved plate analyzer, and between bolt head and the shades. Added electrical ground straps between the shades and the analyzer housing. The straps were required because of thermal isolation.

9. Added balance weight to platform #3, to statically balance the subsatellite for counterbalancing the changed thermal materials.

BOOM FAILURE

During thermal-vacuum testing of the Flight #1 P & F Spacecraft, a structural failure occurred in the inboard fiberglass reinforced plastic tube of one of the spacecraft balance booms on April 26, 1971. The tube had failed at a point approximately one foot from the attachment bracket at the spacecraft and was hanging downward at approximately 90°. A second balance boom had a distinct bow in approximately the same location. The failure was of a ductile nature. In the investigation the boom temperature during the test was calculated as reaching 210°F. Also, the boom material was found to suffer a sharp reduction in mechanical properties above 160°F sufficient to result in the bending failure while the 1g environment of an Earth-bound test chamber is applied. Such failures would not be anticipated in orbit because of the zero "g" conditions. The thermal configuration of the booms at the time of the failure was aluminum tape covering the fiberglass tube. Corrective action was to change the thermal covering to be an 8-layer, 1/4-mil thick alumnized Mylar spiral wrap covered with a layer of 2-mil aluminized Mylar, Mylar side outwards. During the test after the fix boom temperatures were 29°F at the center of the inner segment and thus the problem was solved.

BOOM DAMPER LEAKAGE

A leak developed in the boom damper of the qualification subsatellite during an engineering solar thermal vacuum test. The oil was seen in the upper platform inside the boom brackets. This failure was written up in FIAR #TRW-PFS-0072 of April 8. The problem was localized to the low coefficients of friction teflon seal covers of the secondary piston allowing fluid to leak past the O-ring and out of the assembly at low temperature. These seals are located over the O-rings. The cause of the damper leakage is attributed to relative separation between the piston shaft and the teflon seal covers which was intensified at reduced temperatures (see Figure 1a). This is explained by noting that the piston shaft contracts at reduced temperatures whereas the teflon O-Ring assembly remains relatively unchanged leaving a small gap. The corrective action was to remove the teflon seals from the secondary piston, replace the existing cap with a new part which will accommodate a static seal against the cylinder and redundant O-Ring against the main piston shaft. The cylinder was refaced to provide for the static seal. Lock-wire holes were plugged with epoxy. Lock-wiring of the fill-screws and nut were removed and epoxy fillets were added to prevent loosening during vibration. These changes were made to all P & F units.

BATTERY CASE REDESIGN

Corrosion was found on the Flight #1 Battery Assembly after it had successfully completed the functional portion of its unit level acceptance tests and prior to integration into the Flight #1 sub-satellite (Failure Investigation Action Report (FIAR) #TRW-PFS-0063). The corrosion was due to a small amount of electrolyte leakage. When the case was opened it was found that cell #8 had ruptured and had a "y" shaped crack completely across the header. Also cells 7 and 9 may have had hairline cracks. The cracks were found by milling the header and using a tracer. The case was not hermetically sealed but had a screwed on cover and was completely filled with an encapsulant. The leakage was found under the cover. Corrective action was the addition of a fiberglass header onto the cell pack prior to encapsulation, and also change of the encapsulant from PR4-2-2 to the less brittle RTV 8113 (PR4-1-1).

DIODE REPLACEMENT

A diode failure occurred during the thermal/vacuum portion of acceptance testing of DSU S/N 001 on November 18, 1970. At +100°F error segments of 8 words read "0"'s instead of "1"'s every 64 words indicating the output data was not the same as the data which had been entered. Investigation indicated that two diodes, CR21 and CR58, both of the same type (PT4-2311), failed open. This was attributed to mechanical overstressing of the parts by the hi-temp shrink sleeves due to incorrect application of heat during the manufacturing process. As a result, the procedure was changed to require a closed-loop heat gun, and the use of a different type of sleeving. The analysis was not completely conclusive such that there remained the possibility that the cause might be the part itself, therefore the type of diode, and the dio e manufacturer were also changed as a precautionary measure. All PT4-2311's were replaced by FHA 600's (screened by TRW) in all flight units, and in the qualification unit DSU. This change was particularly significant because of the number of these diodes used throughout the P & F System.

TABLE 1. TECHNICAL PROBLEMS ENCOUNTERED

| FIAR NO. | DATE OF FAILURE | UNIT SERIAL NO. | DESCRIPTION OF FAILURE |
|---|---|---|---|
| 0001 | 10/29/70 | Rcvr 001 | Coherent Drive Level Low |
| 0002 | 10/30/70 | Xmtr 001 | Low Voltage at A2Q3 |
| 0003 | 11/03/70 | Rcvr 001 | Intermodulation Not 15db Below |
| 0004 | 11/12/70 | DSU 001 | Error Lite-Vib |
| 0005 | 11/18/70 | DSU 001 | Readout Incorrect, PT4-2311 Open |
| 0006 | 11/21/70 | DEU 001 | Data Not Shifting, C1276 Short |
| 0007 | 11/24/70 | DSU 001 | Error Lite During X-Vib |
| 0008 | 11/24/70 | DEU 001 | Incorrect Readout, C1276's Shorted |
| 0009 | 11/25/71 | Xpndr 001 | +28V Current Went to Zero |
| 0010 | 11/27/70 | DSU 001 | Improper Vib Inputs |
| 0011 | 11/28/70 | DSU 001 | Memory Address Stopped |
| 0012 | 11/30/70 | Rcvr 001 | Threshold Center Frequency High |
| 0013 | 12/7/70 | DEU 001 | Vibration 30° Off Required Axis |
| 0014 | 1/7/71 | Batt Assy 001 | Protection Circuit Did Not Work |
| 0015 | 1/10/71 | Batt Assy 001 | Protection Circuit Did Not Work |
| 0016 | 12/30/70 | Xpndr 002 | Intermodulation Too High |
| 0017 | 1/4/71 | SEU 002 | Incorrect Output |
| 0018 | 1/23/71 | Batt Assy 001 | Reverse Current Thru Shunt |
| 0019 | 1/27/71 | Batt Assy 001 | Regulator Switching Erratic |
| 0020 | 2/2/71 | Sun Sensor 001 | Sensitivity Out of Tolerance |
| 0021 | 2/2/71 | Sun Sensor 003 | Sensitivity Out of Tolerance |
| 0022 | 2/2/71 | Sun Sensor 004 | Sensitivity Out of Tolerance |
| 0023 | 1/29/71 | DEU 003 | Improper Output |
| 0024 | 2/11/71 | Batt Assy 004 | Protection Circuit Inoperative |
| 0025 | 1/27/71 | Antenna 002 | Power to Acquire is High |
| 0026 | 2/22/71 | FES 002 | Incorrect Response |
| 0027 | 2/27/71 | PES 001 | Potential Mechanical Overstress |
| 0028 | 2/27/71 | PES 001 | C1-A1 Frequency Shift |
| 0029 | 3/2/71 | PES 001 | High Voltage Dropped |
| 0030 | 2/2/71 | Xpndr 003 | Reference TDR 58471 |
| 0031 | 2/18/71 | DEU 003 | X-Axis Intermittent Output Error |
| 0031 | 2/23/71 | DEU 003 | X-Axis Intermittent Output |
| 0032 | 3/3/71 | Xmtr 003 | Low Power Board Output Intermittent |
| 0033 | 3/5/71 | SEU 003 | Low Voltage Of 0.98 mV; Should Be 1.00 mV Min |
| 0034 | 3/8/71 | FES 003 | Noise on Output Lines (Time Zero) |
| 0035 | 1/7/71 | Antenna 002 | Pattern Repeatability Out-Of-Spec |
| 0036 | 12/4/70 | Antenna 002 | Axial Ratio High |
| 0037 | 12/11/70 | PES 1-1 | Anal #1 - Lack of Electron Counting |
| 0038 | 1/17/71 | PES 1-3 | Anal #3 - Test Input Wire Reversed |
| 0039 | 1/20/71 | PES 1-1 | Anal #3 - No Output From 404 Discriminator |
| 0040 | 1/20/71 | PES 1-1 | Anal #4 - No Output From 406 Discriminator |

ABLE 1. TECHNICAL PROBLEMS ENCOUNTERED (Continued)

| FIAR NO. | DATE OF FAILURE | UNIT SERIAL NO. | DESCRIPTION OF FAILURE |
|---|---|---|---|
| 0041 | 1/23/71 | PES 1-1 | Anal #3 - Peak Energy Shifts Lower |
| 0042 | 1/25/71 | PES 1-1 | Experiment Model 112 Has No Output |
| 0043 | 1/25/71 | PES 1-1 | Anal #3 - No Output from Model 405 |
| 0044 | 2/1/71 | PES 1-1 | Anal #4 - High Voltage Output Incorrect |
| 0045 | 2/3/71 | PES 2-2 | Telescope #11 - Shield/Vac. Chamber Resistance Too Hig |
| 0046 | 2/4/71 | PES 2-3 | Anal #1 - Count Rate Problem Due to Test Equipment |
| 0047 | 2/23/71 | PES 1-1 | Experiment Test Interruptions Due to Bad Data |
| 0048 | 2/23/71 | PES 2-2 | Experiment PCU Failed |
| 0049 | 2/25/71 | PES 2-2 | Experiment DS 2 Shorted |
| 0050 | 3/12/71 | Antenna 001 | Axial Ratio High |
| 0051 | 3/15/71 | PES 001 | Experiment 3.75 kv Output Shorted to Ground |
| 0052 | 3/22/71 | FES 002 | Sensor Assembly Out of Spec |
| 0053 | 3/22/71 | FES 003 | Sensor Assembly Out of Spec |
| 0054 | 3/24/71 | PES 001 | At - 35°F and $2.5 \times 10^{-8}$ Pressure High Voltage Erratic |
| 0055 | 3/27/71 | PES 001 | At - 78°F and $5 \times 10^{-8}$ Pressure High Voltage Erratic |
| 0056 | 2/25/71 | PES 1-1 | Mechanical and Electrical Out of Spec Condition |
| 0057 | 3/21/71 | PES 1-1 | No Analog #1 Logic Output |
| 0058 | 2/18/71 | PES 2-2 | Analog #3 - +4.6 Volt Line Shorted |
| 59 | 3/9/71 | PES 2-2 | PES - Corona Discharge at Vacuum |
| 0060 | 3/21/71 | PES 2-2 | PES - High Volt Incorrect |
| 0061 | 3/28/71 | PES 2-2 | PES - Channel A Oscillates at PCU Rate |
| 0062 | 3/28/71 | PES 2-2 | PES - Fund. s/b <49mV for DSU +5V is 54 mV |
| 0063 | 3/31/71 | Batt Assy 002 | KOH Seeping From Battery Case |
| 0064 | 4/3/71 | PES 2-2 | H.V. Does Not Turn-On and +37V Line Shorted |
| 0065 | 4/5/71 | PES 2-2 | H.V. Erratic |
| 0066 | 4/2/71 | Xmtr 003 | |
| 0067 | 3/19/71 | Batt Assy 002 | Cell #8 Voltage Low at Pre Vibration Test |
| 0068 | 4/2/71 | FES 001 | Noise Level Above Spec Requirements |
| 0069 | 11/24/70 | DSU 001 | |
| 0070 | 4/2/71 | SS 001/Batt 001 | Smoke Was Observed From Battery Assembly (R42 & 33) |
| 0071 | 4/1/71 | SS 001/Batt 001 | Battery Assembly 10 & 12 Blown |
| 0072 | 4/8/71 | SS 001/Damp.Assy 4,5&6 | Damper Assemblies Leaking Oil |
| 0073 | 3/3/71 | SS 001 | Battery Assembly & DEU BOnd Resistance Over 50Ω |
| 0074 | 4/10/71 | PES 2-2 | P-P Ripple Spikes & Power Supply Low Volt |
| 0075 | 4/10/71 | PES 2-2 | Unable to Obtain A1 (300V) & (1000) Volts |
| 0076 | 4/10/71 | PES 2-2 | HV Arcing at -35°F/Vacuum |
| 0077 | 4/13/71 | PES 2-2 | HV Oscillation at -36°F in Vacuum |
| 0078 | 4/18/71 | Batt Assy 005 | Board A8, Connect J1, Pins 34 & 35 Reversed |
| 0079 | 4/20/71 | SS 002 | Battery Overheated Due to Facility Air Cond. Problem |
| 0080 | 4/21/71 | PES 2-3 | A3 (Module 403) Has No Output |

TABLE 1. TECHNICAL PROBLEMS ENCOUNTERED (Continued)

| FIAR NO. | DATE OF FAILURE | UNIT SERIAL NO. | DESCRIPTION OF FAILURE |
|---|---|---|---|
| 0081 | 4/26/71 | SS 002/Boom Assy | Boom Assembly Arm Bent |
| 0082 | 4/27/71 | PES 2-3 | Telescope B Assembly 12 Threshold Too High |
| 0083 | 4/28/71 | SS 002/GSE | Word 30 Error due to GSE Frequency Drift |
| 0084 | 5/1/71 | PES 2-3 | Chassis Gnd. 8 mΩ S/B >100mΩ; Anal #1 Damaged |
| 0085 | 5/4/71 | PES 2-3 | No CA-HY Due to Mod 706 Shiled Shorting |
| 0086 | 4/21/71 | PES 2-3 | Analog #3 Mod 403 Noisy or No Output Due to Corona |
| 0087 | 5/5/71 | PES 2-3 | Gross Power Consumption Due to Damaged Resistors |
| 0088 | 5/4/71 | PES 2-3 | Analyzer Plate Voltage Out of Spec |
| 0089 | 5/9/71 | PES 2-2 | All Power Went to "0" While Approaching Qual. Vib |
| 0091(a) | 5/8/71 | SS 002/DEU 002 | DEU Count Error S (A+B) 5 |
| 0092 | 5/15/71 | SS 001/FES 003 | Faulty Calibration Reading Due to Cold Solder Join |
| 0093 | 5/8/71 | PES 2-2 | Out of Spec Voltages/Spec to be Rev. |
| 0094 | 5/21/71 | SS 002/Batt Assy 005 | Fuses F9 & F12 Blown Due to Mishandling |
| 0095 | 5/20/71 | SS 001/Boom Assy 004&005 | Lateral Boom Offset Out of Spec (reqmt too tight) |
| 0096 | 5/21/71 | SS 001/Batt Assy 001 | Fuse F12 Blown Due to Mishandling |
| 0097 | 6/13/71 | PES 2-4 | $E_A$ & $E_B$ Out of Spec Due to Operator Error |
| 8 | 5/16/71 | SS 001/FES 003 | Incorrect Bonding of Washer to S/C |
| 0099 | 6/12/71 | Antenna 001 | Incorrect Test Signal From GSE |
| 0100 | 6/16/71 | PES 2-4 | G1 & G2 Grounds Shorted Due to Pinched Wire |
| 0101 | 6/16/71 | PES 2-4 | "A" Telescope Exhibits Excess & Erratic Noise |
| 0102 | 6/22/71 | PES 2-4 | A1 & A2 HV Erratic Due to Manufacturing Mishandlin |
| 0103 | 6/24/71 | PES 2-4 | Calibration Mode Inoperative Due to Bad IC |
| 0104 | 6/30/71 | PES 2-4 | HV Too Low at -25°F Due to Poor Diode Mounting |
| 0105 | 7/7/71 | SS 003/PES | PES 5V Line too Low Due to GSE Line Losses |
| 0106 | 7/8/71 | SS 003/Batt Assy 003 | Fuses F2 & F8 Blown Due to Handling Accident |
| 0107 | 7/19/71 | SS 003/DEU 002 | No Low Telescope Counts |
| 0108 | 7/20/71 | SS 003/PES 2-4 | High Telescope Counts - Temperature Sensor |
| 0109 | 8/24/71 | SS 003/DEU 002 | No DEU Counts Between 16-31 (ECP #032) |
| 0110 | 11/18/71 | Flt 2 S/C | Flight 2 S/C failure due to Vacuum Chamber Accident |
| 0111 | 12/1/71 | PES 2-2 | Power input current reading dipped to zero. |
| 0112 | 12/6/71 | PES 2-2 | Assembly A2 shorted to chassis. |
| 0113 | 12/13/71 | PES 2-2 | Input current low at -15°F. |
| 0114 | 12/16/71 | PES 2-2 | Input current high during vibration. |
| 0115 | 12/28/71 | PES 2-2 | High voltage "turn-off" during T/V. |
| 0116 | 1/3/72 | Transponder 003 | Spurious Modes on Transmitter - GSE Problem |
| 0117 | 1/8/72 | PES 2-2 | High Voltage arcing in spacecraft T/V. |
| 0118 | 1/14/72 | Battery Assy 003 | Fuse wire F12 blown. |
| 0119 | 2/3/72 | Flight 1 S/C | Data drop-out in space |
| 0120 | 2/25/72 | PES 2-2 | Channel B veto and calibrate light out on GSE during T/V. |

7a. SPACECRAFT TEST HISTORY

Qualification Unit Test History

On completion of fabrication the main structural elements of the subsatellite (substrates, platforms, booms, etc.) were assembled toegther for verification of the mechanical interfaces. The subsatellite was delivered to the integration and test laboratory in this assembled state on November 25, 1970. Here it was disassembled on December 2, kits prepared for a later and more complete assembly, and the substrates sent to the solar panel fabrication shop for the mounting and wiring of the solar cells.

Prior to commencing the integration of the Qualification subsatellite, the top platform (#5) was sent to the engineering test shop for proof loading of the lifting fixture mounting inserts that are bonded into this platform.

With the return of the top platform, the build-up and integration of the subsatellite was started on December 8. The main electrical harness was installed after the antenna, transponder subsystem, command decoder, Subsatellite Electronics Unit (SEU), and Digital Electronics Unit (DEU) had been mounted. The absence of the Digital Storage Unit (DSU), the particles and fields experiments, and a power subsystem severely limited the integration and test activities. However, the installation of the "breadboard" particles experiment power supply did permit integration and test of the transponder and partial data system.

This testing was completed on December 16 to the point that the subsatellite was capable of being used for a compatability test with the MSFN system. It was transported to MSC Houston, on December 17 for the first part of this compatibility test and to KSC on January 4 for the final part of the test, returning on January 9. The spacecraft used for these tests was a partially completed unit but was quite satisfactory for these tests. The unit employed an engineering model PES and did not contain the DSU, Battery Assembly, or FES. These tests included uplink command channel SNR; sub BER and MRR, and downlink SNR and BER. Primary concern was general communications compatability with the MSFN ground station network, and the ability to communicate with the P&F Subsatellite while in lunar orbit from stations using 30-foot antennas. The testing at MSC indicated operation with 30-foot antennas would be marginal. However actual operation of the Flight #1 P&F in lunar orbit confirmed satisfactory operation with even the uncooled paramp 30-foot sites.

When the subsatellite was returned to the integration and test laboratory at TRW the DSU was available for integration, this was done on January 12 and a functional test of the data system performed, including a compatibility check with the TRW ground support equipment (GSE) i.e. the PCM decommutation equipment.

The fields experiment was the next unit available for installation and integration on January 13 and this was followed four days later by the battery assembly i.e. battery, charge control electronics, and shunt assembly, which were also integrated.

Prior to performing further functional tests, the subsatellite was returned to the wiring bench for the installation of the separatin harness and micro-switch assembly. When the installation was completed the earlier portions of the functional tests were repeated, the battery was serviced, and "dry runs" were performed on the telemetry calibration procedure.

On completion of these tests the fields experiment (S/N 001) was removed on February 9 from the subsatellite and returned to the vendor for retest and calibration checkout at UCLA. At the same time the sun sensor (S/N 003) was received and subsequently installed in the subsatellite.

In the course of the earlier functional tests and on further battery checkout, it was found the overvoltage protection circuits were inoperative. The battery was removed from the subsatellite and returned to the unit engineer for further investigation. This investigation showed that several transistors in the inoperative circuit were "blown" (see TDR 60579). Rs this was the "engineering model" battery it was not returned to the subsatellite but was at a later date replaced by the actual qualification battery (S/N 001).

The "breadboard" particles experiment power supply was also removed from the subsatellite at this time and the remainder of the subsatellite, along with the boom assemblies, installed in a thermal-vacuum chamber and exposed to a "bake" test for 60 hours at 140°F $\pm 5$ in a vacuum of $5 \times 10^{-5}$ torr to out-gas unapproved materials on February 12. The solar array panels for this subsatellite were also exposed to the same "bake" test, but in a separate chamber.

After the "bake" test the subsatellite was further disassembled to allow rework of the platforms. This rework consisted of filling the platform edges with an epoxy filler and drilling vent holes into it when it had hardened. Inserts for mounting balance weights were also bonded into several of the platforms at this time. The subsatellite was then reassembled and final installation of the available "black boxes" made, including bonding resistance measurement and torque value verification.

During March the qualification battery (S/N 001) and the fields experiment (S/N 001) were installed in the Qualification Unit subsatellite as they become available, and with the aid of the "bread-board" particles experiment power supply final integration and functional testing of the incomplete assembly was started.

While awaiting delivery of the particles experiment the corrosion damaged antenna (known since unit test, but integrated pending further disposition) was removed from the subsatellite and replaced with the antenna (S/N 003) from the F-2 subsatellite. The S/N 001 antenna was returned to the unit engineer for refurbishment. Also, during this period the subsatellite was installed in the solar thermal-vacuum chamber and used in the checkout and "dry run" of the test set-up.

When a Particles Experiment (S/N 001) was finally received it had an inoperative high voltage system and only a portion of the particles analyzer functioned. Therefore the integration of this experiment was somewhat limited, but it did permit completion of the subsatellite assembly and integration on April 2. At this time the fields experiment was also changed, with experiment S/N 001 being replaced by experiment S/N 003. In parallel with this integration activity the thermal instrumentation was installed.

On completion of an integrated system test the Qualification subsatellite was installed in the 30 foot solar-thermal-vacuum chamber and the thermal proof phase of the qualification solar-thermal-vacuum test started. This test was aborted on the third day when the temperature data indicated unsatisfactory thermal conditions within the subsatellite.

When the subsatellite was removed from the thermal-vacuum chamber the post test inspection showed small pools of oil on the top surface of the subsatellite. Further inspection indicated that the oil had apparently come from the boom damper assemblies. These assemblies were subsequently removed from the subsatellite and sent to an engineering test laboratory for further investigation. The investigation confirmed the damper leakage and recommended a modification to the damper assembly. This modification was made, the damper assemblies retested, and on verification of the leak test results the assemblies returned to the subsatellite.

In parallel with this work the qualification battery was removed from the subsatellite and reworked to incorporate modifications that provided the capability to monitor, via "hardline", the battery temperature and the shunt curves. Also, the experiment was removed from the subsatellite and returned to the respective vendor for rework; the fields experiment for a tuning modification and the particles experiment for incorporation of a working high voltage power supply.

The qualification subsatellite remained inactive for a period while further thermal proof tests were performed on the Flight 1 subsatellite. As a result of these tests, major thermal modifications were made to the qualification subsatellite to correct its thermal design. At the same time the reworked battery and particles experiment were reinstalled in the subsatellite. However the rework on the particles experiment had been unsuccessful and the high voltage power supply was still inoperative. Also, as the fields experiment was at

this time still undergoing retest, a "dummy" experiment, representative as a thermal model, was installed in its place in the subsatellite.

During May the reassembly of the qualification unit subsatellite was followed by the installation of thermal instrumentation, the performance of a limited functional test, and finally installation into the 30 foot chamber for a repeat test of the thermal proof phase of the qualification thermal-vacuum test.

The thermal proof test was discontinued after the performance of only eight orbits and an extended eclipse where the data showed that the thermal design modifications had been successful in correcting the earlier thermal problems. The subsatellite was then removed from the chamber and the particles experiment and "dummy" fields experiment removed from the subsatellite.

When the reworked and retested fields experiment (electronics S/N 003 and sensor S/N 005)were received back from the vendor they were reinstalled in the subsatellite and the assembly closed-up, "bagged", and mounted horizontally in the NAR fit check tool for the performance of a special battery service test. The test was to establish the likely temperature margin available in the SIM Bay when the battery is being charged and discharged in that location. The results of this test indicated that provisions should be made to ensure a flow of cool dry air in the SIM Bay to keep the subsatellite cool during battery servicing.

The formal qualification test program began when a particles experiment (S/N2-2)with a working high voltage power supply was finally received. When this experiment was installed and integrated, the fields experiment was also fully integrated, functional testing completed, power profile measurements and telemetry calibrations repeated, and the subsatellite closed-out. During the close-out the vibration instrumentation was installed and final minor thermal modifications made to "trim" the thermal design for the required orbital temperatures. However, prior to the close-out it was found that the magnetometer Bp axis inflight-calibrate circuit was not functioning and the electronic unit had to be returned to the vendor for repair. This was accomplished the same day, as the problem was found to be the fault of a cold solder joint.

On completion of this work an integrated systems test was performed on the subsatellite, then the subsatellite was moved to the engineering test bay for a pre-vibration measurement of the balance boom position. This was followed by a 3-axis acceptance level vibration test, during which the Z-axis had to be performed twice to resolve instrumentation problems with the micro-switch monitors.

After the completion of the acceptance vibration test a limited functional test was performed. When the data from this test was verified as good the subsatellite was exposed to a further 3-axis vibration, this time to qualification levels. This test was also followed by a limited functional test, and then the positions of the balance booms again measured to verify that they maintained their position within the allowable tolerance, in spite of exposure to prolonged vibration levels.

During the post-vibration measurement of the deployed balance boom positions it was found that the vibration test had caused damage to the boom retaining bracket. But as the bracket was not damaged to the point of causing a premature boom release it was not considered a failure. However, further investigation was continued in the problem, including a special vibration test with the mass model subsatellite.

While the investigation continued on the mass model subsatellite, the qualification subsatellite was thermally instrumented and installed in the 30 foot chamber for the start of the qualification solar-thermal-vacuum test. This test ran, at vacuum, for over 200 hours and was very successful, with no problems being experienced and the particles experiment high voltage power supply remaining stable throughout the test.

The qualification test program was completed with the performance of the final integrated systems test. This test was also successful and a review of the data showed the subsatellite to have met the requirements of the qualification test program.

Key events in integration and test of the qualification unit P&F Subsatellite were:

| Date | Event |
|---|---|
| 25 November | Received Qual spacecraft structure from manufacturing |
| 2 December | Disassembled structure per HC-21M-01 NC. |
| 4-13 December | Partial assembly and integration in preparation for MSFN testing. |
| 13-16 December | Performed engineering run on procedure HC-21S-01. |
| 17 December | Shipped partially assembly qualification spacecraft to MSC Houston for MSFN compatability test. The spacecraft contained an engineering model PES, and did not contain the DSU, FES or Battery Assembly. |

| Date | Event |
|---|---|
| 18-31 Dec. | Engineering MSFN Compatability Tests at MSC |
| 4 Jan. | Shipped Spacecraft to KSC |
| 5-6 Jan. | Performed Engineering Test of TCP-KL-6007-LMID |
| 6 Jan. | Spacecraft Returned to TRW |
| 12 Jan. | Installed DSU S/N 001 |
| 12-15 Jan. | Performed Engineering Run of HC-21S-01 |
| 18 Jan | Installed Battery Assembly S/N 004 |
| 2-11 Feb. | Performed Engineering Run of HC-21S-01 |
| 12-15 Feb. | 60 Hour Thermal/Vacuum "Bake-Out" of Spacecraft for Outgassing |
| 2 March | Install Battery S/N 001 |
| 4 March | Install Engineering Model PES |
| 4 March | Install FES S/N 001 |
| 9 March | Start Test Procedure HC-21S-01A |
| 22 March | Replace Antenna S/N 001 by S/N 003 |
| 24 March | Install Wobble Damper S/N 004 |
| 25-26 March | Perform Engineering Compatability Check out of Thermal Vacuum (Mfg - Non Functional) |
| 26 March | Remove FES S/N 001 for RTV Mods |
| 30 March | Remove Engineering Model PES |
| 31 March | Install FES S/N 003 |
| 1 April | Installed PES S/N 1-1 (non-flight, HV-Inop) |
| 1-2 April | Performed Remainder of HC-21S-01A |
| 3-4 April | Performed Engineering Run of HC-21S-04 (Mfg. Test) |
| 4-8 April | Performed Qual T/V HC-21S-06 Thermo Phase (Eng. Test) |
| 8-9 April | Performed Solar Array Evaluation with S/S in T/V (non-op) |
| 29 April | Install Modified Booms |

| Date | Event |
|---|---|
| 5-6 May | Perform Engineering Run on HC-21S-05A (Mfg. Test) with Non-Flight, HV-Inop PES S/N 1-1 |
| 6-8 May | Perform Thermo Phase HC-21S-06 (Eng. Test) |
| 10 May | Remove PES S/N 1-1 |
| 13-14 May | Perform Engineering Run on HC-21T-03 (Mfg. Test) Without PES |
| 15 May | Install Operative PES S/N 2-2 and Started Formal Test Program on Qualification Unit Spacecraft |
| 15-17 May | Performed HC-21S-01B |
| 17-18 May | Performed HC-21S-04D |
| 18 May | Performed HC-21S-02NC |
| 18 May | Performed HC-21M-02NC |
| 19 May | Performed 3 Axis Acceptance Vibration HC-21A-01B |
| 19 May | Performed HC-21S-05A |
| 19, 20 May | Performed HC-21Q-01NC |
| 20 May | Performed HC-21S-05A |
| 20 May | Performed HC-21S-02NC |
| 21-30 May | Performed Solar T/V HC-21S-06BL |
| 31 May | Performed HC-21S-04D |
| 31 May | The Qualification Program is Completed |

## 7b. FLIGHT 1 TEST HISTORY

The Flight 1 spacecraft structure was received from manufacturing November 25, 1970. The structure was disassembled per HC-21M-01 on December 2, and then EO "A5" was incorporated into the -2 platform to facilitate the new battery configuration.

Assembly and integration of this subsatellite commenced on 11 January. All available units were integrated, which included the "breadboard" particles experiment power supply, an engineering model sun sensor, and the engineering model battery, but excluded the particles and fields experiment. This build-up permitted the performance of preliminary functional tests, which were completed on 3 February. Following this, the subsatellite was disassembled to accomplish rework of the equipment platforms. This rework consisted of filling the platform edges with epoxy to provide solid faces, and drilling vent holes in these faces to permit venting of the honeycomb structure.

During February the separation harness and microswitch assembly was installed and a "fit check" made with the solar array assembly. Further modifications were made to the main electrical harness to monitor the battery temperature and shunt buss current. Mechanical work performed on the subsatellite consisted of "shaving" protruding platform inserts and installing other inserts in the upper and lower platforms to accomodate the attachment of balance weights.

This subsatellite was also "baked" for over 60 hours starting February 13 to help reduce possible contamination from outgassing materials.

After the "bake" test the Flight 1 subsatellite was reassembled and used for engineering tests on various power system anomalies (oscillation and instability) seen on the Qualification subsatellite during its test program. No problem was found on the Flight 1 system and subsequently the problems on the Qualification system were traced to test condition constraints. During this period of time, "blown" transistors were found in the engineering model battery circuit boards. this problem was also found on the Qualification battery and was eventually traced to battery bench test grounding problems.

Integration continued after this test on Flight 1 when the sun sensor and fields experiment became available for installation. This continued integration was likewise performed with "breadboard" particles experiment power supply installed in the subsatellite.

During April power profile measurements, power system calibrations, and magnetometer system checks were performed and battery charging operations verified using the Flight #1 subsatellite with the breadboard PES installed.

While awaiting delivery of the particles experiment and the Flight #1 battery the thermal modification resulting from the thermal proof test on the qualification subsatellite were installed.

When the particles experiment (S/N 2-2) was delivered the high voltage power supply was inoperative, however, this did not prevent it from being integrated in accordance with the procedure. The Flight #1 battery (S/N 005) was also integrated at this time and was found to have the shunt current monitor and battery temperature monitor wired incorrectly. This was reworked by reversing the respective pin connections. The incomplete sections of the integration procedure were completed at this time and telemetry calibrations and system functional testing begun. Also, the power profile measurements were rechecked.

The formal acceptance test program now started with a DCAS inspection of the subsatellite prior to its closeout with the installation of the solar panels. This was followed with the first integrated systems test, which, because of a failure with the laboratory airconditioning, had to be interrupted to allow the subsatellite battery to cool after it had reached its allowable temperature limit. The ambient temperature at this point had reached approximately 85°F.

On completion of the integrated systems test the subsatellite was mated to the Flight #1 launcher assembly, fit checked with the NAR tool, and mounted on the vibration table. The subsatellite completed its three axes acceptance level vibration with no problems evident, other than fixture mating difficulties.

Following a post-vibration limited functional test the subsatellite was demated from its launchers, further thermal taping modifications made, and the thermal test instrumentation installed.

Instead of performing only the acceptance phase of the solar-thermal-vacuum test on the Flight #1 subsatellite, it was agreed between TRW and MSC, to expose it first to the thermal proof phase to determine the effectiveness of the new thermal system modifications. Four orbits in each of the -Cos, + Cos, and Normal Inclination configurations were planned, but as the test progressed it became necessary to increase the number of orbits to eight for each configuration, to allow the subsatellite to thermally stabilize. However, during the fourth orbit of the Normal Inclination phase (twentieth orbit in the test) it was observed that the magnetometer boom was bent.

At this point it was decided to terminate the Normal Inclination orbits and to abort the test on completion of the extended eclipse. This was done and after chamber pump-up the failed boom was examined, then removed from the subsatellite, and subsequently found to have melted at the point of failure.

As a result of this failure, and further errors in the predicted versus test temperatures, resulting from the test, further thermal modifications were made to the subsatellite. The thermal instrumentation was increased on the replaced magnetometer boom and all booms jacketed with a mylar blanket. The subsatellite was again installed in the 30 foot thermal-vacuum chamber and again exposed to thermal proof phase tests. After seven orbits had been completed in the +Cos inclination configuration and two orbits had been completed in the Normal inclination configuration, it was decided that the thermal design was now correct for those configurations and that the extended eclipse could begin.

On completion of the extended eclipse the test was terminated and after the post-test checks were completed the S/N 2-2 particles experiment was removed from the subsatellite and returned to the subcontractor (ATC).

While awaiting delivery of a new particles experiment (with an operative high voltage power supply) a special battery check was made to verify battery charge procedure HC-21T-02. Also during this time further small thermal modifications were made to "trim" the system to the most current predicted temperature requirements.

During the integration of the new particles experiment (S/N 2-3) it was observed that the current being drawn from the particles experiment on +7.8V line was approximately 40% greater than that recorded during the initial integration. Subsequent investigations traced the problem to a failed accumulator circuit in the digital electronic unit (DEU S/N 002). The defective unit was removed from the subsatellite and replaced by the Flight 2 unit (S/N 003).

On completion of the integration of the particles experiment and the DEU, the power profile measurements, telemetry, calibration, and data system functional checks were repeated. Following this the subsatellite was prepared for another integrated systems test. However, this test was aborted when it was found that the flight battery (S/N 005) had an operational buss of approximately 11.6V (compared with approximately 13.2V on the Qualification battery) and could not tolerate operating in an almost fully charged state in the integrated systems test configuration without tripping the under-voltage circuit (11.0V). Further tests were performed on the battery/power subsystem, and after much discussion concerning the battery operating points, it was agreed that the test could be best performed with the battery in a partially discharged state. This was done, and the integrated systems test completed successfully; although some difficulty was experienced with the flux tank test set-up;

and once again the test was also interrupted to allow the battery to cool after it had reached its temperature limit.

After a lengthy data review the subsatellite and launcher were mated, aligned with the NAR tool, and installed on the vibration table. However, after only one vibration run, in the x-axis, direction was received to discontinue the test and to remove the particles experiment from the subsatellite for rework, to replace a zener diode. This was done, but before rework commenced on the experiment, direction was again received, this time to continue with the test and not to rework the experiment. Therefore the experiment was reinstalled in the subsatellite, functionally checked; and the subsatellite reinstalled on the vibration table. After a repeat of the post-x-axis functional test the acceptance vibration test continued for the Z and Y axes.

On completion of the vibration and limited functional tests the subsatellite was demated from the launcher and prepared for the acceptance thermal vacuum test. During these preparations a special battery capacity check was performed. Using the fully powered subsatellite as the load, the systems was left operating at a nominal current of approximately 2 amperes until the under-voltage circuit tripped. The elapsed time was recorded and totaled 6 hours and 10 minutes.

The acceptance solar-thermal-vacuum test, the first with an operating high voltage system in the subsatellite, was very successful. However, one extra high temperature soak was added to the end of the test sequence to verify that a data anomaly observed in the first high temperature soak was not a result of the high temperature environment but was the result of a data system operational sequence constraint. This anomaly was conclusively demonstrated later in a special data system operation test, when it was shown that if a Telemetry Store Fast command is sent to the subsatellite while the data system is in Telemetry Store Normal in the automatic cycle mode, it will knock the sub-com counter out of sequence.

After the acceptance thermal-vacuum test the particles experiment was removed from the subsatellite, reworked and retested for the Zener diode change. It was then reintegrated into the subsatellite, a limited functional test performed and the subsatellite transported to the TRW magnetic test facility at Malibu.

At Malibu, the subsatellite was checked for operational stray fields, 25 gauss magnetized, and 50 gauss demagnetized conditions. The test results from these tests show that the subsatellite meets all of the magnetic specification requirements.

After the magnetics tests the subsatellite was prepared for the final integrated systems test. During these preparations two fuses were replaced in the battery system, these had been found to be "blown" prior to the shipping of the subsatellite to Malibu. After replacing the fuses the battery was charged for several hours and then the final integrated systems test commenced. This test was also completed successfully, and after a careful review of the test data the subsatellite was moved to the alignment test area.

The final subsatellite opertions consisting of alignments, mass properties measurements, subsatellite/launcher mating, and final battery servicing were perormed and the Flight 1 Acceptance Test Program completed.

The subsatellite was shipped to KSC on Saturday, 29 May 1971.

Key Events in integration and test of the Flight 1 Subsatellite were:

| Date | Event |
|---|---|
| 25 Nov. 1970 | Received s/c structure from manufacturing |
| 2 Dec. | Disassembled structure per HC-21M-01 |
| 11-19 Jan. 1971 | Assembly and integration of spacecraft |
| 20-26 Jan. | Engineering run of procedure HC-21S-01 (mfg. test) |
| 13-15 Feb. | 60 hour therma/vacuum "bake-out" of spacecraft for outgassing |
| 25 Feb. | Engineering run of HC-21S-01A |
| 10 March | Install antenna S/N 002 |
| 26 March | Start second engineering run of procedure HC-21S-01A |
| 31 March | Install Sun Sensor S/N 001 |
| 12 April | Completed Engineering run on HC-21S-01A (Mfg. test) |
| 15 April | Installed Wobble Damper S/N 002 |
| 17 April | Installed PES S/N 2-2 with inoperative high voltage |
| 16-19 April | Performed HC-21S-01B |
| 20 April | Performed HC-21S-04B (IST) |

| Date | Event |
|---|---|
| 21 April | Performed Rigging HC-21M-02 N/C |
| 21,22 April | Performed Acceptance Vibration HC-21A-01B |
| 22 April | Performed Limited Functional HC-21S-05 A1 |
| 23 April | Performed De Rigging Hc-21M-02 N/C |
| 23-27 April | Performed Solar T/V HC-21S-06 N/C |
| 27-29 April | Reworked Booms |
| 29 April | Incorporated Thermo Mods |
| 29 April | Started Solar T/V Re-Test for Booms |
| 1 May | Completed Extended Eclipse and Effort on HC-21S-06 NC |
| 2 May | Removed Particles Experiment S/N 2-2. |
| 7 May | Installed Particles Experiment S/N 2-3 (first fully operative PES) |
| 7, 8 May | Performed HC-21S-01B |
| 9-11 May | Performed HC-21S-04C |
| 11 May | Performed Mating per HC-21M-02 |
| 12 May | Started HC-21A-01C1 but Aborted Test for PES S/N 2-3 Removal |
| 13 May | Reinstalled PES S/N 2-3, No Rework Performed |
| 13 May | Performed HC-21S-01B |
| 13 May | Restarted and Completed HC-21A-01C1 |
| 13 May | Performed HC-21S-05A |
| 13 May | Performed Demating Per HC-21M-02 |
| 14-19 May | Performed HC-21S-06A (Solar Thermal Vacuum) |
| 19-20 May | Reworked PES S/N 2-3 With Diode Replacement |
| 21 May | Performed HC-21S-01C1 |
| 21 May | Performed HC-21S-05A |
| 21,22 May | Performed HC-21K-01A at Malibu |
| 23 May | Performed HC-21S-04D |
| 24 May | Performed HC-21S-02NC |
| 24-26 May | Performed HC-21S-03B1 |
| 27 May | Performed HC-21T-03NC |
| 28 May | Performed HC-21M-01A2 |
| 28 May | Performed HC-21M-02NC |
| 28 May | Government Inspected and Accepted |
| 29 May | Shipped to KSC |

## 7c. FLIGHT 2 TEST HISTORY PHASE I (11/25/70 - 7/26/71)

The spacecraft structure was received from manufacturing November 25, 1970. Between December 2 and March 12 limited work was done on the structure and solar panels in preparation for mechanical and electrical assembly. The honeycomb platform edges were epoxy filled and drilled and inserts were installed in the upper and lower platforms to accommodate the attachment of mass balance weights. Also, the lower platform and adapter ring were assembled in preparation for mechanical and electrical assembly.

Approximately June 2 when work was completed on the Flight #1 and Qualification subsatellies integration commenced on the Flight #2 unit. The transponder, command decoder, subsatellite electronics unit, digital storage unit, sun sensor, magnetometer electronics, main electrical harness, and wobble damper were installed and the partial assembly placed in a thermal vacuum chamber for a "bake" test . This "bake" test consisted of exposing the subsatellite units for 60 hours to an environment of 140°F $\pm$5 in a vacuum of 5 x $10^{-5}$ torr, to out-gas unapproved materials. The booms and solar panels were "baked" in a separate and earlier test.

On completion of the "bake" test the digital electronics unit and the "breadboard" particles experiment power supply were installed in the subsatellite and electrical integration started. During the integration of the battery and magnetometer a special tape recording was made of the fields experiment output. This tape recording was delivered to UCLA.

When the particles experiment S/N 2-4 was received on July 3 the integration was completed and system functional tests performed. Following this the solar panels were installed, subsatellite closeout performed, and the integrated system test performed to commence the formal acceptance test program for Flight #2.

On completion of the integrated systems test the subsatellite was mated to its launcher and the complete assembly exposed to a 3-axes acceptance vibration test sequence. The subsatellite was then demated from the launcher, thermal instrumentation and test cables were installed, and the subsatellite installed in the 30foot solar-thermal vacuum chamber.

Following a comprehensive 7 day solar-thermal-vacuum acceptance test the subsatellite was transported to the TRW Magnetic Test Site at Malibu. Here it underwent stray magnetic field measurement and demagnetization. After this it was put through the final integrated systems test and finally aligned, balanced, weighed and moments of inertia and position of center of gravity determined.

During the first integrated systems test it was found that the accumulator channel #4 in the DEU did not show any counts lower than 256; during the solar-thermal-vacuum test and the second integrated systems test it was found that channel #6 in the DEU showed excessive counts from the PES telescope when "calibrate" and "test control" modes were activated; also, during the installation and checkout of the subsatellite in the solar-thermal-vacuum chamber two fuses in the battery/test connector interface were blown. Special tests were performed to verify these

discrepancies and a decision was made to complete final preparation of the subsatellite as a back-up subsatellite for Flight #1 and to remedy these problems after the launch of Apollo 15.

A review of all the acceptance test data verified satisfactory performance of the Flight #2 subsatellite (with the noted discrepancies) and showed it to have successfully completed the acceptance test program.

The subsatellite was given a "conditional acceptance" as a back-up for the launch of the Apollo 15 on July 26, 1971.

FLIGHT 2 SPACECRAFT TEST HISTORY
PHASE 2 (7/27/71-2/29/72)

| | |
|---|---|
| 28 July 1971 | The DEU was tested while installed in the spacecraft and it was verified that two accumulator channels were not operating in the low count range. The DEU was subsequently removed for unit level trouble shooting and repair. |
| 20 September | As a result of the problems noted during spacecraft testing regarding the test control function in the PES, trouble shooting commenced on the above date. During unit level testing a major problem occurred and the unit was subsequently returned to ATC for repair and rework. |
| 22 September | The magnetometer was removed for engineering modifications. The modifications consisted of doubling the magnetometer sensitivity. The subsatellite was placed in the refrigerator for storage and refrigeration. |
| 27 October | The magnetometer, S/N 002, was reinstalled into the spacecraft. The DEU S/N 002 was also reinstalled into the spacecraft. |
| 1 November | The PES, S/N 2-4, was installed in the spacecraft. The new thermal tape was used to cover the curved plate analyzer exposed areas. |
| 6 November | The IST was performed on the spacecraft denoting that the subsatellite was in a completely assembled configuration ready for acceptance level testing. |
| 10 November | The subsatellite was installed on the shake table for acceptance level vibration testing. Only the Y axis acceptance vibration was performed. |

| | |
|---|---|
| 15 November 71 | The subsatellite was installed in the 7 x 12 foot thermal vacuum chamber and the S/C thermal vacuum was started On the morning of 18 November the thermal vacuum chamber lost vacuum causing major electronic circuit damage to the subsatellite. Subsequent testing revealed malfunctions in the following units; PES, DEU, and CDU. In addition the following units were also removed for limited unit level acceptance testing; the transponder, magnetometer, DSU, and SEU. |
| 30 November | The subsatellite consisting of only the battery assembly was placed in cold storage. |
| 22 December | All units with the exception of the particle experiment were reinstalled in the subsatellite. |
| 29 December | Installed PES S/N 2-2 in the subsatellite. Reintegrated all subsatellite units. |
| 1 January 72 | The integrated systems test was performed on the Flight #2 subsatellite. |
| 2 January | Vibration level testing was performed on the subsatellite. Only the Y-Y axes acceptance level vibration was performed. |
| 6 January | The subsatellite was installed in the 30 ft. thermal vacuum chamber for solar thermal vacuum testing. |
| 7 January | High voltage was turned on and the high voltage was observed to be malfunctioning, therefore high voltage was turned off. The satellite high voltage system was allowed to soak in a hard vacuum for a 24 hour period. Upon turning the high voltage on again the abnormal condition still existed. At this point, the solar thermal vacuum test was aborted. |
| 10 January | The PES, S/N 2-2, was removed from the subsatellite for unit level testing in a vacuum chamber. |

19 January 72 PES, S/N 2-4, was installed in the subsatellite and reintegrated per procedure HC-21S-01B.

20 January The IST was performed on the subsatellite. A vibration test was not performed because:

1) Removal and installation of the PES is a minor mechanical operation.
2) Flight 2 subsatellite had 3 previous vibration tests.
3) PES S/N 2-4 was given a full 3 axis vibration test just prior to installation.

21 January The subsatellite was installed in the 30 ft. solar thermal vacuum chamber. Solar thermal vacuum testing commenced on 1/21/72.

23 January The solar thermal vacuum testing consisted of:

1) High temperature soak and functional
2) Low temperature soak and functional
3) High temperature soak and functional
4) Low temperature soak and functional
5) 14 normal orbits

28 January Thermal vacuum testing was successfully completed with no subsatellite anomalies.

29 January The subsatellite and supporting test equipment was transported to the Malibu test site for stray magnetic field measurement and demagnetization.

30 January The last IST was performed on the subsatellite.

31 January The battery was charged and discharged. The battery capacity was determined to be 10.9 ampere hours. No measurable degradation in the battery capacity was indicated.

| | |
|---|---|
| 1 February 1972 | Final adjustments to the subsatellite were performed beginning on 1 February. These included:<br>1) Final mechanical preparation<br>2) Alignment<br>3) Mass properties testing<br>4) Weighing and balance of the subsatellite<br>5) Mating subsatellite and launcher<br>6) Fit Check - NAR interface<br>7) Final functional consisting only of a limited battery charge and discharge<br>8) Preparation for shipment |
| 6 February 1972 | Flight 2 Subsatellite Shipped to KSC |
| 29 February 1972 | Final trim weights on Flight 2 subsatellite changed per ECP 039 at KSC. |

Key events in the integration and test of the Flight #2 Subsatellite are as follows:

| Date | Event |
|---|---|
| 25 Nov. 1970 | Received spacecraft structure from manufacturing |
| 3 June 1971 | Installed subassemblies |
| 4 June 1971 | Performed engineering bake-out thermo/vacuum |
| 8 June 1971 | Installed DEU and breadboard PES power supply |
| 1 July 1971 | Performed engineering run on integration and functional test |
| 3 July 1971 | Installed PES S/N 2-4 |
| 4 July 1971 | Completed integration of spacecraft |
| 5 July 1971 | Performed IST |
| 7 July 1971 | Performed 3-axis acceptance vibration |
| 7 July 1971 | Performed limited functional |
| 8-16 July 1971 | Performed T/V (30 ft chamber) |
| 17 July 1971 | Performed magnetic test at Malibu |
| 18 July 1971 | Performed IST |
| 22 July 1971 | Completed mechanical alignments and mass property measurements. |
| 23 July 1971 | Flight 2 spacecraft placed in shipping container as back-up for Flight 1 spacecraft. |
| 28 July 1971 | DEU removed from spacecraft |
| 20 Sept. 1971 | PES 2-4 removed from spacecraft |
| 22 Sept. 1971 | FES removed from spacecraft |
| 27 Oct. 1971 | FES S/N 002 and DEU S/N 002 installed in spacecraft |
| 1 Nov. 1971 | PES 2-4 installed in spacecraft with modified analyzer thermal tape. |
| 6 Nov. 1971 | IST performed |
| 10 Nov. 1971 | 1-axis vibration performed |
| 15 Nov. 1971 | T/V (7x12 foot) chamber failure |
| 30 Nov. 1971 | Spacecraft completely disassembled except for battery |
| 22 Dec. 1971 | All units except for PES reinstalled in spacecraft |
| 29 Dec. 1971 | PES 2-2 installed |

| Date | Event |
|---|---|
| 1 Jan. 1972 | IST Performed |
| 2 Jan. 1972 | 1-axis vibration test performed |
| 7 Jan. 1972 | T/V (30 foot chamber) high voltage spacecraft failure |
| 10 Jan. 1972 | PES 2-2 removed from spacecraft |
| 19 Jan. 1972 | PES 2-4 installed in spacecraft |
| 20 Jan. 1972 | IST performed |
| 28 Jan. 1972 | T/V test (30 foot chamber) completed |
| 29 Jan. 1972 | Magnetic test performed at Malibu |
| 30 Jan. 1972 | IST performed |
| 31 Jan. 1972 | Battery charged and discharged |
| 5 Feb. 1972 | Final alignment and mass properties performed |
| 6 Feb. 1972 | Flight 2 spacecraft shipped to KSC |
| 29 Feb. 1972 | Trim weight change at KSC |

## 8. KEY MEETING SUMMARIES

The customer review meetings which are perhaps the most important held during the P&F program are listed below and summarized in the following paragraphs. Other particularly important meetings included the monthly customer review meetings which were held at TRW.

| Date | Meeting |
|---|---|
| 5/14-15/70 | P&F System PDR |
| 7/14-15/70 | P&F System CDR |
| 8/4-5/70 | PES CDR |
| 3/8-12/71 | Qualification Unit Phase One C.A.R. |
| 4/6-7/71 | Flight #1 Phase One C.A.R. |
| 5/7/71 | PES Flight #1 C.A.R. |
| 5/26-28/71 | Flight #1 Phase Two C.A.R. |
| 6/21-24/71 | Flight #2 Phase One & Qualification Unit Phase Two C.A.R. |
| 6/29-30/71 | PES Flight #2 C.A.R. |
| 7/21-22/71 | Flight #2 Phase Two C.A.R. |

### P&F System Preliminary Design Review (PDR)

The Preliminary Design Review for the Particles and Fields Subsatellite program was held at TRW on May 14 and 15 of 1970. During this meeting the design approach and the system end item specification were thoroughly reviewed and approved with the exceptions noted in the meeting minutes. The resulting detailed design was to be reviewed at the Critical Design Review (CDR). Detailed review of the GSE was not included in this meeting but was to be performed at the June Monthly Management Meeting. Also the detailed design approach for the scientific instrumentation was not reviewed because of the earlier status of these subcontracts and because these subcontracts were not yet signed. However, the baseline for the design of the scientific instruments was reviewed. Exceptions and action items identified or defined in this design review meeting are formally recorded on Review Item Disposition (R.I.D.) forms or as formal action items, with minor action items simply included as items in the meeting minutes. During the meeting on 15 May, MSC announced that the basic P&F contract had just been signed.

Particles Experiment Subsystem PDR

The Particles Experiment Subsystem Preliminary Design Review (PDR) was held on June 4 and 5, 1970, at the ATC Facilities in Pasadena. The principal purposes were to review the design approach to the Particles Experiment Subsystem as currently configured, and to provide an opportunity for NASA, University of California, TRW, and ATC to reach agreement on an acceptable set of Specifications to be included in the final PES subcontract. Forty (40) RID's were generated during this PDR.

Fields Experiment Subsystem PDR

The preliminary design review for the Fields Experiment Subsystem was held at Time-Zero Corporation on 18 June 1970 at the time of this meeting the status of the magnetometer electronics design and breadboard fabrication was such that the design breadboard has been built and operated, and the deliverable breadboard is in fabrication now. Ten RID's were prepared, of which six were approved. The remaining four contained cost and schedule impact items and required further consideration by Time-Zero. A suspense date of 26 June 1970 was set for action on the four RID's.

P&F System Critical Design Review (CDR)

The Critical Design Review (CDR) for the Particles and Fields Subsatellite Program was held at TRW on July 14 and 15. During this meeting the detailed design of the satellite and its GSE except for the scientific instrumentation were thoroughly reviewed and approved with the exceptions noted in the meeting minutes and approval was given for proceeding with fabrication. The detailed design of the scientific instrumentation would be reviewed at its CDR's in about two weeks. The requirements for the scientific instruments were reviewed in this meeting.

Key documents reviewed in detail by MSC during this meeting included the End Item Specification on the flight hardware, SY1-36B, and the Battery Charger/Simulator EQ3-287B, and considered them approved with the exceptions as noted on RID's and action items. Also reviewed were the Quality Assurance Plan #16763-33B, Reliability Plan #16763-34A, the Configuration Management Plan #16763-35, System Safety Plan #16763-36, Electromagnetic

Compatability Control Plan #16763-37-1, Magnetic Cleanliness Control Plan #16763-38, the Development Schedule, Development Test Plan #16763-19, Certification Plan #16763-18, Parts and Materials List #16763-44, FMEA #16763-14, and the Experiment Support Requirements document #16763-31. The Command List #16763-41, and the Measurement List #16763-40 were also reviewed and were approved.

Props for this CDR included a full-scale, three dimensional mock-up used to illustrate the feasures of the mechanical system including the current spacecraft packaging and boom configuration, the full scale antenna range metal mockup, and sample sections of the solar array configuration. A number of tours were conducted for the visitors with one including operation of the DEU breadboard. The general meeting plan provided for a single central main meeting during the morning of July 14 which was followed by ten parallel team meetings for detailed work. Following this was the formal CDR Board meeting for summation and disposition of action items and RID's.

Fields Experiment Subsystem CDR

The Critical Disign Review for the Fields Experiment Subsystem (FES) was held at Time-Zero Corporation on 29 July 1970. The program status was that the breadboard is in temperature testing, 90% of all parts are in-house and screening of these parts will begin no later than Monday, 3 August 1970. Nine RID's were prepared during this meeting.

Particles Experiment Subsystem CDR

The Particles Experiment Subsystem Critical Design Review (CDR) was held on August 4 and 5, 1970, at the ATC facilities in Pasadena. The primary purposes of this meeting were to review the instrument design in detail, and plans for implementation thereof; and to resolve any questions or objections to the instrument design and/or specification in order to establish a baseline for proceeding with fabrication of the Qual Unit. Required actions resulting from the CDR were defined in formal action items and RID's.

## QUALIFICATION UNIT PHASE ONE ACCEPTANCE REVIEW (C.A.R.)

An acceptance review of the Qualification Unit Particles & Fields Subsatellite black boxes and the Ground Support Equipment was conducted March 8 through 12, 1971 at TRW. With the exception of the Particles Experiment Subsystem, Black Box Data Packages for the qualification subsatellite were reviewed and corrections to the Data Packages were defined, and the flight subsatellite design as defined by the engineering documentation was frozen. The spacecraft level test procedures were baselined and approval was given for proceeding with subsatellite spacecraft level qualification testing. The Subsatellite GSE, and Acceptance Test Equipment Data Packages were reviewed and conditionally accepted pending a demonstration that the test equipment performs satisfactorily when coupled to the flight hardware. Approval was given to procede with spacecraft level testing with the GSE and Acceptance Test Equipment.

## FLIGHT #1 PHASE ONE ACCEPTANCE REVIEW

An Acceptance Review of the Flight #1 Particles and Fields Subsatellite black boxes was conducted April 6 and 7 1971 at TRW and approval was given for proceeding with Flight #1 subsatellite spacecraft level testing. The Particles Experiment Subsystem (PES) was not included in this Acceptance Review due to a high voltage problem.

The Flight 1 Spacecraft level Acceptance Test Plan was reviewed with the following approved recommendations:

1) Start acceptance testing with the qualification PES and qualification battery. The Flight #1 battery will be installed prior to the final integrated system test.

2) The qual (refurbished) magnetometer will be tested and flown with the Flight 1 subsatellite. The recommendation is pending further stress analysis.

3) Flight 1 PES testing will proceed minus high voltage, if a high voltage failure occurs during acceptance testing.

## PES FLIGHT #1 ACCEPTANCE REVIEW

An Acceptance Review of the Flight #1 Particles and Fields Subsatellite Particles Experiment System (PES) was conducted on 7 May 1971. The Flight #1 PES has S/N 003 constituting the subassemblies having S/N's 2-3. Exceptions to the above are subassemblies of the A4, A1, and A3 Channeltron Decoupler Module and B Telescopes which have S/N's 1-1. The baseline design was frozen as of this review. Approval was given to integrate the Flight #1 PES into the Flight #1 Spacecraft.

## FLIGHT #1 PHASE TWO ACCEPTANCE REVIEW

A final acceptance review of the Flight #1 Particles and Fields Subsatellite was conducted May 26-28, 1971.

The formal review board accepted the serial number 002 Particles and Fields Subsatellite conditionally upon performance of action assigned by the board and upon successful completion of design certification. Two items appeared on the shortage report, unapproved waiver requests HC-W18 and W19. The form DD250 was signed. TRW was directed to ship the unit to the Cape on May 29, 1971.

The Flight #1 Particles Experiment Subsystem (PES) (S/N 2-2) contains two analyzers (A1 & A4), the 433 module of the A3 analyzer and two silicone surface barrier detectors which were exposed to qualification level testing in the Prototype (S/N 1-1) instrument. The affects of this testing on these parts is addressed by an ATC Reliability Analysis Report, The board found use of these parts in the Flight I PES Acceptable.

## FLIGHT #2 PHASE ONE & QUALIFICATION UNIT PHASE TWO ACCEPTANCE REVIEWS

A Phase I Acceptance review of the Flight II Particles and Fields Subsatellite was held June 21-24, 1971. All Flight II "black boxes" were covered except the Particles Experiment Subsystem (PES). Review of the data revealed the "black boxes" in question to be acceptable. Flight II failure history was reviewed. Nine failures occurred. All have been closed. The Waiver/Deviations summary showed 3 waivers and 8 deviations granted. None were pending. No RID's were presented. The units under review were found acceptable by the board and approval was granted to integrate them into the subsatellite.

Mr. Johnson, the NASA/MSC P&F Experiment Manager, indicated that the subsatellite level data package for the Qualification Unit has been forwarded to MSC and reviewed there. Based on this review the Qualification Unit Particles and Fields Subsatellite was found acceptable. The DD250 was signed. TRW was directed to place the unit in bonded stores.

## PES FLIGHT #2 ACCEPTANCE REVIEW

The Phase I Acceptance Review for the Particles Experiment Subsystem (PES) only of the Particles and Fields Subsatellite was held June 29th and 30th. Data was reviewed June 29th at Analog Technology Corporation (ATC), Pasadena, California. A formal acceptance board was held June 30th via telecon. Part of the board was at MSC in Houston and Part at ATC in Pasadena. The findings of the data review were presented to the formal board. Unit history was summarized. The Deviation/Waiver review indicated two deviations granted, with none pending. Five failures, one open, were shown in the handout material.
A sixth failure which occurred in the final thermal vacuum test, was presented to the board orally. The board found the Flight II (Serial 2-4) PES would be acceptable for integration into the subsatellite upon 1) completion of the Hazard Circuit change and 2) resolution of the low temperature, high voltage regulation problem.

## FLIGHT #2 PHASE TWO ACCEPTANCE REVIEWS

The Phase II Acceptance Review for the Flight II Particles and Fields Subsatellite was held July 21-22, 1971, at TRW, Redondo Beach, California. A number of technically unacceptable items were identified. These occurred late in the testing program. Repair cycle time made immediate corrective action and use of the unit as a backup to the Apollo 15 unit mutually exclusive. Most probable failure mechanisms, failure propagation mechanisms and flight impacts were investigated at length. The technical review team found the flight impacts acceptable for a backup unit and recommended no repairs be started until after Apollo 15 launch. Four subsatellite level failures were reported; two remain open. Applicable waivers and deviations were listed. Twelve were granted; none pending. The technical data review minutes were reviewed for the board. No RID's were presented. The board deferred consideration of a sectoring logic design change until more data is available. The board agreed that this unit should be held in flight configuration in its present condition as a back-up for the Apollo 15 unit. Thereafter corrective action should proceed. The board found the Flight II Particles and Fields Subsatellite to be acceptable conditional upon 1) Completion of open work items, 2) Resolution of the problems discussed in the meeting minutes.

## FLIGHT #2 PHASE TWO RE-ACCEPTANCE REVIEW I

This meeting was held at TRW on November 4, 1971. It was essentially a review of all open work items before reinitiating a complete reacceptance test cycle.

## FLIGHT #2 PHASE TWO RE-ACCEPTANCE REVIEW II

This meeting was held at TRW from February 1 to February 3, 1972. The formal MSC board accepted the Flight 2 spacecraft.

## 9. FLIGHT #1 IN-ORBIT PERFORMANCE COMMENTS

The P&F Flight #1 Subsatellite was separated from the Apollo 15 CSM in lunar orbit on August 4, 1971 at 1.13 PM PDT. All systems operated satisfactorily. A brief description of performance is provided below.

### ORBIT

The orbit at injection was 75 by 55 nautical miles. Four days later the orbit was 63 miles circular. The orbit is expected to change to 105 by 15 miles within three months. Many unknowns are associated with the orbital changes. The coherent doppler provided by the S-Band Transponder is used to determine orbital parameters. Triangulation (three station tracking) is also being employed.

### COMMUNICATIONS

Tracking and TLM data quality and command link has been excellent during 30' uncooled antennae. Received signal level on 85' antennae is approximately -134 dBm. The Apollo FOD (Flight Operations Directorate) has stated the communications and command system is one of the best they have worked. The subsatellite has consistently responded the first time a command has been sent.

### POWER

The spacecraft power subsystem (solar array/battery/charger) is operating to specification. Typical combinations of operating modes for maintaining power balance is 10 autocycle modes with 1 tracking mode, and 1 charge mode. When maximum is desired the combination is 1 tracking orbit with 1 charge orbit. A tracking orbit is made up of the real time mode when in radio rnage, then memory mode on the backside of the moon, then data dump once radio range is re-established. During autocycle mode the transmitter is on approximately 12 minutes during each 120 minute orbit.

### MAGNETOMETER EXPERIMENT

Average magnetic field measurements have been in the order of 10 gamma, with some intervals (1 to 2 orbit duration) up to 30 gamma. The magnetometer zero crossing system has been working as designed. The sensor has been able to detect vector direction changes. Close correlation has been obtained with magnetometers on the lunar surface.

### PARTICLES EXPERIMENT

All 6 particles detector sensors are working normally and collecting scientific data. The high voltage turn-on was delayed 24 hours as planned to allow the subsatellite to outgas. Turn-on was normal. The range of particles data has been in the order of 0-300 counts/second.

TYPICAL AVERAGE ORBIT PARAMETERS (INITIAL)

| | |
|---|---|
| Spin Speed | 11.85 RPM (12.0 design) |
| Spin Angle Error (initial) | ±0.5° (1.5° design) |
| Wobble | -0 |
| Battery Temperature | 60-75°F |
| Particle Telescope Temperature | 58-68°F |
| Magnetic Sensor Temperature | 62-65°F |

The subsatellite (and Moon) was shadowed by the Earth for 3.5 hours on August 6, 1971. All systems operated normally through the eclipse. The lowest temperatures were about 0°F.

# Apollo 15 Preliminary Science Report: The Particles and Fields Subsatellite Magnetometer Experiment

Paul J. Coleman, Jr.*
Department of Planetary and Space Science
and
Institute of Geophysics and Planetary Physics
University of California
Los Angeles, California 90024

G. Schubert
Department of Planetary and Space Science
University of California
Los Angeles, California 90024

C.T. Russell
Institute of Geophysics and Planetary Physics
University of California
Los Angeles, California 90024

L.R. Sharp
Department of Planetary and Space Science
and
Institute of Geophysics and Planetary Physics
University of California
Los Angeles, California 90024

*Principal Investigator

Publication No. 981
Institute of Geophysics and Planetary Physics

Preprint

September 24, 1971

(Revised September 30, 1971)

68

## Abstract

A preliminary analysis of the data from the UCLA magnetometer on board the Apollo 15 subsatellite indicates that remnant magnetization is a characteristic property of the moon, that its distribution is such as to produce a rather complex pattern or fine structure, and that a detailed mapping of its distribution is feasible with the present experiment. The analysis also shows that lunar induction fields produced by transients in the interplanetary magnetic field are detectable at the satellite orbit and that the magnetometer data will provide estimates of the latitude and longitude dependences in the distribution of interior conductivity. Finally, the analysis indicates that the plasma void or diamagnetic cavity, which forms behind the moon when the moon is in the solar wind, extends to some altitude below the satellite orbit and probably to the lunar surface and that the flow of the solar wind near the limbs is usually rather strongly disturbed.

## 1. Introduction

Magnetic field measurements obtained with the Apollo 12 lunar surface magnetometer and the Apollo 14 hand-held magnetometer have established the existence of a significant lunar remnant magnetization, provided estimates of the distribution of electrical conductivity of the moon's interior, and established an upper limit on the average magnetic permeability of the moon. The objectives of the lunar subsatellite magnetometer experiment are to extend the measurements of the moon's magnetic field, the permanent as well as the induced components, and to study the moon's interaction with the field and charged particles of its environment. Specific objectives include the following: to map the remnant magnetic field of the moon, to map the electrical conductivity of the moon's interior, and to study the properties of the plasmas in cis-lunar space by measuring the magnetic effects of the interactions of these plasmas with the moon. Included in this objective is a search for magnetic disturbances caused by material that leaves the moon by one process or another and is ionized while still nearby. Finally, the magnetometer is part of the instrumentation for the lunar particle shadowing experiment. This experiment and its objectives are described in another paper in this Preliminary Science Report.

The multiplicity of the objectives of the magnetic field study is made possible by the geometry of the moon's orbit which, as shown in Figure 1, passes through three very different regions in near-earth space, i.e., the region in which the solar wind

flow is essentially undisturbed by the presence of the earth, the 'magnetosheath' in which the flow is drastically modified by the obstacle presented by the earth's magnetic field, and the geomagnetic cavity which consists of the space threaded by the magnetic field from the earth. As shown in the figure, this cavity extends to about 10 earth radii in the direction of the sun. Its extent in the opposite direction, i.e., the length of the geomagnetic tail, is unknown, although it is more than 100 earth radii.

The lunar orbiting satellite, Explorer 35, has also yielded a great deal of information on the electromagnetic properties of the moon and its interactions with its plasma environment. Orbits of this satellite for times separated by 6 months are shown in Figure 2. The area traversed by Explorer 35 during a 12-month period is indicated by bounding circles marking the loci of perilune and apolune. Also shown is the orbit of the subsatellite.

When the moon is in the solar wind, the region directly behind the moon, i.e., the region directly downstream from the moon, is essentially devoid of solar wind plasma. This downstream cavity and the rarefaction waves on its boundary, shown schematically in Figure 2, were discovered by Colburn et al. (1967) with the Explorer 35 magnetometer. The sketches in Figures 1 and 2 show the essential difference between the interaction of the solar wind with the moon and that with the earth. Specifically, most of the solar wind that interacts with the moon

simply hits the moon and stops (Figure 2), whereas most of the solar wind that interacts with the earth is diverted around the entire geomagnetic cavity and forms the magnetosheath (Figure 1).

12

## 2. The Magnetometer

The magnetometer system carried on board the Apollo 15 subsatellite consists of two orthogonal fluxgate sensors mounted at the end of a 6-foot boom and an electronics unit housed in the spacecraft. A block diagram of the instrument is shown in Figure 3 and a photograph of the magnetometer hardware is shown in Figure 4. The specifications of the instrument are listed in Table 1.

The two magnetometer sensors are oriented parallel ($B_p$) and transverse ($B_T$) to the spin axis of the spacecraft. The measured quantities used to define the vector field are the magnitudes of the parallel component, the absolute value of the transverse component, and the angle between the transverse component and the component of the sun-spacecraft vector transverse to the spin axis.

An important item of subsatellite equipment is the data storage unit. This unit records field measurements on the far side of the moon for playback when the subsatellite is in view from the earth.

3. Remnant Magnetization

At times of relatively low levels of geomagnetic activity, the magnetic field in the geomagnetic tail is quite constant. Thus, the best possibilities for the detection of lunar remnant magnetism are provided by the subsatellite magnetometer data recorded when the moon is in the geomagnetic tail during quiet intervals. Our preliminary analysis of the quick-look data recorded during the first traversal of the geomagnetic tail revealed the existence of measurable levels of remnant magnetism over much of the subsatellite orbit. Figure 5 shows average values of $B_P$ and $B_T$ computed for nine successive orbits during which the moon was in the geomagnetic tail.

The major features of the structure in the traces are associated with large craters lying within 10° of the band defined by the ground tracks of the nine orbits. The most obvious feature is that apparently associated with the crater Van de Graff, which produces a 1 gamma variation in the field as the satellite sweeps past it. Van de Graff is approximately 9° across and its center is located about 8° from the satellite ground track. Other prominent features of the data are associated with the craters Hertzsprung, Korolev, Gagarin, Milne, and Mare Smythii. It should be kept in mind that the process of averaging over nine orbits effectively filters out variations over latitude and longitude ranges smaller than 5° as well as temporal variations in the earth's tail field. Figure 6 shows the location of the satellite ground track relative to these major craters.

74

The magnetic field measurements used in this preliminary analysis do not include the final pre-flight calibrations. Thus, although the measured variations are accurate, the absolute values may be off by a few gammas. Further, the data processing performed to date has been done entirely by hand and this precluded our determining the orientation of the component perpendicular to the satellite spin axis. However, the preliminary results show that we will be able to obtain a detailed mapping of the lunar remnant magnetization from the subsatellite orbit.

The plot of $B_T$ in the nine-orbit average shown in Figure 5 suggests that the remnant field is weaker on the near side than on the far side and that most of the major craters, with the exception of Gagarin, are associated with local minima in $B_T$. This near side/far side asymmetry leads us to the speculation that the remnant field observed is due to irregularities in a magnetized crust. This crust has been grossly disturbed over a broad region of the near side, possibly by the infall of the bodies which created the ringed maria, but disturbed primarily by more localized crater formation on the back side.

Samples returned from the Apollo 11 and 12 sites show remnant magnetization as great as $10^{-2}$ emu/cm$^3$. If one takes this value as an upper limit on the magnetization of lunar material, then the minimum scale size of a spherical body magnetized at this level and producing a 1 gamma variation at the subsatellite orbit is approximately 10 km. The field at the surface of such a region, and therefore the maximum field that

could be produced by such a region on the surface of the moon, is roughly 1000 gamma. Such a volume would have a magnetic dipole moment of approximately $10^{16}$ gauss $cm^3$. For a more typical remnant magnetization of $10^{-5}$ emu/$cm^3$, the scale size would be 100 km and the surface field would be about 10 gamma for this dipole moment. The data shown in Figure 5 also indicate that any lunar centered magnetic dipole must have a magnetic moment less than $4 \times 10^{19}$ gauss $cm^3$ corresponding to a surface field strength in the range 1.5 to 3 gamma.

A permanent magnetic field of $38 \pm 3$ gamma was detected at the Apollo 12 site with the lunar surface magnetometer (Dyal et al., 1970). Permanent fields of $103 \pm 5$ gamma and $43 \pm 6$ gamma were detected at sites separated by 1.17 km in the Fra Mauro region explored by the Apollo 14 astronauts (Dyal et al., 1971). The lunar subsatellite has passed directly over both these sites, but no significant field variation was observed over either. Thus, the surface fields observed to date must be of relatively small scale size as indicated by the field gradient measured at the Apollo 14 site.

As the altitude of perilune of the subsatellite decreases, we will obtain more information on the fossil fields at the Apollo 12 and 14 sites. As pointed out by Sonett et al. (1971), if both were produced by the same magnetizing field, a field in excess of $10^3$ gamma must have existed some billion years after the formation of the moon, or 3.4 billion years ago, and further, it must have existed for 300 million years, since the magnetized rocks from the Apollo 11 and 12 sites are respectively 3.4 and

and 3.7 billion years old. A detailed map of the permanent magnetization on the moon will provide additional information on the ancient magnetizing field, and the history of the magnetized material subsequent to its magnetization.

77

## 4. Electrical Conductivity

Information on the electrical conductivity of the moon's interior has been obtained through an analysis of simultaneous magnetic field measurements at the Apollo 12 site and at the lunar orbiting satellite, Explorer 35. The results already obtained include the radial conductivity profile that provides information on mantle-core stratification, the temperature of the mantle, the near-surface thermal gradient and heat flux, and the composition of the interior (Dyal and Parkin, 1971; Sonett et al. 1971a, b). The experimental technique employed in these studies is essentially a measurement of the moon's response to changes in the solar wind magnetic field.

Data recorded at the lunar subsatellite during several successive orbits when the moon was in the solar wind are plotted in Figure 7. From the point of view of the conductivity studies, the important feature of these plots is the greater variability of the magnetic field on the day side or upstream side of the moon. The observed behavior shows that the magnetic field measured at the subsatellite when the moon is in the solar wind includes a component due to lunar induction. The pressure of this component indicates that data from the subsatellite magnetometer, along with simultaneous data from the lunar surface magnetometers and Explorer 35 magnetometer, can be used to produce a detailed, three-dimensional model of the interior conductivity. At this writing, the conductivity studies are only just beginning and no further results are available.

78

5. Boundary Layer Studies

Observations of the magnetic field and plasma obtained with the lunar orbiter, Explorer 35, have revealed a fairly consistent picture of the large-scale interaction of the solar wind with the moon. As shown schematically in Figure 2, the absence of a lunar bow shock allows most of the solar wind plasma to reach the lunar surface where it is absorbed. As a consequence of this absorption, a so-called diamagnetic cavity exists behind the moon, or downstream from the moon, when the moon is in the solar wind. The essential magnetic feature of this cavity is an interior magnetic field stronger by about 1.5 gamma, on the average, than the exterior field. At the boundary of this cavity, there is a sharply localized decrease in the field magnitude approximately coincident with the boundary of the moon's optical shadow.

The preliminary analysis of the data from the subsatellite magnetometer indicates that a diamagnetic increase also appears at the lower altitude of the subsatellite. Figure 8 shows a 12-orbit average of the measurements recorded while the moon was in the solar wind. The field enhancement between satellite sunset and satellite sunrise is readily distinguishable and is approximately 1 gamma.

Data from Explorer 35 have also revealed the existence of sporadic field disturbances adjacent to the rarefaction wave at the boundary of the diamagnetic cavity (see Figure 9). Mihalov et al. (1971) have shown that these disturbances in the solar wind flow occur when certain regions of the lunar surface are at the limbs. The greatest concentration of disturbance sources was

found to be in a 15° square near the crater Gagarin.

Our preliminary analysis of the subsatellite magnetometer data indicates that strong disturbances, or limb effects, are present most of the time. These disturbances produce more or less characteristic variations in the subsatellite magnetometer record. Record sections from orbits 183-187 are shown in Figure 7. The data analyzed so far suggest that the disturbances such as those apparent near the sunset line occur when near-side regions are at the limbs as well as far-side regions are at the limb. A 12 orbit average plotted in Figure 8 shows that limb effects at satellite sunrise, i.e., at the sunset limb on the moon, are more persistent than those at the other limb. It remains to be seen whether this persistence is a consequence of this area's being more effective in producing disturbances or some property of the solar wind, such as the orientation of its magnetic field. Thus, on the one hand the detection of relatively strong remnant fields in the vicinity of Gagarin would be consistent with the suggestion of Mihalov et al. that the limb effects detected at Explorer 35 are caused by localized regions of enhanced magnetic fields. On the other hand, the preliminary indication from the subsatellite data that limb disturbances are present more often than not and that they are just as great when many other regions are at the limb indicates that further study is required to establish the causes of these disturbances in the solar wind flow.

## 6. Summary

A preliminary analysis of the data from the UCLA magnetometer on board the Apollo 15 subsatellite indicates that remnant magnetization is a characteristic property of the moon, that its distribution is such as to produce a rather complex pattern or fine structure, and that a detailed mapping of its distribution is feasible with the present experiment. The analysis also shows that lunar induction fields produced by transients in the interplanetary magnetic field are detectable at the satellite orbit and that the magnetometer data will provide estimates of the latitude and longitude dependences in the distribution of interior conductivity. Finally, the analysis indicates that the plasma void or diamagnetic cavity that forms behind the moon when the moon is in the solar wind extends to some altitude below the satellite orbit and probably to the lunar surface and that the flow of the solar wind near the limbs is usually rather strongly disturbed.

It should be emphasized that these conclusions are, for the most part, tentative. Their verification must await more detailed analysis, improvements in statistical accuracy, and comparisons with the lunar surface magnetometers and the Explorer 35 magnetometer.

## Acknowledgments

We are indebted to G. Takahashi and his staff at Time Zero, Inc., for their efforts in the design and fabrication of the subsatellite magnetometer; and to T. Pederson, R. Brown, and their staff at TRW Systems, Inc., for their work in the design and fabrication and testing of the subsatellite and the integration of the magnetometer. We are particularly grateful to C. Thorpe who was charged with the difficult task of controlling the magnetic fields of the subsatellite.

The UCLA engineering team was led by R.C. Snare. Preliminary circuit designs were done by the late R.F. Klein. The testing and calibration of the magnetometer was supervised by F.R. George. We are also grateful to the many people at the Manned Spacecraft Center who contributed to the success of this project, especially J. Johnson, the program manager, and P. Lafferty, the contract technical monitor.

No list of acknowledgments for this experiment can be complete without an expression of appreciation to astronauts Scott, Irwin, and Worden. Through their efforts Apollo 15 opened a new era of space exploration.

## References


Colburn, D.S., R.G. Currie, J.D. Mihalov, and C.P. Sonett, Diamagnetic solar-wind cavity discovered behind Moon, Science, 158, 1040, 1967.

Dyal, P., C.W. Parkin, and C.P. Sonett, Apollo 12 magnetometer: Measurements of a steady magnetic field on the surface of the moon, Science, 196, 762, 1970.

Dyal, P., and C.W. Parkin, The Apollo 12 magnetometer experiment: Internal lunar properties from transient and steady magnetic field measurements, Preprint, NASA-Ames Research Center, 1971.

Dyal, P., C.W. Parkin, C.P. Sonett, R.L. DuBois, and G. Simmons, Lunar portable magnetometer experiment, Preprint, NASA Ames Research Center, 1971.

Mihalov, J.D., C.P. Sonett, J.H. Binsack, and M.D. Moutsoulas, Possible fossil lunar magnetism inferred from satellite data, Science, 171, 892, 1971.

Sonett, C.P., D.S. Colburn, P. Dyal, C.W. Parkin, B.F. Smith, G. Schubert, and K. Schwartz, Lunar electrical conductivity profile, Nature, 230, 359, 1971a.

Sonett, C.P., G. Schubert, B.F. Smith, K. Schwartz, and D.S. Colburn, Lunar electrical conductivity from Apollo 12 magnetometer measurements: Compositional and thermal inferences, to appear in Proc. Apollo 12 Lunar Science Conf., Geochim. Cosmochim. Acta. Suppl., 1971b.

Strangway, D.W., E.E. Larson, and C.W. Pearce, Magnetic studies of lunar samples - breccia and fines, Proc. Apollo 12 Lunar Sci. Conf., Geochim. Cosmochim. Acta. Suppl. 1, 3, 2534, 1970.

Table 1

Apollo Subsatellite Magnetometer Specifications

| | |
|---|---|
| Type: | Second-harmonic, saturable core fluxgate. |
| Sensor Configuration: | Two sensors, one sensor parallel to the satellite spin axis ($B_P$) and one perpendicular to this axis. |
| Mounting: | Sensor unit at end of 6-foot boom. Electronics unit in spacecraft body. |
| Dynamic Range: | Two ranges, automatically selected. 0-±50 $\gamma$ at higher sensitivity. 0-±200 $\gamma$ at lower sensitivity. |
| Resolution: | 0.4 $\gamma$ and 1.6 $\gamma$ depending on range. |
| Sampling Rates: | |
| Real Time: | $B_P$ every 2 seconds, $B_T$ every second. |
| High Rate Storage: | $B_P$, $B_T$ magnitude and $B_T$ phase once every 12 seconds. |
| Low Rate Storage: | $B_P$, $B_T$ magnitude and $B_T$ phase once every 24 seconds. |
| Power: | 0.70 watts |
| Weight: | Electronics Unit: 1.8 lb.<br>Sensor Unit: 0.5 lb. |
| Size: | Electronics Unit: 11"×6.25"×1.5"<br>Sensor Unit: 0.6" diam. × 3". |
| Operating Temperature Range: | +160°F to -60° F. |

## Figure Captions

1. Schematic diagram showing the three regions of near-earth space traversed by the moon. For most of each lunation the moon is in the solar wind. The other two regions are the magnetosheath and the tail of the geomagnetic cavity. The plane of the figure is essentially the ecliptic plane. The large dot adjacent to the lunar surface marks the approximate location of the Apollo 12 lunar surface magnetometer.

2. Schematic diagram showing the interaction of the solar wind with the moon. Also shown are the orbits of the lunar subsatellite and Explorer 35. The sketch is drawn as though the orbital planes of both are parallel to the ecliptic plane. Actually, the former is inclined to the ecliptic by about 25-30° while the latter is inclined by about 15° Orbits of Explorer 35 are shown for times separated by 6 months. The region swept out by the Explorer 35 orbit over a 12-month interval is indicated by bounding circles.

3. Block diagram of the Apollo 15 subsatellite magnetometer.

4. Apollo subsatellite magnetometer.

5. Measurements of $B_p$ and $B_T$ obtained while the moon was in the geomagnetic tail. The values plotted are averages over nine successive orbits. The longitudes of the intersections of perpendiculars from the centers and rims of nearby major craters with the satellite ground track are also shown. The measured values were derived from telemetered data using a preliminary calibration. Consequently, the absolute values may be in error by a few gammas although the indicated variations are accurate. The saw-tooth nature of the plots in certain regions

is the result of statistical noise and the high resolution used for this plot.

6. Mercator projection of the far side of the moon showing the ground track of the satellite for the fifth orbit in the nine orbit sequence used in Figure 5.

7. Plots of $B_p$ and $B_T$ for five consecutive orbits during which the moon was in the solar wind.

8. Averages of $B_p$ and $B_T$ computed from 12 orbits during which the moon was in the solar wind.

9. Diagram depicting the relative geometry of the moon and a rarefaction wave at the boundary of the diamagnetic cavity.

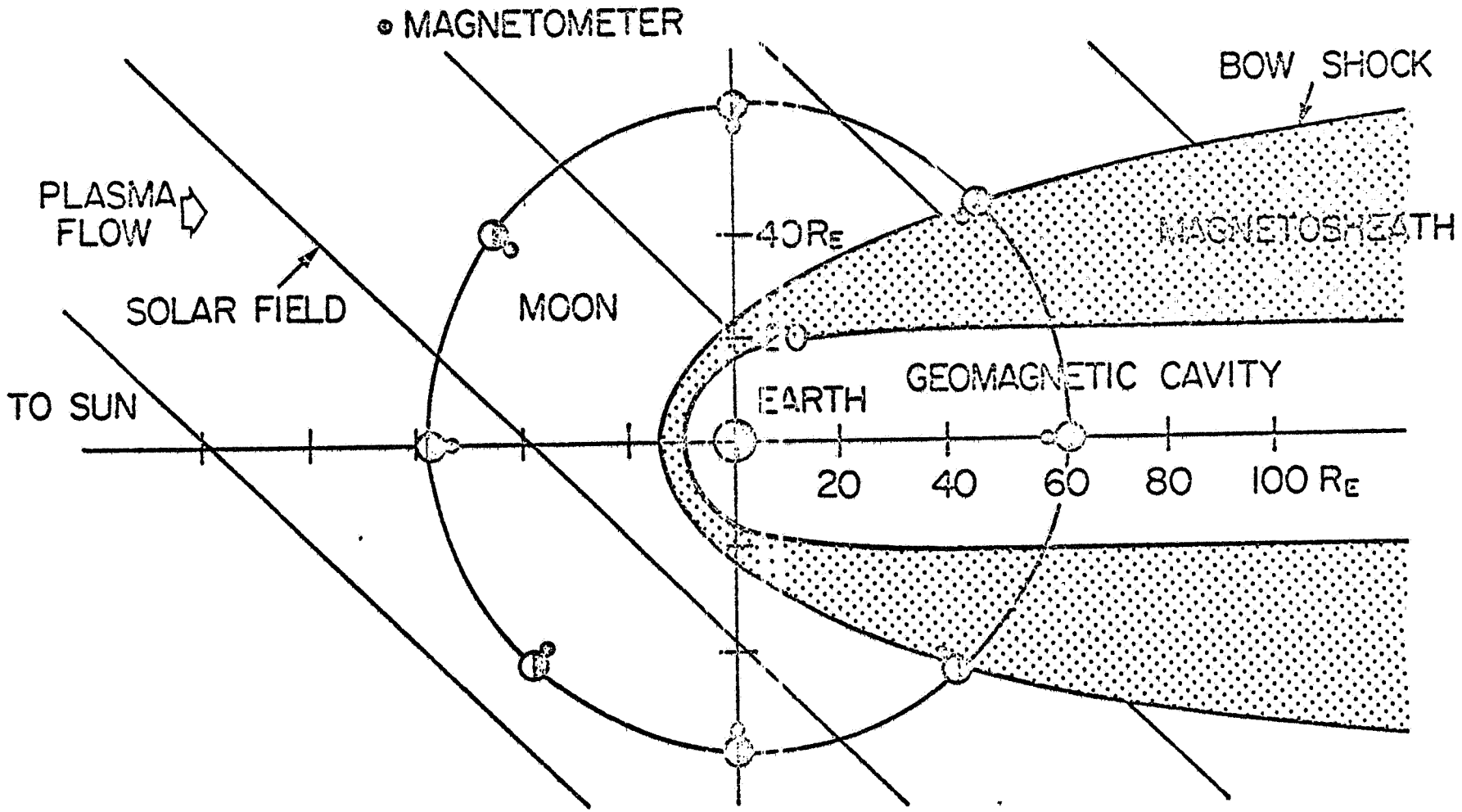
MAGNETOMETER
BOW SHOCK
PLASMA FLOW
SOLAR FIELD
MOON
40 $R_E$
MAGNETOSHEATH
20
GEOMAGNETIC CAVITY
TO SUN
EARTH
20
40
60
80
100 $R_E$
EARTH AND MOON NOT TO SCALE

Figure

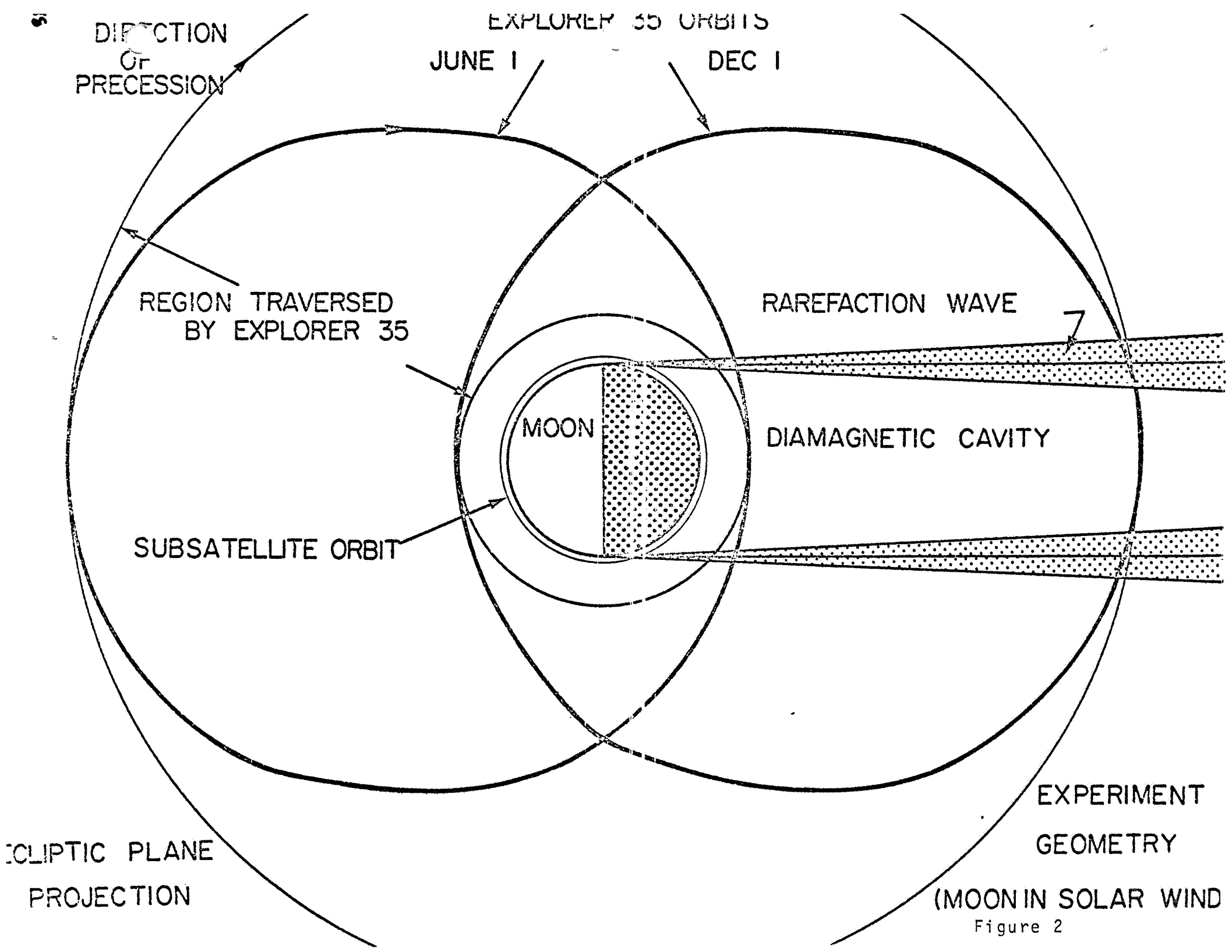
DIRECTION
OF
PRECESSION
EXPLORER 35 ORBITS
JUNE 1
DEC 1
REGION TRAVERSED
BY EXPLORER 35
RAREFACTION WAVE
MOON
DIAMAGNETIC CAVITY
SUBSATELLITE ORBIT
ECLIPTIC PLANE
PROJECTION
EXPERIMENT
GEOMETRY
(MOON IN SOLAR WIND

Figure 2

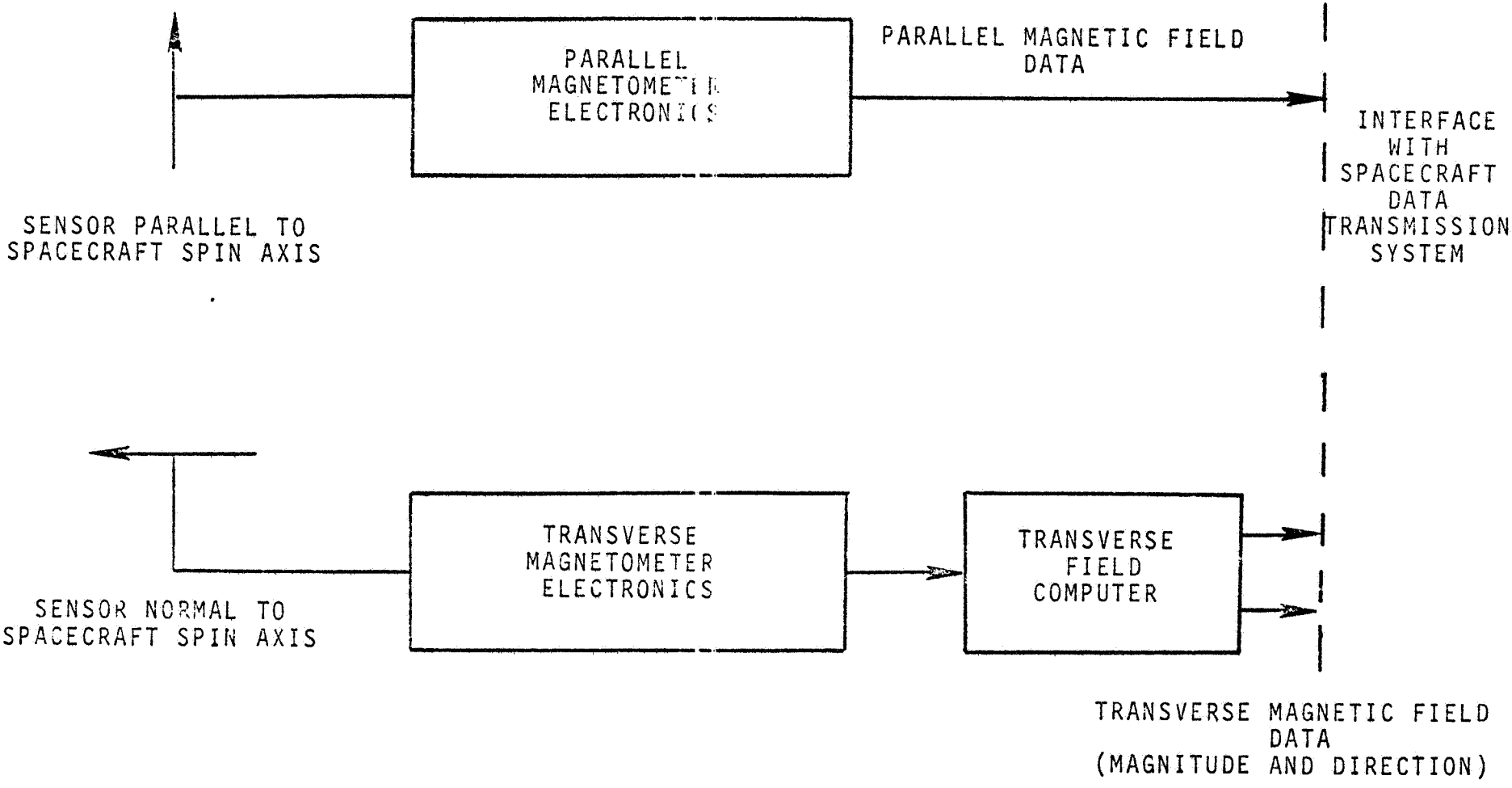


LUNAR SUBSATELLITE MAGNETOMETER

BLOCK DIAGRAM
Figure 3

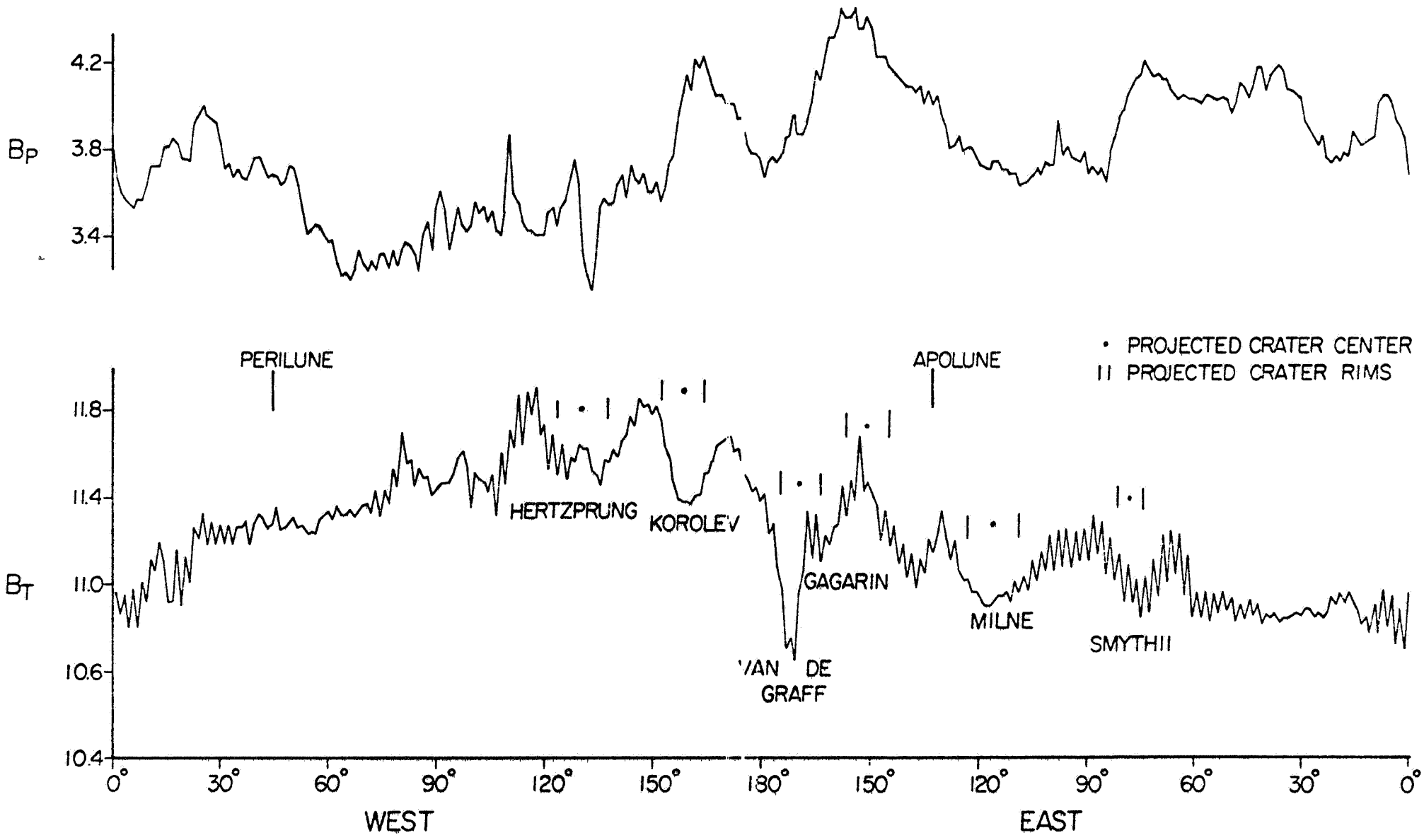
4.2
3.8
3.4
$B_P$
PERILUNE
APOLUNE
• PROJECTED CRATER CENTER
| | PROJECTED CRATER RIMS
11.8
11.4
11.0
10.6
10.4
$B_T$
HERTZPRUNG
KOROLEV
GAGARIN
MILNE
SMYTHII
VAN DE GRAFF
0°
30°
60°
90°
120°
150°
180°
150°
120°
90°
60°
30°
0°
WEST
EAST

Figure 5

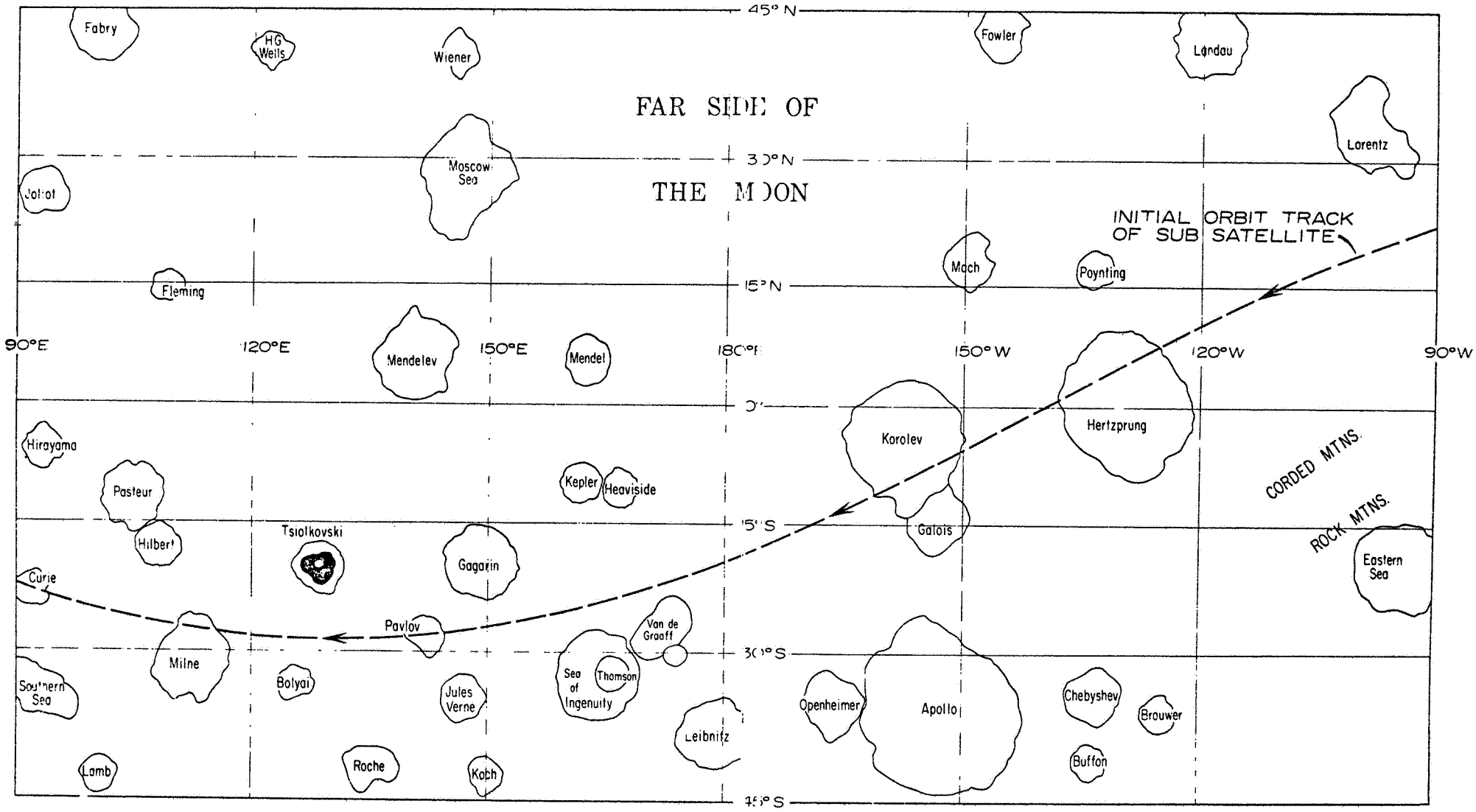
FAR SIDE OF
THE MOON
INITIAL ORBIT TRACK
OF SUB SATELLITE
45° N
30° N
15° N
0°
15° S
30° S
45° S
90°E
120°E
150°E
180°E
150° W
120° W
90° W
Fabry
HG Wells
Wiener
Fowler
Landau
Lorentz
Moscow Sea
Joliot
Fleming
Mach
Poynting
Mendelev
Mendel
Hirayama
Pasteur
Hilbert
Tsiolkovski
Kepler
Heaviside
Korolev
Hertzprung
Galois
CORDED MTNS.
ROCK MTNS.
Eastern Sea
Curie
Gagarin
Pavlov
Van de Graaff
Milne
Sea of Ingenuity
Thomson
Jules Verne
Bolyai
Southern Sea
Leibnitz
Openheimer
Apollo
Chebyshev
Brouwer
Buffon
Lamb
Roche
Kohh

Figure 6

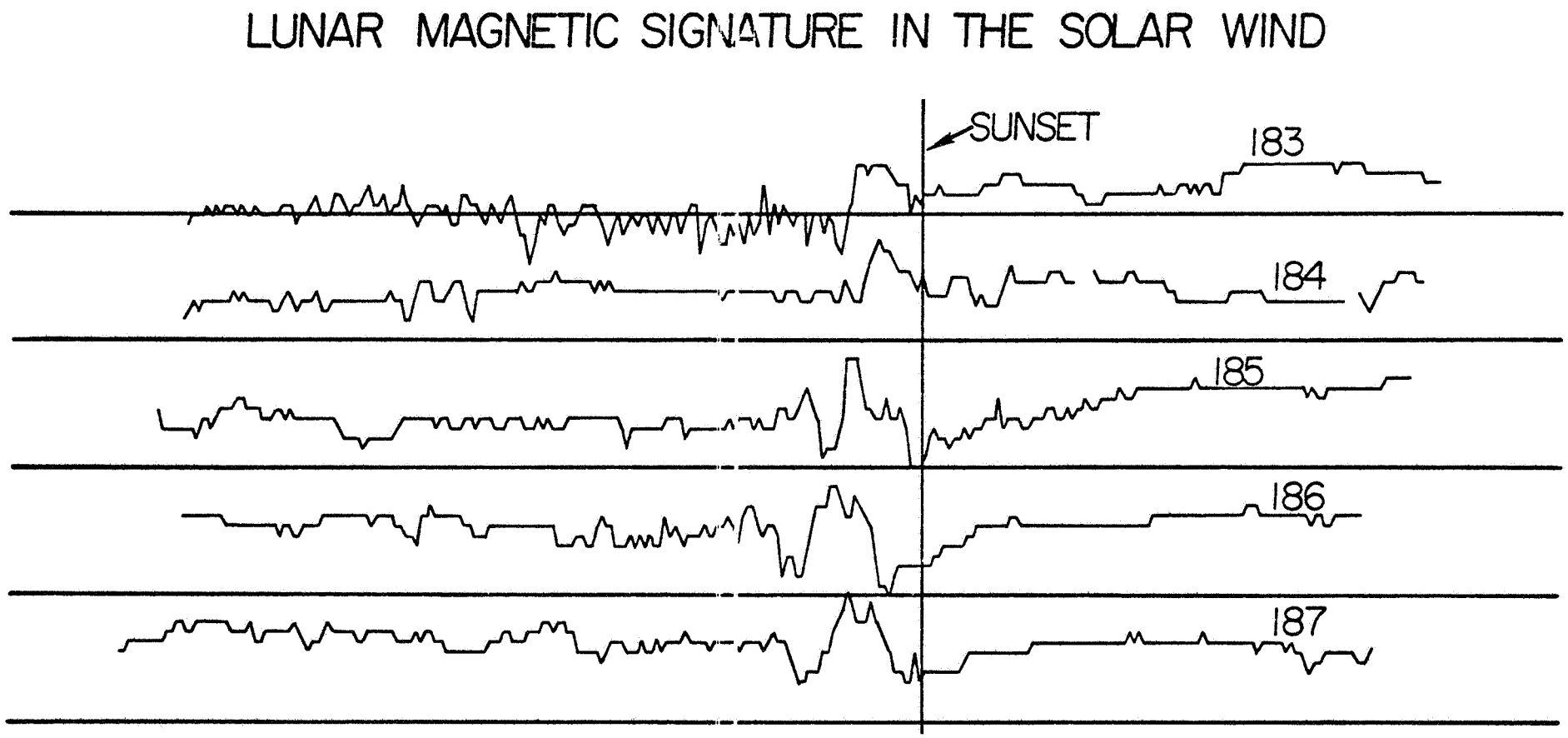
LUNAR MAGNETIC SIGNATURE IN THE SOLAR WIND
SUNSET
183
184
185
186
187
Bp

Figure 7a

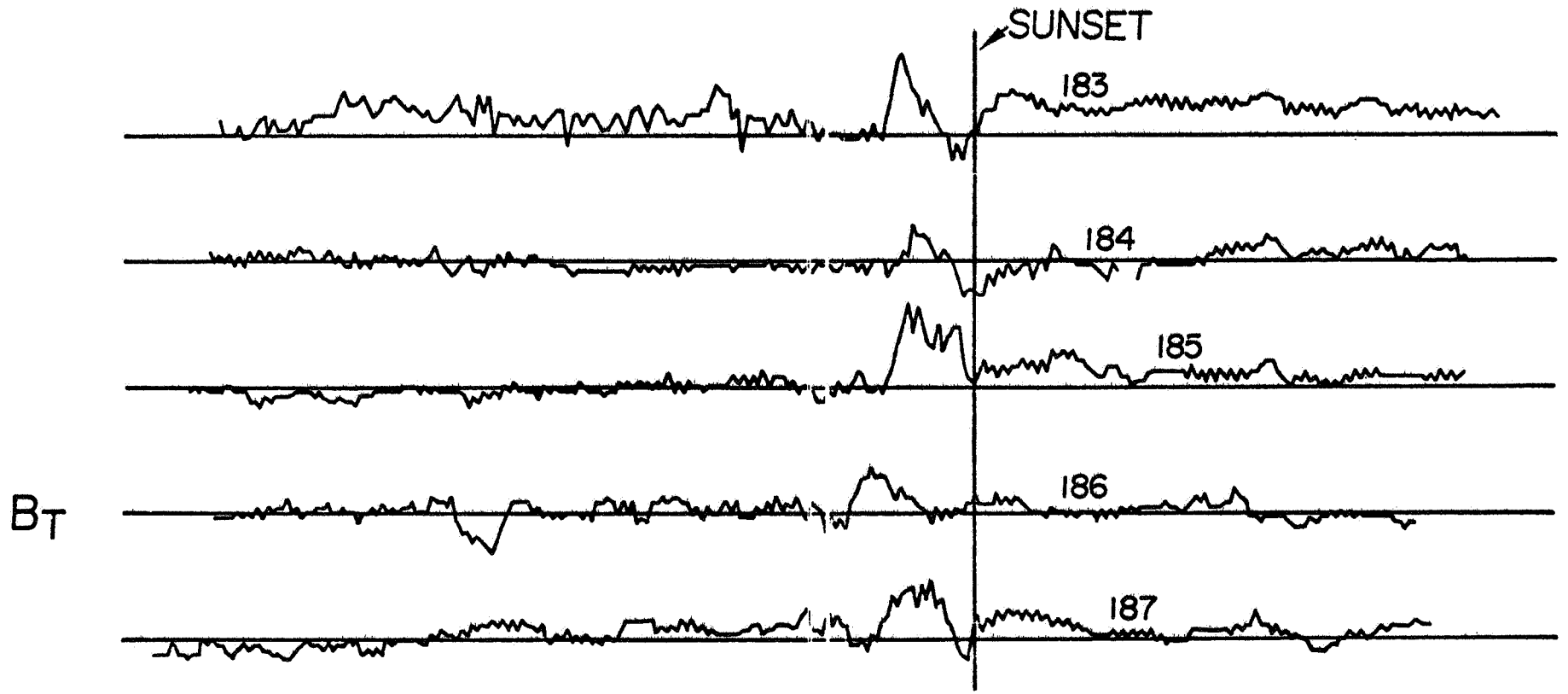
LUNAR MAGNETIC SIGNATURE IN THE SOLAR WIND
SUNSET
183
184
185
186
187
$B_T$

Figure 7b

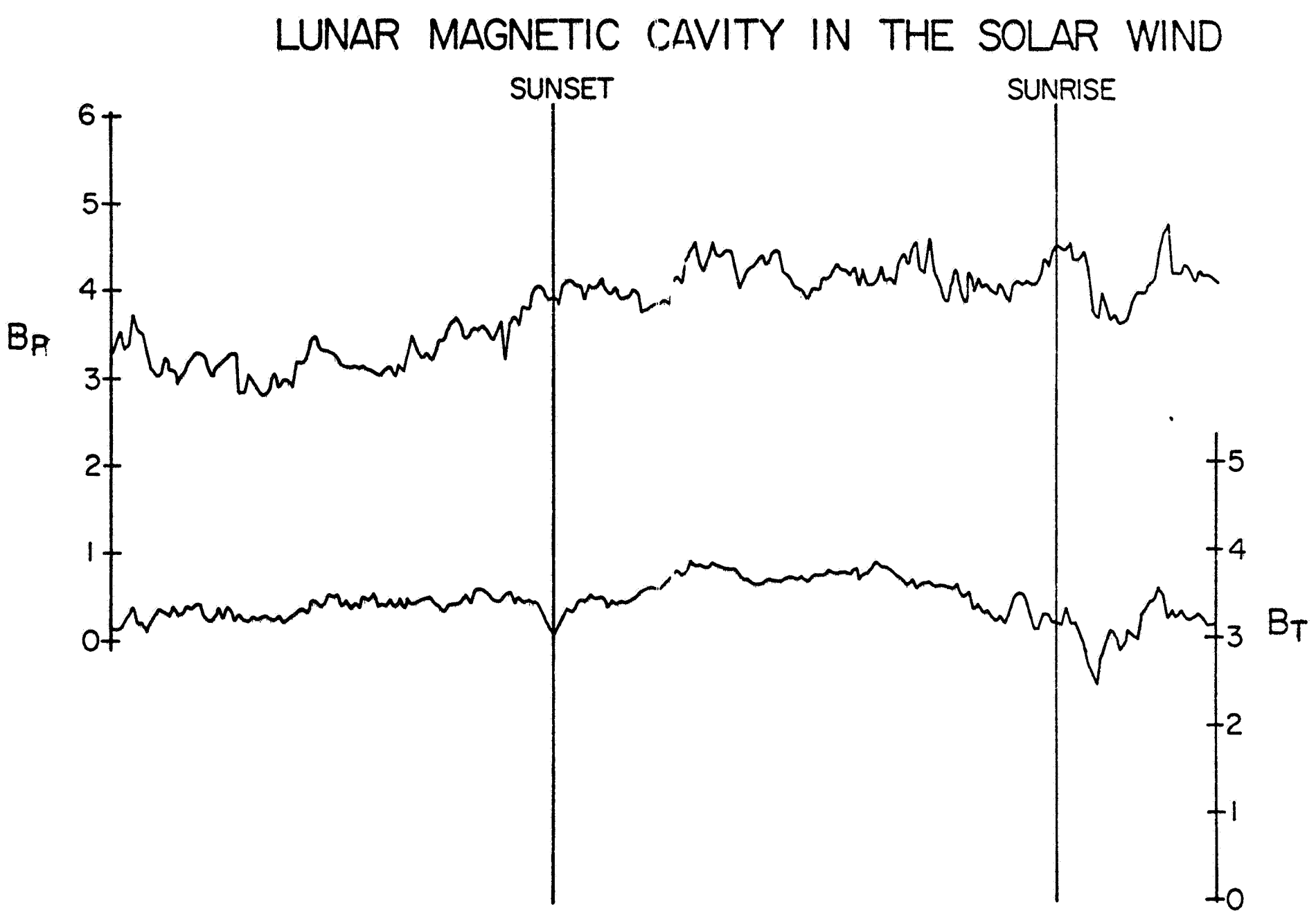
LUNAR MAGNETIC CAVITY IN THE SOLAR WIND
SUNSET
SUNRISE
6
5
4
3
2
1
0
$B_R$
5
4
3
2
1
0
$B_T$

Figure 8

# RELATIVE GEOMETRY OF LIMB SHOCK AND SUBSATELLITE

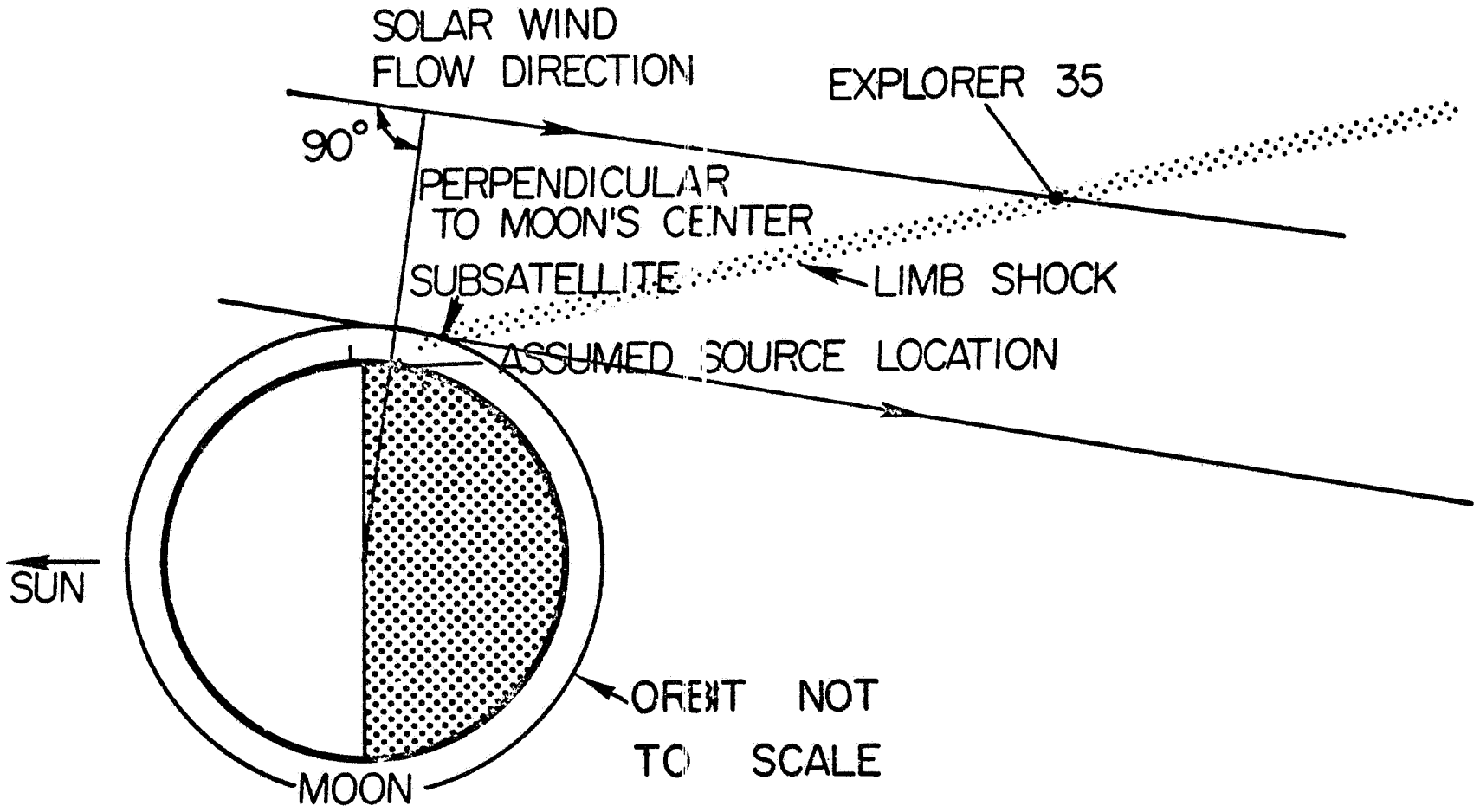


Figure 9


# SOLAR WIND INTERACTION WITH THE MOON: RESULTS FROM THE APOLLO 15 SUBSATELLITE

K.A. Anderson
L.M. Chase
R.P. Lin
J.E. McCoy
R.E. McGuire

December 6, 1971

UNIVERSITY OF CALIFORNIA, BERKELEY

97

# SOLAR WIND INTERACTION WITH THE MOON: RESULTS FROM THE APOLLO 15 SUBSATELLITE

K. A. Anderson,[1] L. M. Chase,[2] R. P. Lin,[2]
J. E. McCoy,[3] and R. E. McGuire[1]

December 6, 1971

[1]Physics Department and Space Sciences Laboratory, University of California, Berkeley 94720

[2]Space Sciences Laboratory, University of California, Berkeley 94720

[3]NASA Manned Spacecraft Center, Houston, Texas 77058

98

## ABSTRACT

Measurements of high energy solar wind electrons have been made from a low orbit around the moon. Solar wind electrons can be identified up to energies of ~3000 eV, where an electron population of different origin becomes dominant. The solar wind cavity on the moon's antisolar side shows evidence of being filled by plasma coming from the downstream direction. When the direction of the interplanetary field corresponds to $\varphi \sim 90^{o}$ a partial solar wind cavity extends across most of the Eastern sunlit side of the moon to within $\sim 20^{o}$ of the noon meridian. There are increases in the ~600 eV electron flux over much of the sunlit hemisphere. These increases are highly persistent and stable in their location over a $2\frac{1}{2}$ day period and hence are not due to intrinsic variations in the solar wind. They are usually associated with disturbances in the magnetic field. These increases are interpreted to be the result of an interaction between the solar wind on the sunlit sude of the moon which deflects some of the solar wind flow and which generates limb shocks.

## INTRODUCTION

On 4 August 1971 at $21^h00^m30.81$ GMT, the Apollo 15 astronauts launched a small scientific spacecraft into an orbit about the moon. Within 20 minutes, information concerning the magnetic fields, plasmas and energetic particles in the close vicinity of the moon was transmitted to earth. The Apollo 15 particles and fields subsatellite (P and FS) has already provided several months of nearly continuous data coverage and is designed to have a lifetime of about one year.

Immediately following its launch, the astronauts observed and photographed the satellite in space; the first time this has been possible for a scientific satellite. A photograph of the spacecraft several seconds after launch is shown here as Figure 1.

The P and FS is instrumented to make the following measurements (Principal Investigators are indicated in parentheses):

1. Plasma and energetic particle intensities (K.A. Anderson, University of California, Berkeley)
2. Vector magnetic fields (P.J. Coleman, Jr., University of California, Los Angeles)
3. Velocity of the P and FS to high precision for the purpose of determining gravitational anomalies (W. Sjögren, Jet Propulsion Laboratory).

The main objectives of the plasma and energetic particle experiment on the subsatellite are:

1. To describe the various plasma regimes in which the moon moves.
2. To determine how the moon interacts with the plasmas and magnetic fields of its environment.

3. To determine certain features of the earth's magnetospheric structure and dynamics.

In what follows here we briefly describe the main features of the spacecraft, the particle detectors and results obtained to date from the plasma and energetic particle detectors concerning the interaction of the solar wind with the moon.

## DESCRIPTION OF THE PARTICLES AND FIELDS SUBSATELLITE

This small scientific spacecraft has a mass of about 38 kilograms and a length of 78 cm. The cross-section is hexagonal and the distance between opposite corners is about 36 cm. The satellite has three deployable booms hinged from one of the end platforms. One of the booms carries the two-axis fluxgate magnetometer sensor while the other two carry tip masses to provide balance and a proper ratio of moment of inertia to avoid precession. The satellite has a short cylindrical section attached to one of the end platforms. This cylinder fits into a barrel attached to the Service and Instrument Module of the Apollo CSM. A compression spring pushes the satellite away and at the same time imparts a spin. Precessional and nutational motion imparted by the launch and boom deployment was removed by a wobble damper. The spin axis of the satellite was initially pointed normal to the ecliptic plane. Very precise pointing of the CSM by the astronauts resulted in an error less than one degree. The spin period is 5 seconds. Each of the six sides of the satellite forms a solar panel. The power output of the array is about 24 watts. Averaged over an orbit about the moon, the power is 14 watts. The power subsystem also includes a battery pack of 11 silver-cadmium cells.

The particle detectors, described in some detail in the Appendix, include several electrostatic analyzers and two solid state telescopes. These instruments cover the electron kinetic energy range 530 eV to 300 keV in 10 intervals, and 25 keV to 6 MeV for protons in six intervals. One of the analyzers (13.5 to 15 keV electrons) is sectored using as a reference the zero crossings of the transverse magnetic field component from the UCLA magnetometer. The telescopes point along the spin axis. The counting rates of the C1, C2, C3 and C4 analyzers are accumulated for one spin period. Therefore they provide spatially averaged intensity data over a certain (rather large) pitch angle interval. The C5 analyzer provides unidirectional intensities averaged over $45^{o}$ pitch angle intervals.

The detector characteristics are summarized in Tables 1 and 2.

A basic scientific requirement placed on the subsatellite was that it must take particle and field data everywhere in the orbit about the moon. This required a data storage capability. The magnetic core memory unit employed provides a capacity of 49,152 bits. Data can be read into the memory at a rate of 8 bits per second which allows coverage of nearly the entire orbit (2 hour period). Data can also be read in at 16 bits per second if it is desired to obtain better time resolution in the measurements at the expense of covering only about one-half the orbit. Real time data at the rate of 128 bits per second can also be acquired from the experiments but the tradeoff here is that battery power as well as solar cell power is being used beyond a certain point. In normal operation, the transmitter is commanded on after the subsatellite appears from behind the moon. Real time housekeeping and scientific data are transmitted for a short time to insure that the receiving stations are locked onto the signal. Then the data in the

memory unit are dumped in 512 seconds at a rate of 128 bits per second. The transmitter is then turned off and accumulation of data in the storage units begins again. A system block diagram of the fields and particles subsatellite is given in Figure 2.

The perilune altitude of the satellite on its first revolution about the moon was 102 km and its apolune altitude, 139 km. The orbital period is 120 minutes to within a few seconds, and the orbit inclination with respect to the moon's equator is $28.5^{\circ}$. The sense of revolution about the moon is clockwise viewed from the North. Perturbations on the orbit affect the perilune. After about 50 revolutions the orbit had become nearly circular at an altitude of 120 km. The perilune then decreased to 100 km on the 120th revolution after which it again began to increase. The inclination of the orbit is not appreciably changed by the perturbations. There is also a long term variation of the lowest perilune reached in the shorter term cycle. It is expected that after some months the subsatellite may reach altitudes as low as 30 km before again increasing.

## RESULTS

Analysis of data from the Apollo 15 subsatellite has so far provided information on the following topics:

1. The energy spectrum of the solar wind electrons at the highest energy end of the distribution, and their angular distribution.
2. The shape of the cavity produced in the solar wind by the moon as seen in ~500 eV solar wind electrons.
3. The flow of plasma over the sunlit side of the moon. We have found enhanced fluxes of particles at certain fixed

locations on the sunlit side of the moon, evidently indicating that at times some of the incident solar wind is deflected around the moon.

Before turning to the results it is necessary to describe the orbit of the spacecraft in some detail, because of its extreme closeness to the moon.

A drawing of the orbit viewed from directly above the orbital plane of the spacecraft is given in Figure 3. Orbital positions of particular interest are marked by Greek letters and by SS and SR. At SS (sunset) the spacecraft moves into the shadow of the moon, at SR (sunrise) it emerges. We have analyzed about 30 orbits over a $2\frac{1}{2}$ day period when the moon is in interplanetary space. The ecliptic longitude of the moon at this time varied from about $335^{\circ}$ to $0^{\circ}$ so that the moon is essentially directly upstream from the earth. During the first part of this period the interplanetary magnetic field tended to lie close to $\varphi = 180^{\circ}$ with variations of up to $\pm 15^{\circ}$. It slowly changed to $\varphi \sim 90^{\circ} \pm 15^{\circ}$ and remained that way for about 20 hours. During this time the field was usually close to the ecliptic plane although for brief periods it would become rather steeply inclined. The magnetometer data has been furnished to us by the UCLA group. It is therefore possible to compare the solar wind cavity characteristics for the cases of $\varphi \sim 180^{\circ}$ and $\varphi \sim 90^{\circ}$. At these times the spacecraft orbit was oriented in such a way that when $\varphi \sim 180^{\circ}$ the orbital plane was parallel, to within a few degrees, to the magnetic field. When $\varphi \sim 90^{\circ}$, the orbit plane made an angle of $\sim 25^{\circ}$ with respect to the field. The effects of orbital plane inclination with respect to the magnetic field at angles as small as this are inconsequential and in order to simplify the explanation of the orbit we now assume that the

interplanetary field always lies in the plane of the spacecraft orbit. Turning to Figure 3 with this assumption in mind we see that the straight lines $\overline{ab}$ and $\overline{cd}$ correspond to interplanetary field lines with $\varphi = 180^{\circ}$ (or $0^{\circ}$) tangent to the moon's surface and which are not distorted by the presence of the moon. This latter assumption deserves a great deal of attention which it will be given by the UCLA magnetometer group. In a preliminary way, it is clear that the moon does indeed interact with the interplanetary medium and produce disturbances on the interplanetary field line. However, the changes in direction and magnitude are nonetheless relatively small, being on the order of 10 to 20% at 120 km altitude so that for the purposes we now have in mind the assumption of straight field lines is a realistic one.

The straight lines $\overline{ef}$ and $\overline{gh}$ then correspond to idealized interplanetary field lines tangent to the moon for which $\varphi = 90^{\circ}$ (or $270^{\circ}$). The positions marked on the orbit then have the following significance: When $\varphi = 180^{\circ}$ (or $0^{\circ}$) the segments of the orbit $\gamma$SS and SR$\lambda$ represent the only times when the spacecraft is on field lines which do not intersect the moon. (If the gyroradius of the particles is comparable with the altitude of the spacecraft the moon can still affect the particle intensities on these field lines. For a detailed treatment of this problem see McGuire, 1972. In the case of 600 eV electrons the gyroradius at $90^{\circ}$ pitch angle is only 8 km.) Corresponding statements may be made for the $\varphi = 90^{\circ}$ (and $270^{\circ}$) case, although it should be noted that the field lines encountered as the spacecraft moves from $\zeta$ to $\theta$ completely cross the solar wind cavity region.

Figures 4 and 5 show particle and magnetic field data for two revolutions about the moon, one for the case of $\varphi \sim 180^{\circ}$ and the other for $\varphi \sim 90^{\circ}$. There is a data gap of about 10 minutes on each orbit

due to the memory readout. These examples are highly representative of other revolutions during this $2\frac{1}{2}$ day period and therefore we need to show only these two. Before and after this $2\frac{1}{2}$ day period, the features seen in Figures 4 and 5 are considerably altered for reasons we do not yet understand. In particular, the increases A, B, C, D and E seen on the sunlit side of the moon which we attribute to a complex interaction of the solar wind with the moon are not nearly as clearly defined. However, for a considerable fraction of the time during that part of a lunation when the moon is well upstream of the earth's bow shock, Figures 4 and 5 represent the observations very well.

One more remark should be made before further discussion of Figures 4 and 5. We are quite certain that the observed 530 to 680 eV electrons are indeed part of the solar wind. This is because, independent of the interplanetary field direction, their lowest intensity is always encountered on the dark side of the moon even when the interplanetary field is directed across the cavity ($\varphi \sim 90^{o}$). This behavior is imposed on them by the collective properties of the solar wind plasma. On the other hand, higher energy particles such as those measured by C4 and C5 (5 to 8 keV and 13.5 to 15 keV electrons) are guided by the magnetic field lines and are not affected by collective properties of the solar wind since they are observed to completely penetrate the cavity. As will be shown in a later section, we believe these higher energy electrons belong to a population of particles having different origin than the solar wind electrons.

106

The Solar Wind Cavity in 500 eV Electrons for $\varphi \sim 180^{\circ}$ (or $0^{\circ}$)

1. The main feature of the solar wind cavity at an altitude of about 120 km above the moon's surface is the order of magnitude decrease in the ½ keV electron flux on the dark side of the moon. The cavity is confined to the region between sunset and sunrise on the spacecraft as one expects it to be from earlier work on Explorer 35 (Lyon et al., 1967).

2. The edges of the cavity are not completely sharp. Figure 4 shows that at the western shadow edge (the one nearest sunset), the electron flux does not reach a minimum until the subsatellite is 530 km from the shadow edge defined by a ray oriented $4^{\circ}$ to the east with respect to the sun-moon line. (This takes into account the aberration of the solar wind.) Thus there is penetration by a small fraction of the ~500 eV electrons into the cavity to distances much greater than the gyroradius of these particles. It seems quite possible that this penetration is associated with the much larger gyroradius of the ions. Most of the ions have thermal energies of around 20 eV, but a small fraction (comparable with the fraction of electrons with energy $\geq$ 500 eV) will have energies up to a few hundred eV. The shadow edges for $\varphi \sim 180^{\circ}$ typically decrease by a factor of 1/e when the spacecraft moves in from the shadow edge by about 150 km. A 100 eV proton with $90^{\circ}$ pitch angle has a gyroradius of 140 km.

3. The deepest part of the cavity is displaced toward the western edge of the cavity. There is then a gradual increase of the ½ keV electron flux toward the eastern terminator. This asymmetry could be due to a leaking into the cavity of plasma. The moon is moving westward at ~30 km/sec and field lines are

presumably slipping through the moon at this same rate. Therefore the field lines toward the western edge of the cavity are the ones most recently to have passed into the moon and therefore should be the ones most depleted of plasma. The field lines then emerge from the eastern edge of the moon about two minutes later. We therefore interpret the gradual increase in flux as due to "back filling" of the cavity by a source with a characteristic time on the order of 10 minutes.

4. The flux of electrons in the energy ranges 1.75 to 2.25 keV (C2) and 5.5 to 6.5 keV (C4) are also decreased in the cavity region behind the moon. C2 drops to its background level while C4 does not, i.e., some 5.5 to 6.5 keV electrons penetrate completely into the cavity. From the $\varphi \sim 180^{o}$ results above it is not possible to establish that the higher energy electrons ($\geq$ 1.75 keV) are indeed part of the solar wind distribution. Below we will show that somewhere between 2 and 5 keV the observed electron fluxes have a different character than the $\frac{1}{2}$ keV electrons which can clearly be shown to belong to the solar wind distribution. Somewhere between 2 and 5 keV the electrons become guided completely by the interplanetary magnetic field and do not respond to the collective properties of the solar wind.

10B

<u>The Solar Wind Cavity in ~500 eV Electrons for $\varphi \sim 90^{o}$</u>

1. There is nearly a two order of magnitude decrease in the $\frac{1}{2}$ keV electron intensity on the dark side of the moon.

2. The western edge of the cavity is again not sharp. The cavity begins very close to sunset on the spacecraft with a 30% decrease in the ½ keV electron intensity. However, the minimum intensity in the cavity is not reached until well past the center of the moon's dark side, corresponding to position θ of Figure 3 at which point the field line intersects the moon. Following this the shadow is very deep until a partial recovery of the electron flux occurs at sunrise on the spacecraft. However, the recovery is not complete until the spacecraft reaches the orbital position μ at which time it can receive electrons from all directions. The presence of a flux of $\sim 5 \times 10^4$ electrons $(cm^2\ sr\ sec\ keV)^{-1}$ across this region extending from sunrise (SR) to μ can be interpreted in terms of a pitch angle anisotropy in the ~500 eV solar wind electrons: Only electrons from the West will be detected when the spacecraft is somewhere on the segment β to SS. This flux is $\sim 3 \times 10^5$ $(cm^2\ sr\ sec\ keV)^{-1}$. When the spacecraft is on the segment SR to μ only electrons moving from the East could be detected. Their flux is $\sim 5 \times 10^4$. This large flux anisotropy (a front to back ratio of ~6), corresponds to a "temperature" anisotropy of roughly 100%. This is much larger than the 10 to 20% reported at much lower energies by the VELA group so that other effects may be involved. There is a further pecularity about the particle fluxes along the orbit segment SR to μ: When the sectored C5 analyzer points directly at the moon it receives a flux of 1 to 2 $(cm^2\ sr\ sec\ keV)^{-1}$ due to electrons of 13.5 to 15.0 keV energy (see Figure 6). This is several times background for this detector. The flux of electrons looking directly away from the moon (toward the East) is $\sim 5$ $(cm^2\ sr\ sec\ keV)^{-1}$.

On the other side of the moon no such effect is observed. We do not believe that the Eastern sunlit quadrant of the moon is emitting ~15 keV electrons, nor do we believe that the moon's surface will coulomb scatter electrons off the moon's surface to this extent. The other parts of the orbit show that this scatter efficiency must be less than 10%. (From theoretical considerations we expect the backscatter efficiency to be about 5%). However, we do note that the magnetic field is generally disturbed over the sunlit side of the moon and perhaps ~20% of the incident ~15 keV electrons can be magnetically scattered or reflected upward.

3. As the interplanetary field direction moves from $\varphi \sim 180^{o}$ to $\varphi \sim 90^{o}$ the increases in 5.5 to 6.8 keV electrons also shift around by approximately $90^{o}$. The increases no longer occur above the optical terminators where they occurred when $\varphi$ was about $180^{o}$. They are now above the subsolar point on the sunlit side (corresponding to the segment $\mu$ to $\beta$) and above the midnight sector on the dark side (segment $\zeta$ to $\theta$). It is thus clear that electrons of 5 keV energy and above can move through the cavity as freely as they can move past the front of the moon where there is no cavity. This can be seen in Figure 5 where it is evident that the 5.5 to 6.8 keV electrons have the same intensity behind the moon as in front. A similar statement applies to the 13.5 keV electrons. It is thus clear that the electrons observed above 5 keV are not bound by the collective properties of the solar wind plasma. The only external influence on their motion is the interplanetary magnetic field and the physical presence of the moon.

4. For both this case and $\varphi \sim 180^{o}$, the magnetic field in the cavity is very stable. The magnetic field in this region has previously been studied at greater distances by Colburn et al. (1967) and Ness et al. (1967).

Energy Spectrum of the Solar Wind Electrons Above 500 eV

The electron component of the solar wind was studied by Montgomery et al. (1968) over the energy range 20 to 700 eV. They found that at low energies (up to about 70 eV) the electron population could be fit by a Maxwellian distribution. At energies above ~100 eV, a non-Maxwellian tail became dominant. One of our electrostatic analyzers, C1, responds to electron energies between 530 and 680 eV thus overlapping the energy range measured by the Vela experiment. As shown above this detector is responding to solar wind electrons. We also detect solar wind electrons in the C2 analyzer at energies between 1750 and 2250 eV. We are unable to determine a velocity distribution function with this information but we are able to measure fluxes with considerable precision. At a mean energy of 600 eV the flux is variable but usually lies between 1.5 and $5 \times 10^{5}$ $(cm^{2}$ sr sec keV$)^{-1}$. At a mean energy of about 2000 eV the flux is approximately 150 $(cm^{2}$ sr sec keV$)^{-1}$ at a time when the flux at 600 eV was $4.5 \times 10^{5}$ $(cm^{2}$ sr sec keV$)^{-1}$. The thermal speeds of the electrons measured in this experiment are much higher than the solar wind bulk speed: at 600 eV the speed is 14,000 km/sec.

The low orbit of the spacecraft and the conclusion that there is a moderate strength interaction of the solar wind with the moon makes it difficult to know if any distribution function measured from this orbit represents the free flowing solar wind. There are directions of the interplanetary magnetic field and positions in the orbit for which least perturbation of fluxes and energies of the solar wind particles would

be expected. When $\varphi \sim 90^{o}$ (or $270^{o}$) and the spacecraft is on field lines which pass at least 2 gyroradii above the lunar surface we might expect the least effect, especially if the interaction region B is avoided. Choosing data in this way leads to the differential energy spectrum plotted in Figure 7. In that figure we have plotted data from the four electrostatic analyzers and the solid state telescopes. In the case of the latter instruments we have made use of their ability to discriminate electrons and protons by means of the foil technique and we have also confirmed this identification using the fact that electrons and protons at the same energy have very different gyroradii and hence are shadowed very differently by the moon. The telescopes respond to pitch angles of $\sim 90^{o} \pm 15^{o}$ while the C1, C2 and C4 analyzers average over a wide range of pitch angles. The 13.5 to 15 keV electron analyzer directly shows, however, that the electrons at these higher energies are nearly isotropic (see Figures 8a and 8b). The fluxes are ~5 from the direction of the sun and 4 $(cm^{2}\ sr\ sec\ keV)^{-1}$ from the antisolar direction when measured in the solar wind cavity.

The question now arises, does the entire spectrum shown in Figure 6 apply to solar wind electrons? The answer is probably not. It is quite clear that the 530 to 680 keV electrons are undergoing collective interactions and it appears that this is also true of the 1.75 to 2.25 keV electrons. However, the 5.8 to 6.5 electrons are definitely being guided by the magnetic field as are all the higher energy electrons, and they completely penetrate the solar wind cavity on the moon's dark side. Using these criteria we would say that the solar wind electron energy spectrum extends to ~2000 eV but that somewhere above this energy a new component of electrons become dominant. The slope of the solar wind differential energy spectrum based on the

two points, one at 530 to 680 eV and the other 1750 to 2250 eV when fitted by a power law, is represented by $E^{-5.2}$. Beyond ~2000 eV the spectrum becomes much less steep for a time, then falls as $E^{-3.5}$ above 20 keV. The origin of the new component is unknown. We can only comment that there are three logical possibilities for its origin:

1. Terrestrial
2. Solar activity (flares, active centers)
3. A "runaway" component of the solar wind electrons

Increases in Solar Wind Electron Intensity on the Sunlit Side of the Moon

In Figures 4 and 5 it is seen that there is a great deal of variation in the intensity of the ~500 eV solar wind electrons. These variations extend over the sunlit portion of the moon to somewhat behind the Western terminator. The region of the Eastern terminator is not so well studied at the present time because of data readout occurring during these times. The increases marked D and E are the largest and extend over the greatest distance. It should be noted that for $\varphi \sim 180^{\circ}$ the increase can be accounted for, in part at least, as a simple shadowing effect of the moon. The increase coincides with the orbital segment marked $\gamma$-$\delta$-SS in Figure 3. On this segment the detector receives electrons from all directions since these field lines do not intersect the moon. However, the fact that when $\varphi \sim 90^{\circ}$ the increases at D and E are still present means that the simple unblocking of field lines cannot account for all of this effect.

The increases at B extend over a rather broad region ($\sim 60^{\circ}$) more or less centered at the noon meridian. The increase at C is smaller but very persistent and highly stable in its location. This fact and others are best seen in Figure 8 where the increases of the type A, B, C, D, and E are displayed for all available orbits over a two day period. A few orbits are missing because of battery charging. The individual orbits are lined up using a reference fixed with respect to the sun. This reference is the time at which sunset occurs on the spacecraft. These orbits include a wide range of azimuthal angles of the interplanetary field. In the first several orbits, $\varphi$ is around $180^{\circ}$. The last several orbits have $\varphi \sim 90^{\circ}$ while in the remaining orbits the field varies between $90^{\circ}$ and $180^{\circ}$.

Feature C is seen to be present in 21 out of 22 orbits. It lies in nearly the same position from orbit to orbit. Its average position is $57.6^{\circ} \pm 3.6^{\circ}$ sunward of the sunset position over these 21 orbits. The average position of C lies about $37^{\circ}$ ahead of the western terminator. Search for a symmetrically placed feature on the Eastern side of the moon has been inhibited by the presence of the data readout. In some cases a feature corresponding to C on the Eastern side, at other times it would fall into or near the cavity where it extends around to the sunlit side of the moon corresponding to $\varphi \sim 90^{\circ}$. There are a very few cases when the corresponding feature on the eastern side seems to be absent, suggesting that feature C may be weaker on one side than the other.

There is no discernible tendency for feature C to change its location with respect to a solar fixed reference. For example, features on the lunar surface move with respect to a solar fixed reference at a

rate of about 13° per day as the moon turns about its axis. By measuring the average position of C for three consecutive intervals during this two day period we find it moves at only a rate of 2° ± 2.5° per day.

The increase over the subsolar region marked B contains a good deal of structure. In Figure 7 it can be seen that increases located very close to the noon meridian ($\Sigma = 0^{\circ}$) and at ~18° to the west of the noon meridian are quite persistent and stable in location, although not so much so as feature C. Figure 4 and other examples show that the magnetic field is generally disturbed across the sunlit side of the moon and especially above the terminators. There is a tendency for there to be magnetic disturbances at B (across the subsolar region) and sometimes coincident with the ~500 eV electron increase at location C. It is clear that the ~500 eV electron increases marked A, B, C, D and E and the associated magnetic disturbances are not entirely caused by intrinsic variations in the solar wind. The effects we have just described must therefore be due to the interaction of the moon with the solar wind.

## SUMMARY AND DISCUSSION

### Properties of Solar Wind Electrons ~500 to 2200 eV

Electrons belonging to the solar wind electron component are present in the ranges 530 to 680 eV and 1.75 to 2.25 keV. Electrons are present in the interplanetary medium with energies above these energies but do not exhibit collective properties as do the 530 to 2200 eV electrons. For example, electrons ≥6 keV are observed to be guided along interplanetary field lines and they are able to completely penetrate the solar wind cavity behind the moon. Thus somewhere

115

C 3

between 2 keV and 6 keV electron population of a different solar or terrestrial origin become dominant. No doubt the exact energy at which the solar wind electrons become obscured by other particle populations is highly variable, depending on solar and/or magnetospheric conditions.

When represented as a power law the solar wind energy spectrum in the energy range ~500 to 2200 eV falls as $E^{-5.2}$. This seems to be somewhat variable, and in particular there are times when the higher energy electron channel (1.75 to 2.25 keV) is enhanced proportionately more than the 530 to 680 eV electron.

The pitch angle distribution of solar wind electrons from ~500 to 2200 eV is highly anisotropic. The directional flux along the interplanetary field from the sun may be 2 to 5 times the flux directed back toward the sun. This effect can be explained by a temperature anisotropy but it would apparently have to be somewhat larger than the 10 to 20% reported by the VELA group. When the anisotropic pitch angle distribution is used to interpret certain features of the solar wind cavity, "temperature" anisotropies of almost 2 to 1 would be required. However, this would be required only in the highest energy portion of the non-Maxwellian component.

## The Solar Wind Cavity

There are regions behind the moon at an altitude of ~120 km where the intensity of ~500 eV solar wind electrons drops by at least 30 to 100 times below their intensity in front of the moon. This is true for all directions of the interplanetary magnetic field.

When $\varphi \sim 180^{\circ}$ the 500 eV solar wind electrons penetrate into the cavity to distances of ~100 km which is much greater than the gyroradius of the electrons (about 8 km).

For interplanetary field directions of $\varphi \sim 90^{o}$, there is also penetration of the ~500 eV electrons into the night side solar wind cavity. Electrons are completely excluded only in a sector about $25^{o}$ wide lying on the Eastern side of the moon's dark side. A partial cavity extends from somewhat behind the Eastern limb all the way to within $\sim 20^{o}$ of the noon meridian. This effect can be understood, at least in part, in terms of a highly anisotropic pitch angle distribution with most of the electrons moving from West to East at these times.

Upstream Interaction of the Solar Wind with the Moon

The increases in the 500 eV solar wind electron fluxes across the entire sunlit side of the moon are not associated with intrinsic variations in the solar wind. These features are highly stable in spatial location with respect to a sun-fixed reference (or the solar wind flow direction). These increases are often associated with disturbances of the magnetic field.

Although present for 2 days these features seem to have been less definite and weaker before and after the two day period.

These spatially fixed features evidently represent an interaction between the solar wind and the moon. For example, if only a Mach (Whang and Ness, 1970) cone is present tangent to the moon slightly ahead of the solar wind terminator, there should be no effects sunward of an orbital location near or somewhat behind $\delta$ in Figure 3. The behavior of the solar wind electrons and the magnetic field near the moon, as shown in Figures 4, 5 and 8, seems to us to be best interpreted in terms of a partial deflection of the solar wind around the moon, accompanied by a shock (located at A and C in Figures 4,

5 and 8). Behind the shock there is a region in which the solar wind flow is considerably disturbed as evidenced by both the behavior of the solar wind electrons and the magnetic field. (Note, for example, in Figure 5 the disturbed field between 35° ahead of the terminator back to the terminator. The increased flux of ~600 eV electrons at D and E are also characteristic of this region.) If the effects at A and C are indeed due to a shock, it cannot be a detached bow shock because of its low altitude location far off the sun-moon line. The idea of an attached limb shock, however, seems to best explain the observations presented here. The theory of limb shocks has been partly developed for the case of the moon by Michel (1964), Hollweg (1968) and by Sousk and Lenchek (1971).

Previously, there has been experimental evidence for an interaction involving partial deflection of the solar wind flow around the moon. Siscoe et al. (1969) found plasma and magnetic field effects outside the expected position of a Mach cone. These measurements were made at much larger distances (~2500 km) from the moon's surface than those described here. The distance beyond the expected position of the Mach cone at which they believed they found a disturbed solar wind flow is in rough agreement with the extrapolated position of a limb shock attached approximately 45° ahead of the moon's terminator.

It remains to understand the disturbances in the solar wind electrons and magnetic field near the moon's noon meridian (B in Figures 4, 5 and 8). These necessarily lie outside a limb shock and therefore appear to be incompatible with this idea. However, it is known that effects do exist upstream from the earth's bow shock.

Also, it could be that more than one form of interaction is involved. At this point we can only say that there exists at least one mechanism for the interaction of the solar wind with the moon over its sunlit hemisphere. At least some of the observed effects of the interaction can be understood in terms of limb shocks attached to the moon roughly halfway between the subsolar region and its terminators.

It is interesting to ask if there is a relation between the umbral increases in the magnetic field (Colburn et al., 1967; Ness et al., 1968) beyond the Mach cone behind the moon at the orbit of Explorer 35 with the low altitude magnetic field and plasma electron disturbances on the sunlit side of the moon reported here. We note the following:

1. The penumbral increases are not present on all occasions. This is also true of the field and plasma disturbances over the sunlit surface of the moon.
2. A penumbral increase may be present over one side of the cavity but not on the other. This asymmetry (or time variation) also occurs in the field and plasma disturbances over the sunlit surface.
3. The penumbral increases lie several hundred kilometers outside the surface of the Mach cone (Ness et al., 1968). If the plasma and field effects present over the sunlit side of the moon are interpreted as disturbances due to the presence of limb shocks an extrapolation of these shock surfaces behind the moon to the Explorer-35 orbit would place them several hundred kilometers outside the Mach cone.
4. If the disturbances in the solar wind lying outside the Mach cone are interpreted as being due to limb shocks, then the remarks above lead to the conclusion that the limb shocks come and go, and may perhaps be asymmetrical. This implies that the agent deviating the plasma flow is variable in its effect, i.e., if it is a lunar atmosphere that deviates the flow, the atmosphere is in some sense variable.

## ACKNOWLEDGMENTS

The success of the Apollo 15 subsatellite is due to the efforts of many people at the Manned Spacecraft Center, NASA Headquarters, TRW Corporation and Analog Technology Corporation. The magnetic field data shown in Figures 4 and 5 from the on-board magnetometer have been made available to us by Dr. P.J. Coleman, Jr., Principal Investigator for that experiment. The scientific work at the University of California, Berkeley was carried out under support from NASA contract NAS 9-10509.

## REFERENCES

Colburn, D.S., R.G. Currie, J.D. Mihalov and C.P. Sonett, Diamagnetic solar-wind cavity discovered behind moon, Science, 158, 1040, 1967

Hollweg, J.V., Interaction of solar wind with the moon and formation of lunar limb shock wave, J. Geophys. Res., 73, 7269, 1968

Lyon, E.F., H.S. Bridge and J.H. Binsack, Explorer 35 plasma measurements in the vicinity of the moon, J. Geophys. Res., 72, 6113, 1967

Michel, F.C., Interaction between the solar wind and the lunar atmosphere, Planet. and Space Sci., 12, 1075, 1964

Montgomery, M.D., S.J. Bame and A.J. Hundhausen, Solar wind electrons: Vela 4 measurements, J. Geophys. Res., 73, 4999, 1968

Ness, N.F., K.W. Behannon, C.S. Scearce and S.C. Cantarano, Early results from the magnetic field experiment on lunar Explorer 35, J. Geophys. Res., 72, 5769, 1967

Sousk, Stephen F. and Allen M. Lenchek, Magnetogasdynamic interactions of the solar wind with planetary bodies, University of Maryland Technical Report No. 71-126, June, 1971

Siscoe, G.L., E.F. Lyon, J.H. Binsack and H.S. Bridge, Experimental evidence for a detached lunar compression wave, J. Geophys. Res., 74, 59, 1969

Whang, Y.C. and N.F. Ness, Observations and interpretation of the lunar Mach cone, J. Geophys. Res., 75, 6002, 1970

121

# APPENDIX

The subsatellite scientific instrumentation includes several fixed-voltage electric field analyzers for electron measurement over the range 500 to 15,000 eV. Because of power, weight and volume limitations, there are no proton measurements in this range. The decision in favor of emphasizing electrons rather than protons was due to the fact that electron shadowing by the moon gives more physical information. However, protons as well as electrons are measured in the two solid state telescopes over the energy range 20 keV to 4 MeV. Tables 1 and 2 list the main parameters of the detectors. In this Appendix we describe in some detail the plasma and energetic particle detectors.

## Energetic Particle Telescopes

Absolute intensities and energy spectra of electrons and protons in the range 20 to about 700 keV are obtained from two telescopes utilizing solid state particle detectors (see Figure 9). Each telescope contains a 25 $mm^2$ silicon surface barrier detector. In terms of particle kinetic energies this detector has a thickness that stops electrons below 320 keV and protons below 4 MeV. Behind this detector is a second one of 50 $mm^2$ area. The output of the back detector is placed in anticoincidence with the front detector.

The front detector is a fully depleted surface barrier detector mounted with the active surface barrier side away from the collimator. Thus the positively biased (aluminum coated) surface is the particle entrance surface. This orientation minimizes radiation damage effects and light sensitivity while providing a thin (40 $\mu g/cm^2$) entrance window. The opposite surface of the front detector is the surface barrier covered by evaporated gold with a thickness of 40 $\mu g/cm^2$. The rear detector is oriented oppositely so that the surface barriers of the two detectors directly face one another.

One of the telescopes has an organic foil of thickness 375 $\mu g/cm^2$ ahead of the front solid state detector. This foil, uniform in thickness to 10%, stops incident protons with energy up to 310 keV but reduces the energy of a 26 keV electron by only 5 keV. Thus, except for a small energy shift, a flux of electrons with energies in the 20 to 320 keV range would cause both telescopes to count at the same rate. However, when protons are incident on the telescopes the counting rates will show large differences. In addition to this means of particle discrimination we can also make use of the fact that protons and electrons of the same energy are shadowed by the moon quite differently.

Detector pulses are analyzed into eight energy channels whose nominal thresholds are given in Table 2. The upper two channels are transmitted in calibration mode only, being substituted for low-energy proton data as shown in the Table. The electron thresholds are switched when the analyzer is switched from one telescope to the other so that the channel edges correspond to the same incident electron energy to compensate for the loss in the foil (approximately 5 keV at the lowest threshold). The foil and the 320 and 520 keV thresholds are adjusted so that:

1. 40 to 340 keV protons detected by the open telescope are degraded below the lowest threshold of the shielded telescope.
2. 340 to 520 keV protons detected by the open telescope deposit 20 to 320 keV in the shielded telescope.

When the 340 to 520 keV proton fluxes detected by the telescope covered by the foil are low then these constraints allow a subtraction of the proton and electron spectra.

A weak radioactive source (plutonium 239) is placed near the front detector in each telescope. Alpha particles from these sources provide well defined and known energy losses as a check on detector and electronics stability.

The low energy thresholds of the telescopes may be varied by ground command. This feature was included since it was desired to operate the telescope as near the thermal noise levels as possible. The two threshold settings available on the Apollo 15 subsatellite are 18 and 21 keV. Because of somewhat higher temperatures than anticipated the threshold was raised to 21 keV during the first week of operation in orbit.

## The Electrostatic Analyzers

The electrostatic analyzer assembly consists of four electrostatic analyzers, analog electronics, high voltage power supplies, and logic circuits in the programming and data handling subassembly. Each electrostatic analyzer consists of two concentric sections of spherical copper plates. The outer plate in each pair is grounded, while the inner plate is raised to a positive potential. The plates are shaped to provide a $180^{\circ} \times 90^{\circ}$ volume between them for the electron trajectories. One of the analyzers (C5) is shown in Figure 10.

Analyzers C1 and C2 are geometrically identical, and employ one channel multiplier (without funnel) to detect intense fluxes of low energy electrons. They differ only in the plate voltage, and hence in the mean detected energy. Analyzers C3 and C4 use the same set of plates but the output of C4 is derived from two funnel-mouthed multipliers in parallel. The output of C3 is derived from one small-aperture multiplier. This arrangement permits a wider dynamic range. The funnel multipliers are surrounded by a plastic scintillator viewed by a photomultiplier, which is connected in anticoincidence to eliminate charged particle counts induced by cosmic rays.

The electrostatic analyzers are oriented perpendicular to the spin axis. To avoid spin biasing of the data due to directional anisotropy of particle flux, data are accumulated for integral spin periods only.

In addition, the output of the C5 detector is time division multiplexed such that particle intensities from various sectors of satellite rotation can be obtained. The sectoring is made with respect to the magnetic field line as sensed by the transverse magnetometer. The sectors are defined as follows:

| | |
|---|---|
| Sector I | $-45^{\circ}$ to $+45^{\circ}$ of B field vector |
| Sector II | $+45^{\circ}$ to $+90^{\circ}$ and $+270^{\circ}$ to $315^{\circ}$ |
| Sector III | $+90^{\circ}$ to $+135^{\circ}$ and $225^{\circ}$ to $270^{\circ}$ |
| Sector IV | $+135^{\circ}$ to $225^{\circ}$ of B field vector |

The precision to which each sector edge is determined is $\pm 5^{\circ}$. This technique of sectoring off the magnetometer output allows us to obtain a particle pitch angle distribution directly, thus avoiding costly and time consuming merging of magnetometer and particle data at a much later date.

125

## FIGURE CAPTIONS

1. The subsatellite a few seconds after ejection from the SIM. The photograph is from a frame of the motion picture film taken by the astronauts.
2. Functional block diagram of the subsatellite.
3. The Apollo 15 subsatellite orbit is approximated for the purposes here as having constant altitude of 120 km and $0^{\circ}$ inclination. The lines ab and cd may be thought of as undisturbed interplanetary field lines with $\varphi = 180^{\circ}$ (or $0^{\circ}$) and $\theta = 0^{\circ}$. Lines ef and gh represent interplanetary field lines with $\varphi = 90^{\circ}$ (or $270^{\circ}$) and $\theta = 0^{\circ}$.
4. Electron and magnetic field data for an orbit about the moon during which $\varphi$ was close to $180^{\circ}$. Many orbits show the same features. The magnetic field in the solar wind cavity is seen to be very quiet but it is disturbed over the sunlit side. The features A, B, C, D and E arise in an interaction between the solar wind and the moon.
5. The electron and magnetic field data for about $1\frac{1}{2}$ orbits when $\varphi$ remained close to $90^{\circ}$. The interaction features still appear. A partial cavity in the solar wind electrons extends well into the sunlit side of the moon.
6. One of the electron analyzers is sectored. When the spacecraft is on orbit segments $\gamma$ to SS and SR to $\lambda$ nearly equal fluxes are received in the direction of the interplanetary field and antiparallel to it. From the lower panel it is seen that these particles completely penetrate the cavity on the night side. These electrons are not part of the solar wind electron distribution.

7. Energy spectrum obtained over a several hour period when the moon was close to the sun-earth line. The solar wind electron spectrum disappears into a different particle population around ~3 keV.

8. The features A, B, C, D and E of Figures 4 and 5 appear on nearly all orbits during a two day period in the solar wind. Feature C appears most regularly and is very stable in its position with respect to a sun-fixed system. These features are therefore due to an interaction of the solar wind with the moon, evidently involving some deflection of the flow.

9. One of the solid state telescopes used on the subsatellite to detect electrons and protons in the energy range 20 to 4000 keV. The other telescope is identical to this except it has no foil. The foil has a very large effect on protons in the range of interest thereby allowing particle identification.

10. The largest electrostatic analyzer (C5) flown on the subsatellite. It measures electrons in the energy interval 13.5 to 15 keV with high sensitivity and is sectored using the magnetometer output as reference. The other analyzers are similar but measure electrons at lower energies.

Table 1 Summary of Detector Characteristics

| Designation | Detector Type | Energy Range | | Geometric Factor | Angular Aperture | Angle to Spin Axis | Minimum Detectable Flux $(cm^2 sec\ sr)^{-1}$ |
|---|---|---|---|---|---|---|---|
| | | Protons | Electrons | | | | |
| $SA_{1-6}$ | Open solid state detector with anticoincidence detector in back. (Six channel pulse height analyzer) | 0.02 MeV | 20-300 KeV | 0.45 $cm^2 sr$ | $40^\circ$ cone | $0^\circ$ | ~0.01 |
| $SB_{1-6}$ | Same as $SA_{1-6}$ except with 500 $\mu gm/cm^2$ foil over detector | 0.3-6 MeV | 25-300 KeV | 0.45 $cm^2 sr$ | $40^\circ$ cone | $0^\circ$ | ~0.01 |
| $C_1$ | Channel electron multiplier in hemispherical plate analyzer | No response | 0.53-0.68 KeV | $3.2 \times 10^{-4}$ | $20^\circ \times 60^\circ$ FWHM | $90^\circ$ | $\sim 10^4$ |
| $C_2$ | Channel electron multiplier in hemispherical plate electrostatic analyzer | No response | 1.75-2.25 KeV | $3.2 \times 10^{-4}$ | $20^\circ \times 60^\circ$ | $90^\circ$ | $\sim 10^4$ |
| $C_3$ | Channel electron multiplier in hemispherical plate electrostatic analyzer | No response | 5.8-6.5 KeV | $1.4 \times 10^{-3}$ | $15^\circ \times 60^\circ$ | $90^\circ$ | $\sim 10^4$ |
| $C_4$ | Funnel-mouthed channel electron multiplier hemispherical plate electrostatic analyzer | No response | 5.5-6.5 KeV | 0.27 $cm^2 \cdot sr$ | $18^\circ \times 60^\circ$ | $90^\circ$ | ~0.1 |
| $C_5$ | Funnel-mouthed channel electron multiplier in hemispherical plate electrostatic analyzer | No response | 13.5-15.0 KeV | 0.63 $cm^2 \cdot sr$ | $13^\circ \times 60^\circ$ | $90^\circ$ | ~0.1 |

Table 2. Solid State Telescope Energy Channels

| Channel No. | Normal Mode Energy Range, keV | Calibration Mode Energy Range, keV |
|---|---|---|
| 1 | 20*-320 | 20*- 320 |
| 2 | 40 - 80 | 40 - 80 |
| 3 | 80 - 160 | 80 - 160 |
| 4 | 160 - 320 | 160 - 320 |
| 5 | 320 - 520 | 2000 - 4000 |
| 6 | 520 - 670 | >4000 |

*Lowest threshold is adjusted to provide a specified noise counting rate. This threshold can be increased approximately 5 keV by ground command.

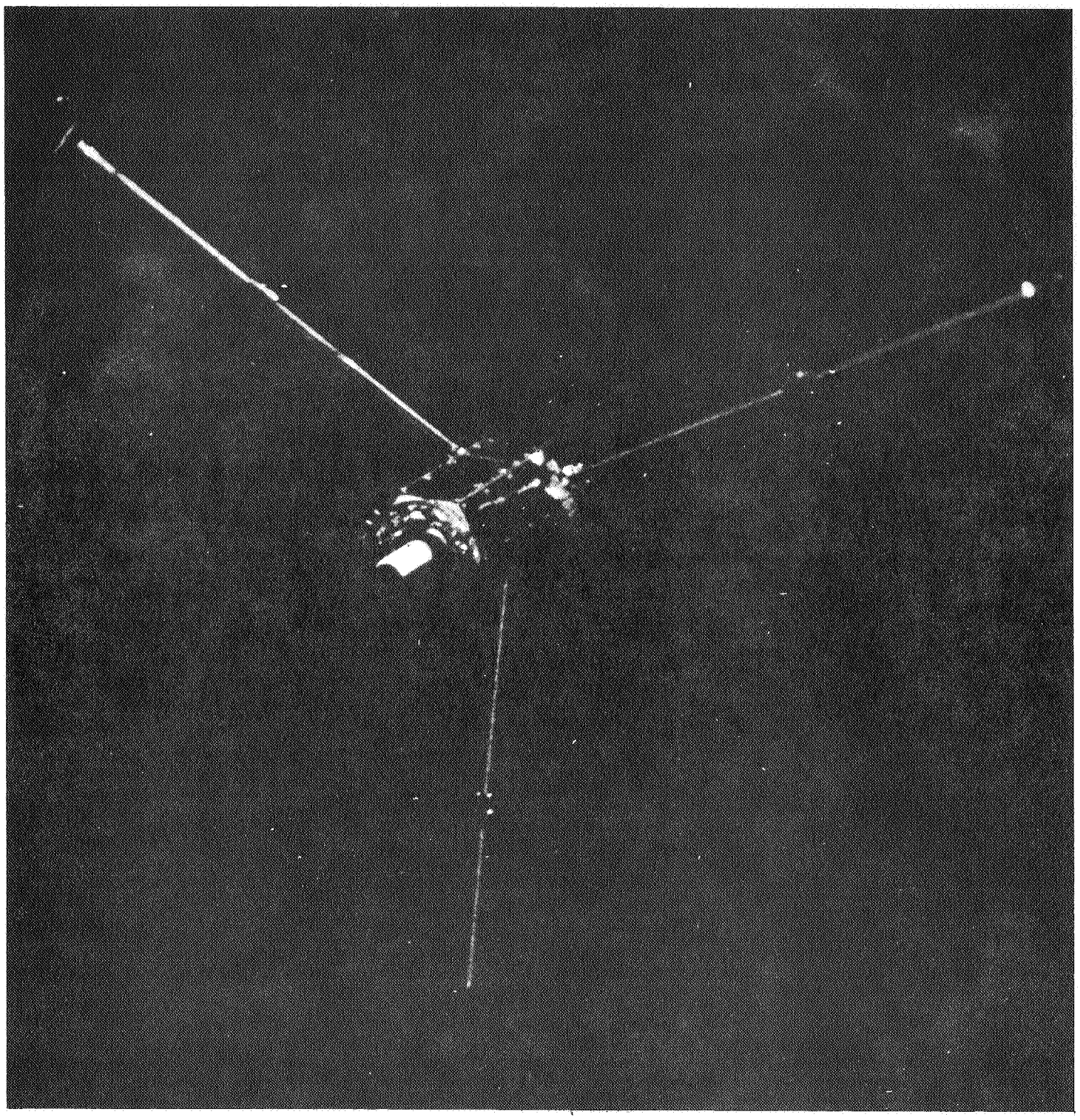

Figure 1

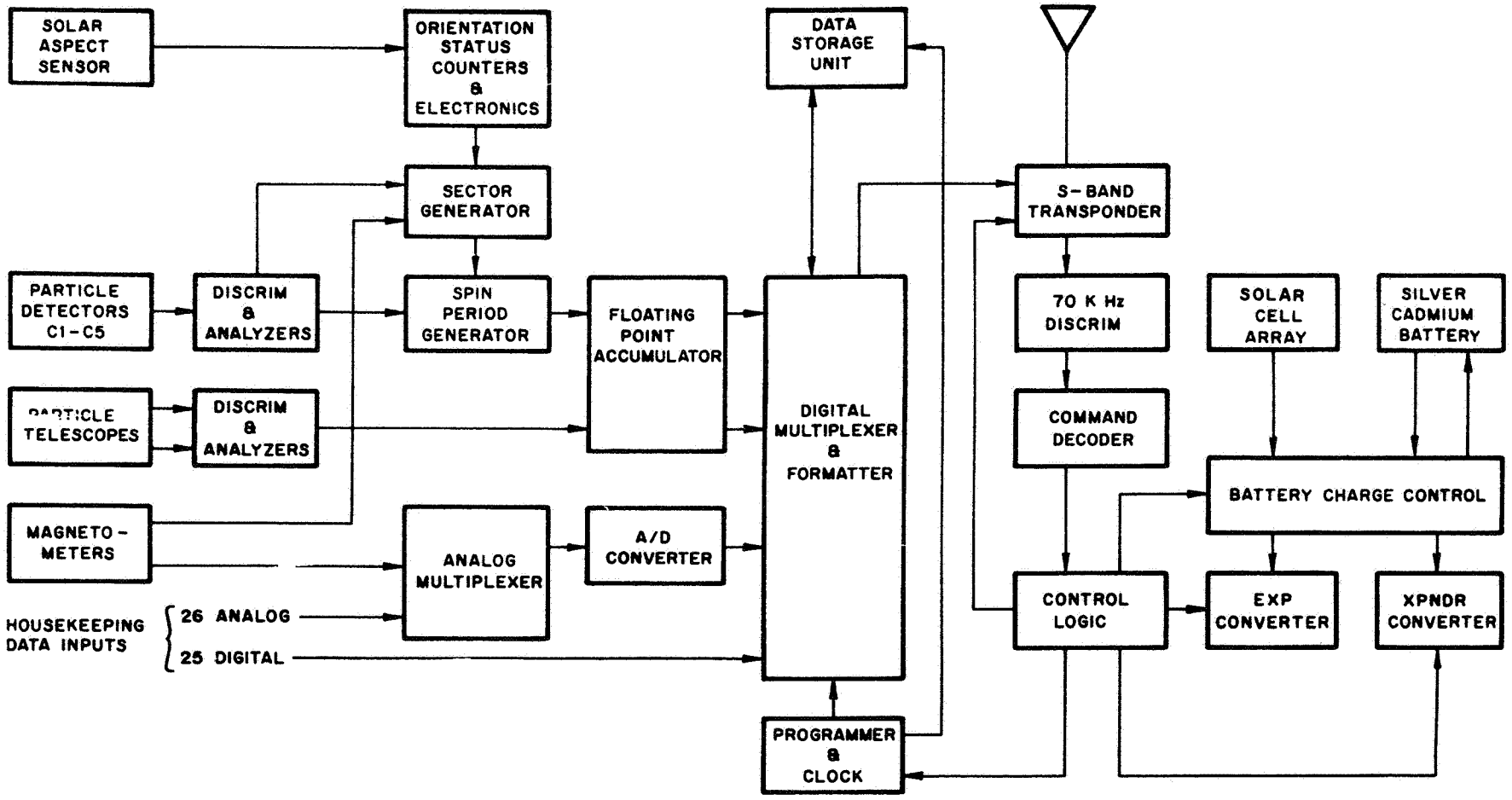
SOLAR ASPECT SENSOR
ORIENTATION STATUS COUNTERS & ELECTRONICS
DATA STORAGE UNIT
SECTOR GENERATOR
S-BAND TRANSPONDER
PARTICLE DETECTORS C1-C5
DISCRIM & ANALYZERS
SPIN PERIOD GENERATOR
FLOATING POINT ACCUMULATOR
DIGITAL MULTIPLEXER & FORMATTER
70 K Hz DISCRIM
SOLAR CELL ARRAY
SILVER CADMIUM BATTERY
PARTICLE TELESCOPES
DISCRIM & ANALYZERS
COMMAND DECODER
BATTERY CHARGE CONTROL
MAGNETO-METERS
ANALOG MULTIPLEXER
A/D CONVERTER
CONTROL LOGIC
EXP CONVERTER
XPNDR CONVERTER
HOUSEKEEPING DATA INPUTS
26 ANALOG
25 DIGITAL
PROGRAMMER & CLOCK

Figure 2

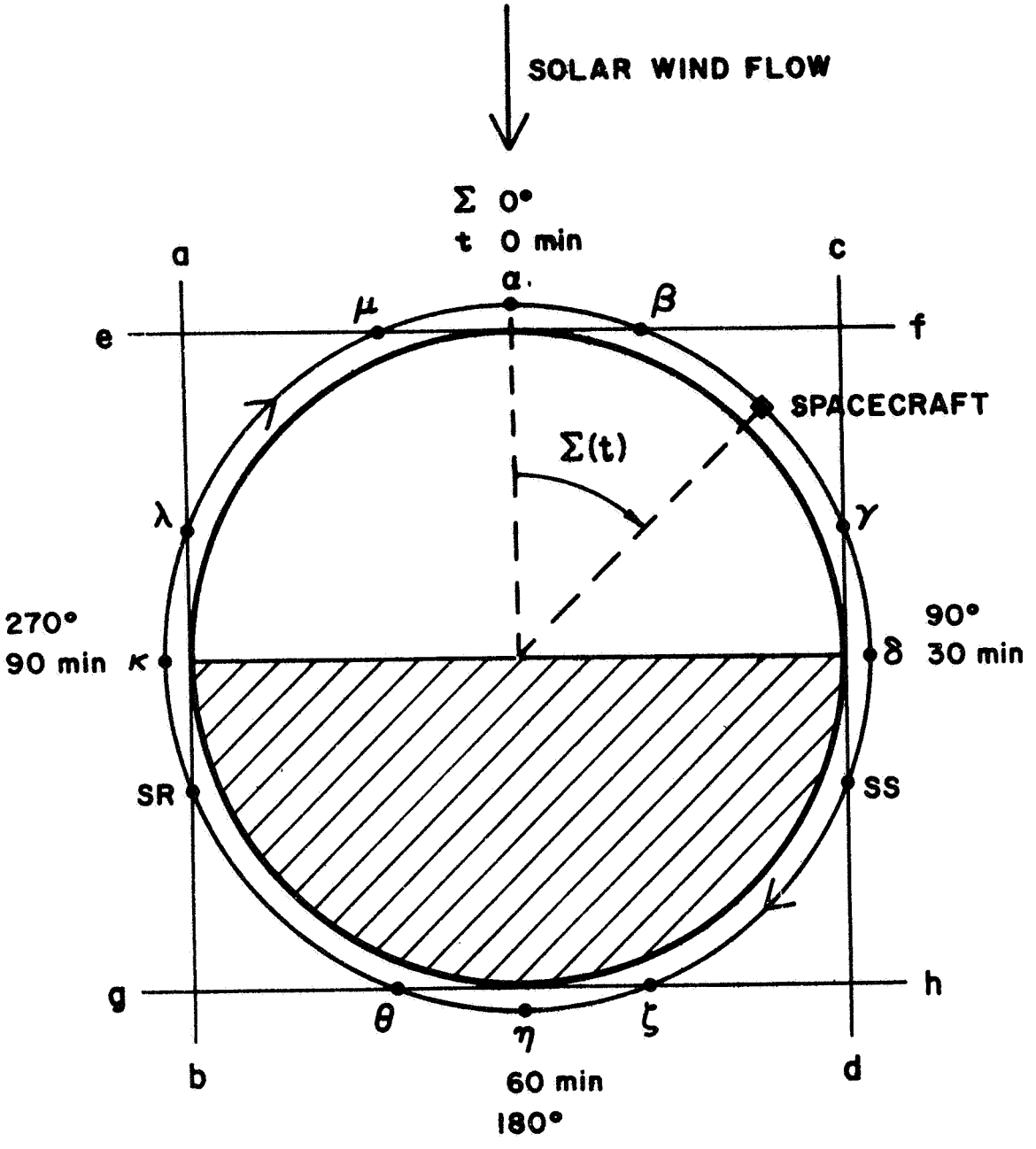


SPACECRAFT ALTITUDE : 120 Km
ORBITAL PERIOD : 120 MINUTES
$\Sigma(t)$ (in degrees) $\cong$ 3t (in minutes)

Figure 3

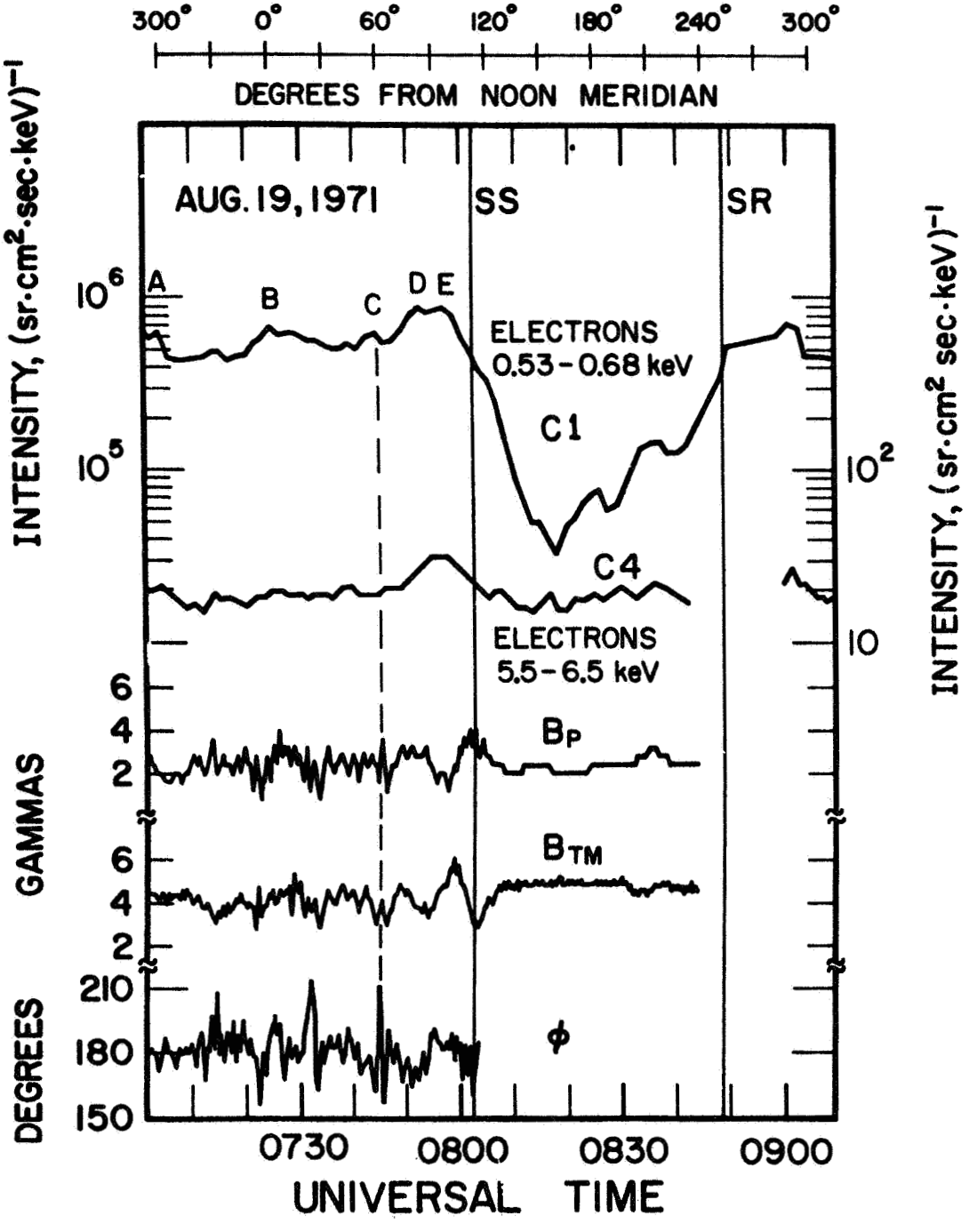
300° 0° 60° 120° 180° 240° 300°
DEGREES FROM NOON MERIDIAN
AUG. 19, 1971
SS
SR
A
B
C
D E
ELECTRONS
0.53 - 0.68 keV
C1
C4
ELECTRONS
5.5 - 6.5 keV
Bp
BTM
φ
INTENSITY, (sr·cm²·sec·keV)⁻¹
GAMMAS
DEGREES
10⁶
10⁵
10²
10
6
4
2
210
180
150
0730
0800
0830
0900
UNIVERSAL TIME

Figure 4

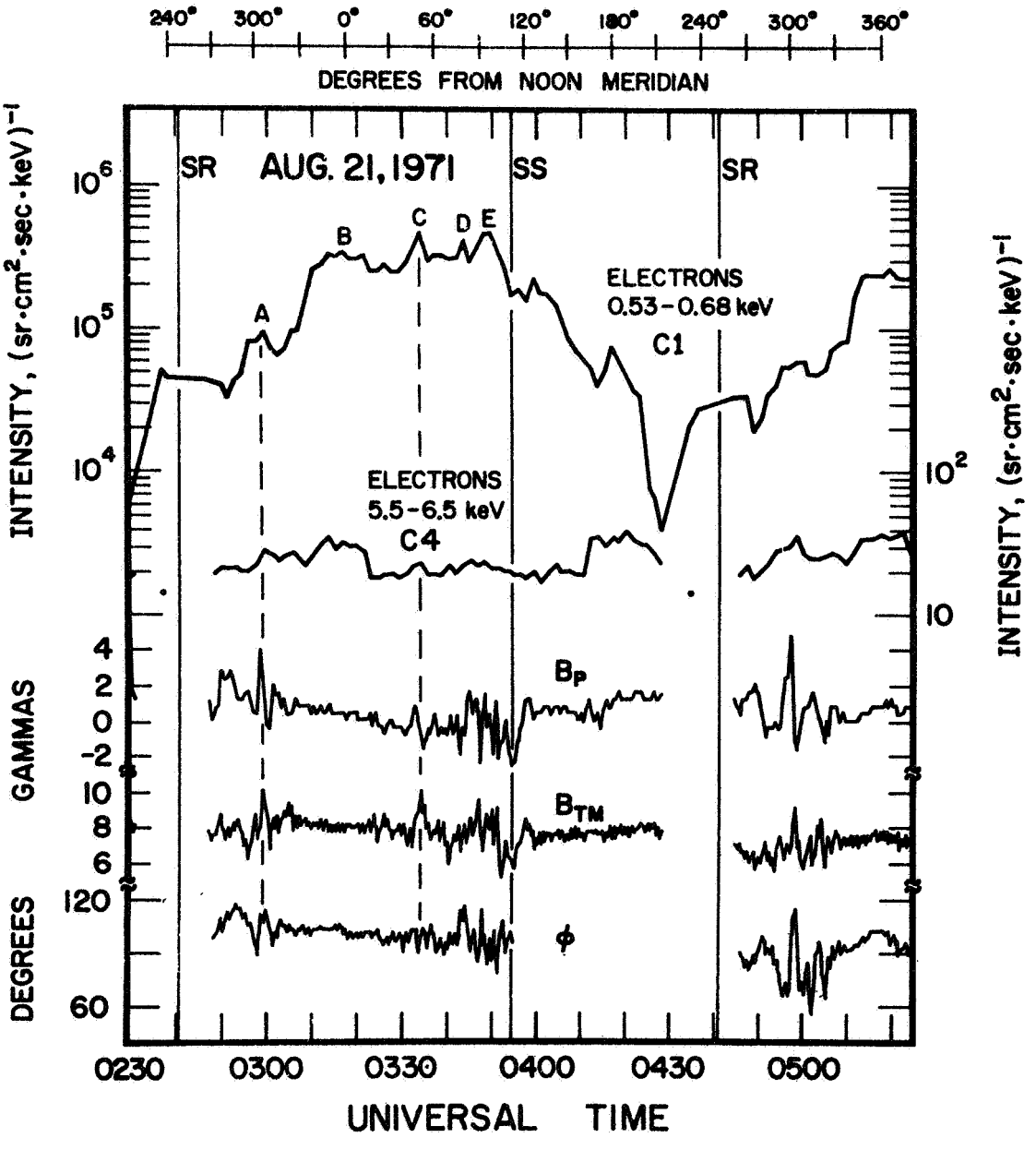
240° 300° 0° 60° 120° 180° 240° 300° 360°
DEGREES FROM NOON MERIDIAN
SR
AUG. 21, 1971
SS
SR
A
B
C
D E
ELECTRONS
0.53-0.68 keV
C1
ELECTRONS
5.5-6.5 keV
C4
INTENSITY, (sr·cm²·sec·keV)⁻¹
10⁶
10⁵
10⁴
10²
10
GAMMAS
4
2
0
-2
$B_P$
10
8
6
$B_{TM}$
DEGREES
120
60
$\phi$
0230
0300
0330
0400
0430
0500
UNIVERSAL TIME

Figure 5

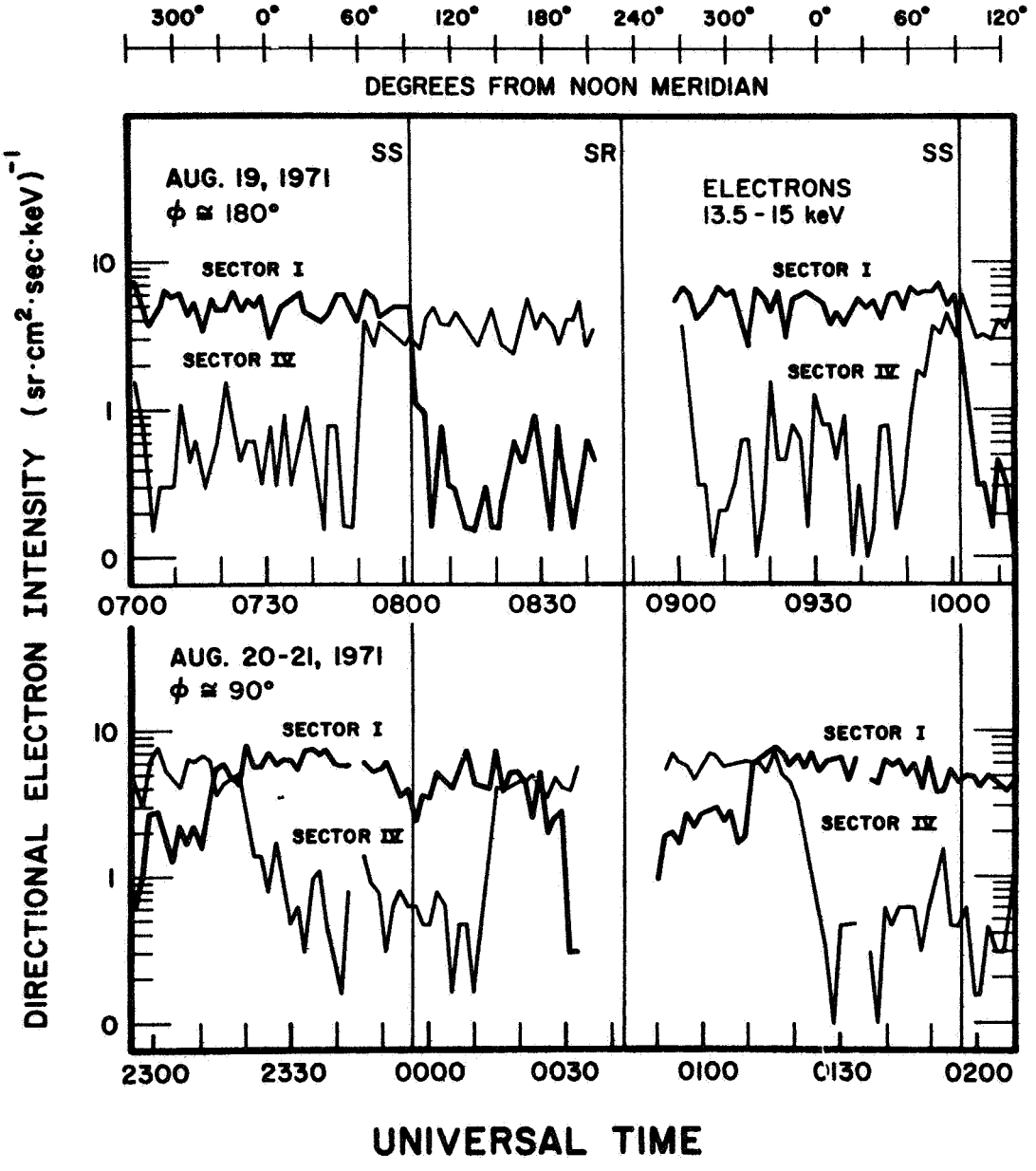
300° 0° 60° 120° 180° 240° 300° 0° 60° 120°
DEGREES FROM NOON MERIDIAN
SS
SR
SS
AUG. 19, 1971
ϕ ≅ 180°
ELECTRONS
13.5 - 15 keV
SECTOR I
SECTOR IV
10
1
0
0700 0730 0800 0830 0900 0930 1000
AUG. 20-21, 1971
ϕ ≅ 90°
2300 2330 0000 0030 0100 0130 0200
DIRECTIONAL ELECTRON INTENSITY (sr·cm²·sec·keV)⁻¹
UNIVERSAL TIME

135

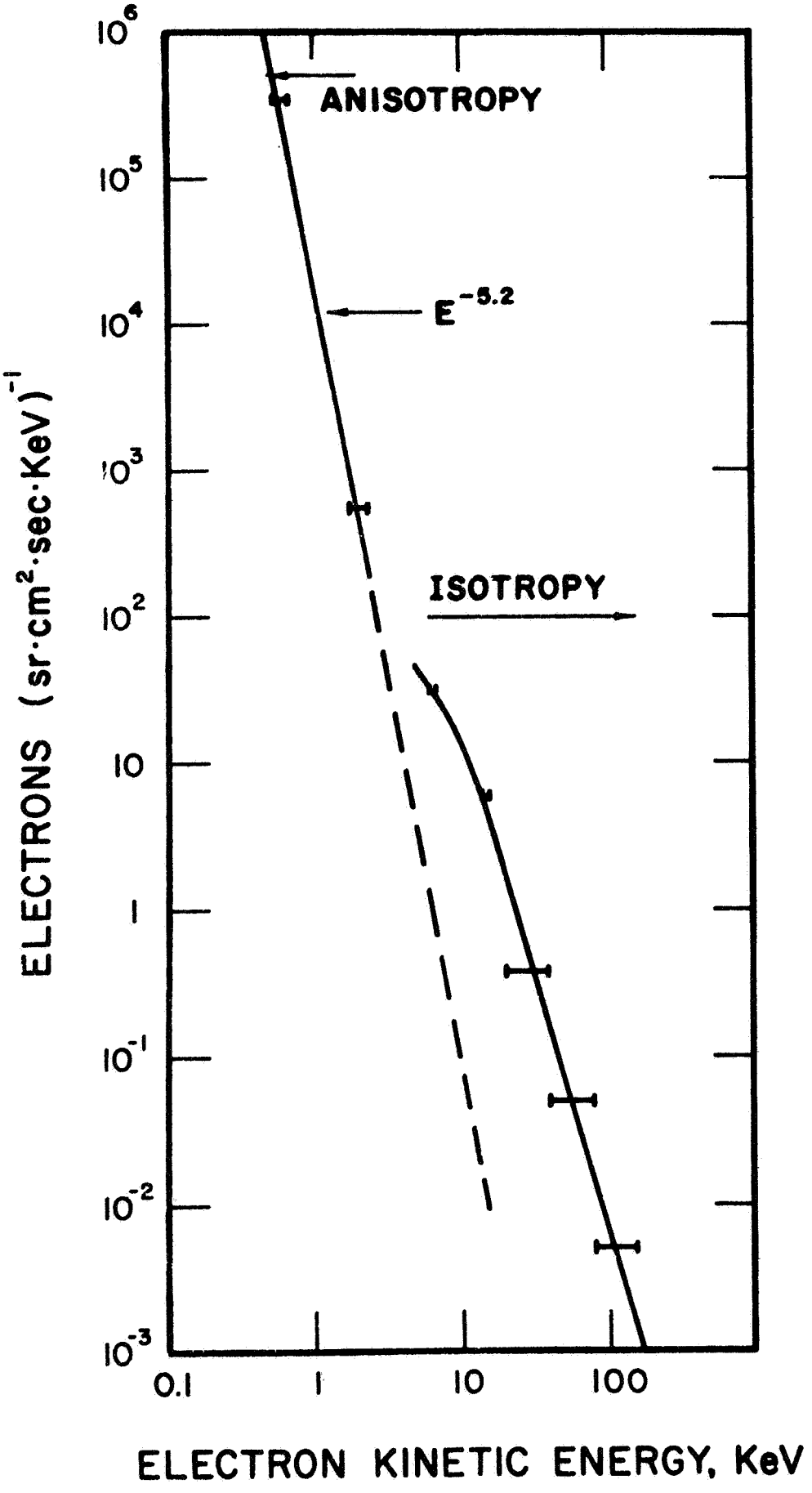
ANISOTROPY
$E^{-5.2}$
ISOTROPY
ELECTRONS (sr·cm²·sec·KeV)⁻¹
$10^6$
$10^5$
$10^4$
$10^3$
$10^2$
10
1
$10^{-1}$
$10^{-2}$
$10^{-3}$
0.1
1
10
100
ELECTRON KINETIC ENERGY, KeV

Figure 7

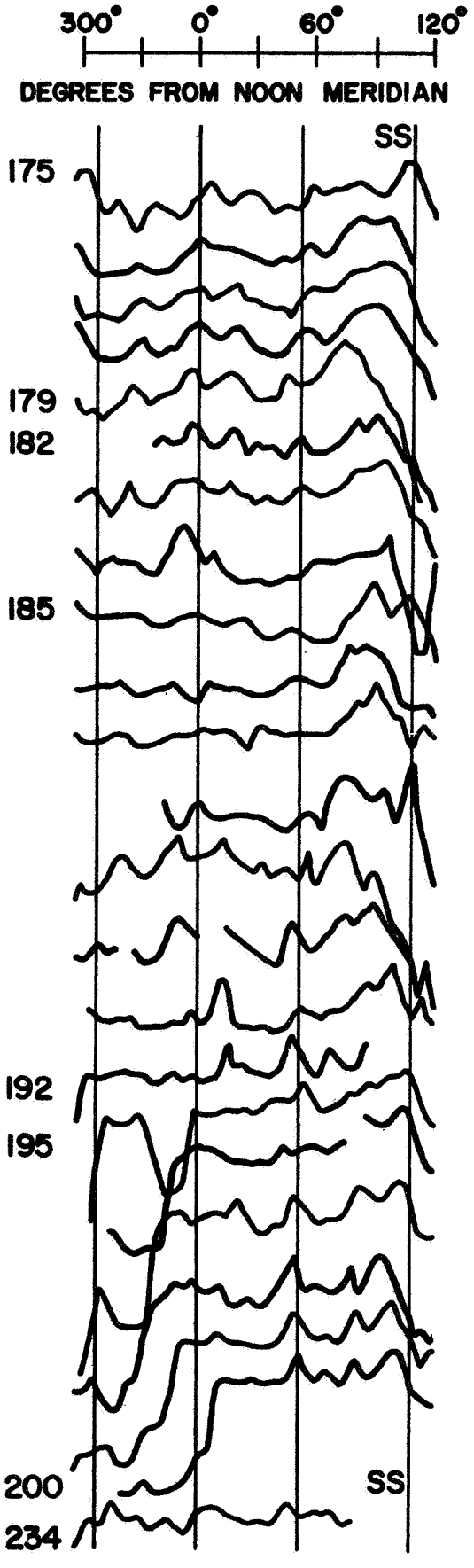
300°
0°
60°
120°
DEGREES FROM NOON MERIDIAN
SS
175
179
182
185
192
195
200
234
SS

Figure 8

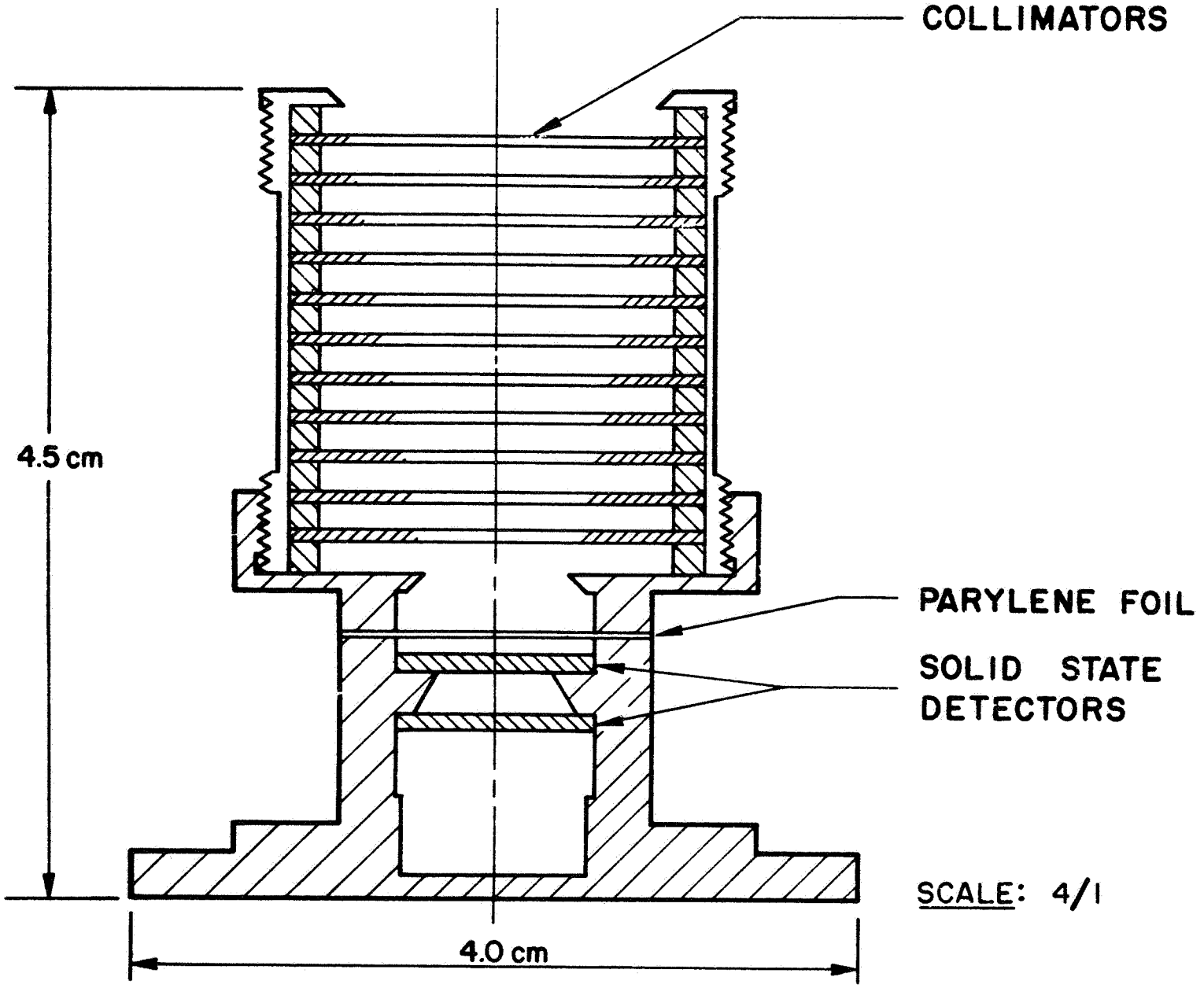
COLLIMATORS
4.5 cm
PARYLENE FOIL
SOLID STATE
DETECTORS
SCALE: 4/1
4.0 cm

Figure 9

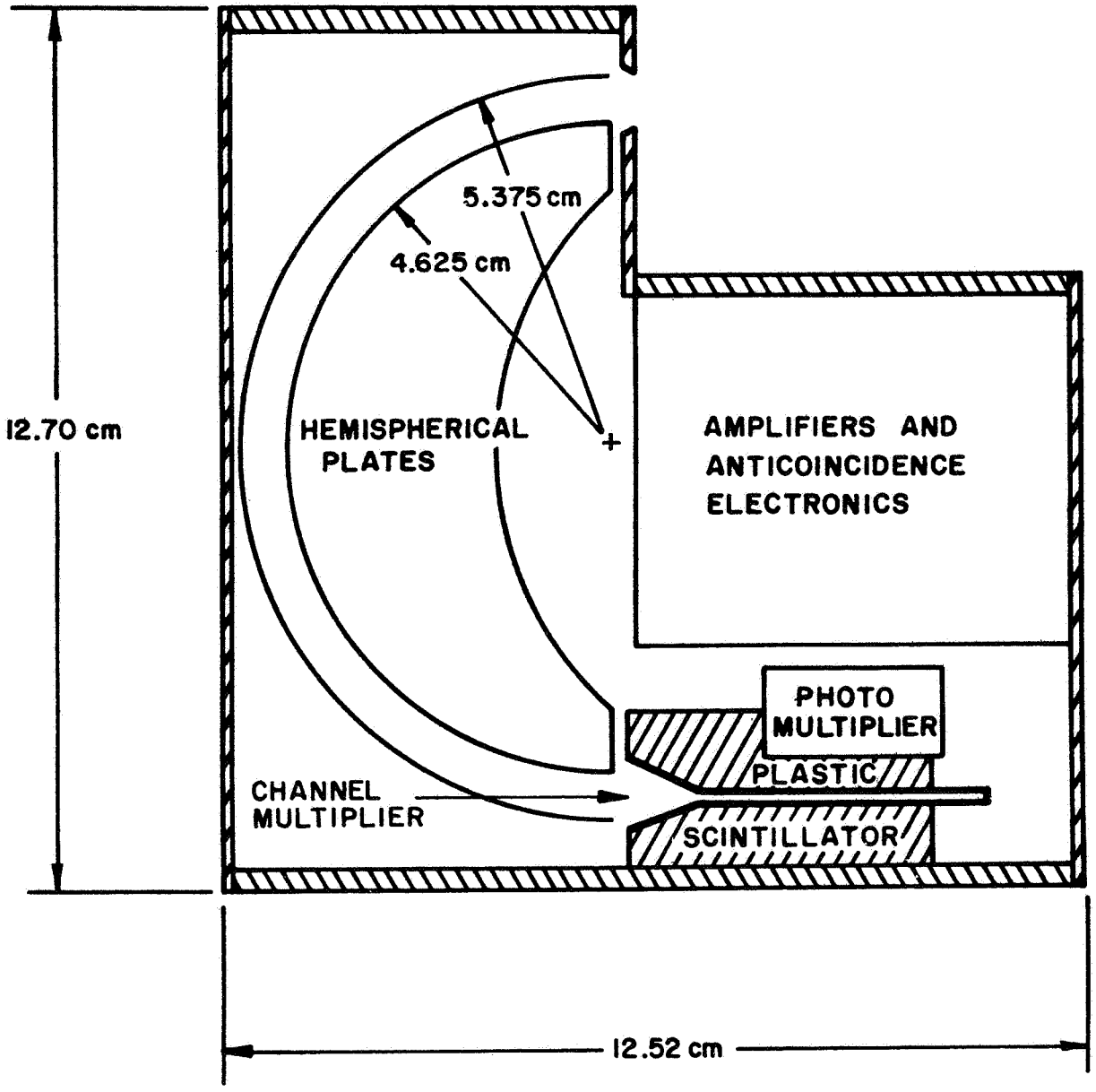
5.375 cm
4.625 cm
12.70 cm
HEMISPHERICAL
PLATES
AMPLIFIERS AND
ANTICOINCIDENCE
ELECTRONICS
PHOTO
MULTIPLIER
PLASTIC
CHANNEL
MULTIPLIER
SCINTILLATOR
12.52 cm

Figure 10

# APPENDICES

TO

FINAL

REPORT

# PARTICLES AND FIELDS SUBSATELLITE PROGRAM

A. COMMAND LIST

B. MEASUREMENT LIST

TRW
SYSTEMS GROUP

ONE SPACE PARK • REDONDO BEACH, CALIFORNIA

CODE IDENT 11982

TITLE

# PARTICLES AND FIELDS SUBSATELLITE

# COMMAND LIST

NAS9-10800
EXH. A, Par. 4.6.4
NO. 16763-41B

DATE 24 September 1970

SUPERSEDING: 16763-41A
11 August 1970

PREPARED BY: J.B. Gardner

APPROVAL SIGNATURES:

E L Baines 9/8/70
DATE
E.L. Baines
Data Handling APM - TRW

T.N. Pedersen 9/9/70
DATE
T.H. Pedersen
P&F Program Manager - TRW

DATE

Darius Hall 10-9-70
DATE
Darius Hall
MSC Contracting Officer

J.H Johnson 9/25/70
DATE
J.H. Johnson
MSC Experiment Manager

DATE

1492

SYSTEMS 1391 REV. 3-67

TRW
SYSTEMS GROUP
ONE SPACE PARK • REDONDO BEACH, CALIFORNIA

# REVISION RECORD

| REV | DATE | AUTHORIZATION | CHANGE | PAGES AFFECTED |
|---|---|---|---|---|
| Basic | 9 July 70 | Contract NAS9-10800 | | |
| A | 11 Aug. 70 | CDR direction and subsequent agreement with Mr. J. Johnson/MSC Experiment Manager. | Changes:<br>1) Change in title of 4 commands<br>2) Modification of the operation of 2 commands<br>3) All command descriptions rewritten to be more user oriented (operational rather than functional) | All |
| B | 8 Sept 70 | Direction from Mr. Jack Johnson/MSC Experiment Manager | 1) Incorporation of MSC's changes<br>2) Correction of 1 error | iii, iv, 1,4,6, 7-11 |
| | 24 Sept 70 | MSC direction at Sept Management Review<br>E. L. Baines<br>T. H. Pedersen | 1) Incorporation of MSC's changes | 5,6,11 |





(FILE DIRECTLY AFTER COVER SHEET)

# FOREWORD

Provided herein is the P & F Subsatellite command list. Included are the modulation type, information bit encoding, vehicle address, system address, word format, verification code format, command list, and functional descriptions.

This document has been prepared in accordance with Contract NAS9-10800, Exhibit A, Paragraph 4.6.4, and Exhibit C Document Table Item 41.

Revision A incorporated the changes identified during the Critical Design Review (CDR) of July 14 and 15, and of subsequent agreements with the NASA/MSC Experiment Manager.

B Revision B incorporates NASA/MSC's comments on Revision A made subsequent to the CDR. Changes for revision B are spotlighted by the presence of a "B" indicator in the left hand margin adjacent to the changed line, or top line of a changed paragraph or section. The indicator is not used for minor changes such as typographical error corrections. Revision B also incorporates the changes from MSC & PI review of the first version of Revision B as identified at the September Management Review.

# TABLE OF CONTENTS

## 1.0 INTRODUCTION AND SCOPE

This document specifies all of the uplink command interfaces between the NASA MSFN (Manned Space Flight Network) and the Particles and Fields Subsatellite (hereinafter referred to as the Subsatellite). It specifies:

a. Modulation type
b. Information bit encoding
c. Vehicle address
d. System address
e. Word formats
f. Verification code formats (downlink telemetry)
B g. Command list
B h. Functional descriptions

## 2.0 RELATED DOCUMENTATION

| | |
|---|---|
| a. MSC: NAS 9-10800 | Contract for design, development, fabrication, test, and delivery of flight qualified S-band Particles and Fields Subsatellites. |
| b. TRW: SY1-36B | Particles and Fields Subsatellite End Item Specification. |
| B c. TRW: 16763-42 | Particles and Fields Subsatellite MSFN Communications System Signal Performance and Interface Specification. |
| d. TRW: EQ4-918 | Equipment Specification - Command Decoder Unit, P & F Subsatellite. |

## 3.0 MODULATION

### 3.1 Subcarrier

The Subsatellite is designed to receive digital (subbit) information from the MSFN ground transmitters via S-band (2101.802 MHz). This subbit information (5 subbits equals one information bit) is transmitted by the ground station through the use of phase shift keyed - frequency modulation (PSK-FM) of the 70 KHz S-band subcarrier. The center frequency and the frequency deviations are defined as follows:

S-band Subcarrier

$f_o$ = 70 KHz

$f_o + \Delta f$ peak = 75 KHz

$f_o - \Delta f$ peak = 65 KHz

### 3.2 PSK Composite

The composite audio (see Figures 1.c., and 1.d.) used to modulate the subcarrier frequency is produced by phase shift keying a 2 KHz information signal (sinewave) in conjunction with a 1 KHz sync signal (sinewave). The digital information is defined as follows:

a. A subbit "one" begins when the positive transition of the 1 KHz sync signal and the 2 KHz information signal cross each other in phase (see Figure 1.a.).

b. A subbit "zero" begins when the positive transition of the 1 KHz sync signal crosses the 2 KHz information signal 180° out of phase (see Figure 1.b.).

c. The subbit period is one millisecond.

### 3.3 Signal Polarity

The polarity of the overall command system shall be defined as follows:

a. With the composite input voltage waveform shown in Figure 1.c., the frequency-time relationship shall be as presented in Figure 1.e., which shall be recognized by the Subsatellite as a subbit "one."

b. With the composite input voltage waveform shown in Figure 1.d., the frequency-time relationship shall be as presented in Figure 1.f., which shall be recognized by the Subsatellite as a subbit "zero."

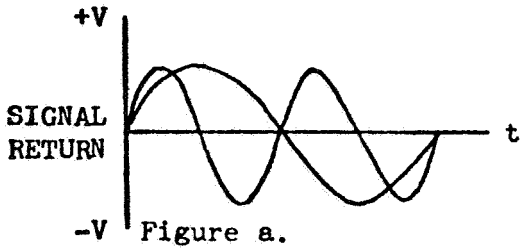


Figure a.
1 KHz SYNC WITH 2 KHz INFORMATION IN PHASE (SUBBIT "ONE")

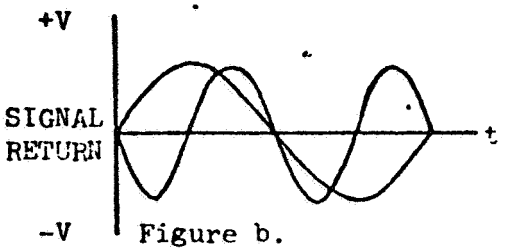


Figure b.
1 KHz SYNC WITH 2 KHz INFORMATION 180° OUT OF PHASE (SUBBIT "ZERO")

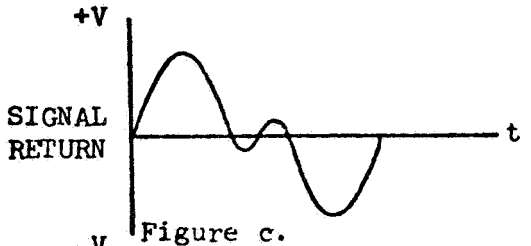


Figure c.
(COMPOSITE INPUT VOLTAGE WAVEFORM FOR SUBBIT "ONE")

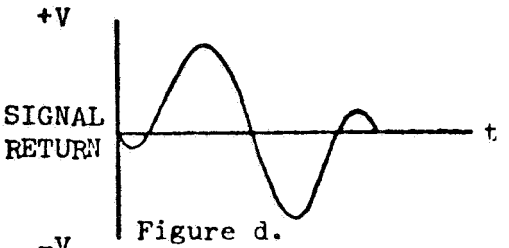


Figure d.
(COMPOSITE INPUT VOLTAGE WAVEFORM FOR SUBBIT "ZERO")

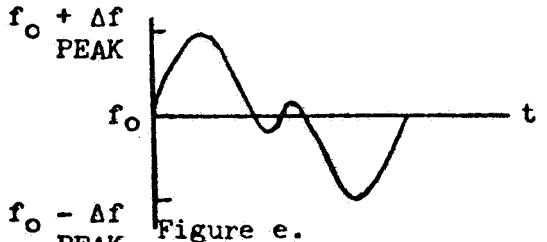


Figure e.
(FREQUENCY-TIME RELATIONSHIP FOR SUBBIT "ONE")

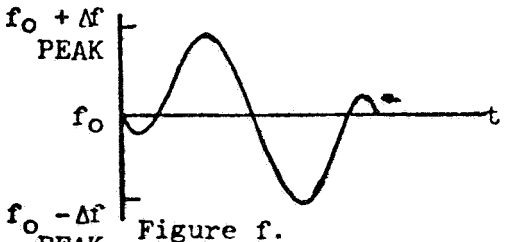


Figure f.
(FREQUENCY-TIME RELATIONSHIP FOR SUBBIT "ZERO")

S-BAND SUBCARRIER

$f_o$ = 70 KHz

$f_o$ + Δf PEAK = 75 KHz

$f_o$ - Δf PEAK = 65 KHz

FIGURE 1. COMMAND SIGNAL POLARITY

## 4.0 INFORMATION BIT ENCODING

### 4.1 Vehicle Address Subbit Encoding

B The first three information bits transmitted are the Vehicle address and are subbit encoded (5 for 1) as defined in equipment specification EQ4-918.

### 4.2 System Address and Data Subbit Encoding

B The next three information bits transmitted (the Systems Address)
B and the remaining information bits (the Data) are subbit encoded (5 for 1) as defined in equipment specification EQ4-918.

## 5.0 VEHICLE ADDRESS

The Vehicle Address for Subsatellite #1 is "010" (octal 2). The Vehicle Address for Subsatellite #2 is "101" (octal 5). Left information bit is transmitted first.

## 6.0 SYSTEM ADDRESS

The System Address for both Subsatellites is "110" (octal 6). Left information bit is transmitted first.

## 7.0 MESSAGE FORMAT

### 7.1 Real-Time Commands

FIGURE 2.

| VEHICLE | VEHICLE ADDRESS | | | SYSTEM ADDRESS | | | DATA WORD | | | | | |
|---|---|---|---|---|---|---|---|---|---|---|---|---|
| | 1 | 2 | 3 | 4 | 5 | 6 | 7 | 8 | 9 | 10 | 11 | 12 |
| Subsatellite #1 | 0 | 1 | 0 | 1 | 1 | 0 | X | X | X | X | X | X |
| Subsatellite #2 | 1 | 0 | 1 | 1 | 1 | 0 | X | X | X | X | X | X |

RTC (real-time command) message bits are shifted into the Subsatellite discriminator/decoder serially, bit 1 first and sequentially through and including bit 12 at a nominal rate of 200 message (information) bits per second.

There are a total of 24 commands that are implemented including 5 spare commands and 2 preflight test commands.

B

'50

## 7.2 Real Time Command List

| | INFO BITS 7 | 8 | 9 | 10 | 11 | 12 | OCTAL COMMAND* | FUNCTION |
|---|---|---|---|---|---|---|---|---|
| | 0 | 0 | 0 | 0 | 1 | 0 | 2602 | PHA THRESHOLD HIGH |
| B | 0 | 0 | 0 | 1 | 0 | 0 | 2604 | PHA THRESHOLD LOW |
| | 0 | 0 | 0 | 1 | 1 | 1 | 2607 | CALIBRATE ON |
| | 0 | 0 | 1 | 0 | 0 | 0 | 2610 | CALIBRATE OFF |
| | 0 | 0 | 1 | 1 | 0 | 1 | 2615 | TRANSPONDER ON |
| | 0 | 0 | 1 | 1 | 1 | 0 | 2616 | TRANSPONDER OFF |
| B | 0 | 1 | 0 | 1 | 0 | 1 | 2625 | EXPERIMENT/DATA POWER ON |
| | 0 | 1 | 0 | 1 | 1 | 0 | 2626 | EXPERIMENT/DATA POWER OFF |
| | 0 | 1 | 1 | 0 | 0 | 1 | 2631 | HIGH VOLTAGE OFF |
| | 0 | 1 | 1 | 0 | 1 | 0 | 2632 | HIGH VOLTAGE ON |
| | 0 | 1 | 1 | 1 | 0 | 0 | 2634 | UNDERVOLTAGE PROTECTION OUT |
| | 0 | 1 | 1 | 1 | 1 | 1 | 2637 | UNDERVOLTAGE PROTECTION IN |
| | 1 | 0 | 0 | 1 | 0 | 1 | 2645 | REAL TIME DATA MODE |
| | 1 | 0 | 0 | 1 | 1 | 0 | 2646 | MEMORY READOUT MODE |
| | 1 | 0 | 1 | 0 | 0 | 1 | 2651 | TELEMETRY STORE NORMAL |
| | 1 | 0 | 1 | 0 | 1 | 0 | 2652 | TELEMETRY STORE FAST |
| | 1 | 0 | 1 | 1 | 0 | 0 | 2654 | SPARE |
| | 1 | 0 | 1 | 1 | 1 | 1 | 2657 | AUTOMATIC CYCLE MODE |
| | 1 | 1 | 0 | 0 | 0 | 1 | 2661 | SPARE |
| | 1 | 1 | 0 | 0 | 1 | 0 | 2662 | SPARE |
| | 1 | 1 | 0 | 1 | 1 | 1 | 2667 | SPARE |
| | 1 | 1 | 1 | 0 | 0 | 0 | 2670 | SPARE |
| B | 0 | 1 | 0 | 0 | 0 | 0 | 2620 | Pre-Flight Test Control-On |
| B | 0 | 1 | 0 | 0 | 1 | 1 | 2623 | Pre-Flight Test Control-Off |

*Octal commands indicate vehicle address for subsatellite #1. To obtain the octal codes for subsatellite #2, octal 2602, for example, becomes 5602, etc.

Figure 3

## 8.0 VERIFICATION CODE FORMAT

B The following codes are transferred by the command decoder to the
B Data Handling System which are injected in the PCM format.

| MESSAGE | 1 | 2 | 3 | 4 |
|---|---|---|---|---|
| Decoder Standby | 0 | 0 | 0 | 0 |
| Valid Command Verified | 1 | 0 | 1 | 1 |

FIGURE 4.

NOTE: Bit 1 (most significant bit) is transmitted first.

## 9.0 COMMAND FUNCTIONAL DESCRIPTION

The normal subsatellite response to each command is described in this section.

9.1 PHA Threshold High - The minimum threshold of the solid state telescope pulse height analyzer is set to the high level. This raises the minimum detectable particle energy to nominally 20 kev.

9.2 PHA Threshold Low - The minimum threshold of the solid state telescope pulse height analyzer is set to a low value, established on the basis of pre-flight calibrations.

9.3 Calibrate ON - This command performs three functions: 1) The anti-coincidence logic in the electrostatic analyzer is inhibited enabling background pulses to be counted. 2) The discriminator level in the solid state telescope PHA is shifted such that counts from a radio active source are detected. 3) A known magnetic field is applied to the magnetometer sensors as a calibration of the sensor level. The calibrate mode may be used in real time or telemetry store modes.

9.4 Calibrate OFF - The calibrate mode is terminated by this command.

9.5 Transponder ON - With an uplink signal present, the transmitter turns on in the coherent tracking mode. If the receiver is not locked to an uplink signal, the transmitter turns off automatically. Each time the receiver locks to an uplink signal, the transmitter will turn on, and each time the uplink disappears, the transmitter turns off. This command does not affect the mode of operation of the subsatellite data system. If the subsatellite is already in a data transmitting mode, this command will produce no observable change in operation until the data transmitting mode is terminated.

9.6 Transponder OFF - The transmitter turns off, unless it has also been turned on by a Real Time Data or Memory Read Out command, or is ON in the data transmitting portion of the Automatic Cycle mode. This command does not affect the experiment or data handling system mode of operation.

B

9.7 Experiment/Data Power ON - The low voltage power supply in the particle detector electronics turns on, supplying power to the data handling system and to the scientific instruments. Power applied to the DEU will result in the real time data mode of operation, however, the time required for actuation of the RTD mode may be up to 24 seconds from power turn-on since the DEU performs the mode change at the end of the main frame. Since at initial turn-on, the DEU can be in any mode, including data storage normal, the main frame period may be 2, 12, or 24 seconds long. Thus with this command, the transmitter may come on with modulation at any time from 0 to 24 seconds after command execution.

9.8 Experiment/Data Power OFF - The low voltage power supply in the particle detector electronics turns off, removing power from the data handling syster and the scientific instruments. Note that removal of power from the DEU turns OFF the satellite clock and time correlation before and after power interruption will be disrupted. The power off command should only be used when the battery is in jeopardy of being depleted or when power consumption must be conserved for extended tracking operations.

9.9 High Voltage OFF - The high voltage power supply in the particle detector electronics turns off, removing high voltage from the analyzer plates, the channeltrons and the photomultiplier tubes and thereby deactivating the electrostatic analyzers.

9.10 High Voltage ON - The high voltage power supply in the particle detector electronics turns on, activating the electrostatic analyzers. The high voltage must not be turned on except under very high vacuum or in-flight conditions and is inhibited from turn-on by the shorting plug during pre-flight testing.

9.11 Undervoltage Protection OUT - The undervoltage sensing circuit is inhibited from turning off the transmitter and experiment/data power supply during an undervoltage condition. With this command, the battery is vulnerable to irreversible depletion since load protection is removed. Thus this command should only be sent for emergency diagnostic purposes and as a last resort that risks the end of life of the power system.

9.12 Undervoltage Protection IN - The undervoltage sensing circuit is enabled such that if an undervoltage condition occurs the undervoltage circuit turns off the experiment power supply and the transmitter, if on. With the undervoltage circuit enabled, the battery is protected from irreversible depletion. If an undervoltage condition occurs and the battery voltage subsequently recovers to an operating level, the experiment/data power converter may be turned on by the command sequence octal 26 (Experiment/Data Power Off) followed by Octal 25 (Experiment/Data Power On). No response within 24 seconds would indicate the battery is still in an undervoltage condition. If the transmitter was on due to transponder on command when the undervoltage occured, the transmitter can be turned on again if the battery has recovered by Transponder Off command followed by Transponder On. No response to this sequence indicates the battery remains in a low voltage condition. If the battery is in an undervoltage condition, the experiment/data power supply and/or the transmitter can be turned on only by command Undervoltage Protection Out and then the two command sequences given above.

B

9.13 Real Time Data Mode - The DEU switches to the real time data mode of operation. Note that mode changes within and controlled by the DEU occur at the end of a main frame of data, thus there can be a delay of up to the main frame period of the existing mode when the command was sent which means up to 2 seconds in the MRO mode, 12 seconds in the TSF mode, or 24

9.13 Real Time Data Mode (Continued)

seconds in the TSN mode. The transmitter is switched in (if Off) at the instant of mode change with data modulation. In the RTD mode, the transmitted bit rate is 128 bps and the frame rate is 0.5 frames per second. See the measurement list, document No. 16763-40 for details on the data format. The subsatellite will remain in this mode until commanded into an alternate mode or until an undervoltage condition occurs. With an uplink signal present the downlink signal will be coherent with
B the uplink with the addition of the 32.768 KHz NRZ-M bi-phase modulated subcarrier.

9.14 Memory Read Out Mode - The DEU switches to the Memory Read Out (MRO) mode of operation. The mode change occurs at the end of a main frame of the previous operating mode, thus a delay of up to 24 seconds may occur before the mode change. At the change to MRO mode the transmitter turns on (if off) with data modulation in the stored data format. The subsatellite remains in this mode until the end of memory pulse occurs after 256 main frames of data (512 seconds) and the subsatellite switches to an idling mode with the transmitter off and awaits a command to an active mode. In the idling mode, the scientific instruments and data handling system are powered but the DEU is not processing any data.

9.15 Telemetry Store Normal - The DEU switches to the telemetry store normal (TSN) mode. The mode change occurs at the end of the main frame of the previous operating mode, thus there may be a delay of up to 2 seconds normally, or up to 12 seconds if the previous mode is Telemetry Store Fast. The transmitter will turn off, if on previously, unless the Transponder On (octal 15) command has been sent whereby the transmitter would remain on in the presence of an uplink signal. In the TSN mode, the data is being stored in the memory at an 8 bps rate. The subsatellite remains in this mode for 256 frames of 24 seconds each (6144 seconds) at which time the end-of-memory pulse occurs and puts it into an idling mode.

9.16 Telemetry Store Fast - The DEU switches to the Telemetry Store Fast (TSF) mode in the same manner as with TSN command. In the TSF mode, the data is stored in the memory at 16 bps and the subsatellite remains in this mode for 256 frames of 12 seconds each (3072 seconds) at which time the end-of-memory pulse occurs switching the subsatellite to an idling mode and holds the data until an alternate command is received.

9.17 Spare

B 9.18 Automatic Cycle Mode - This command initiates the automatic cycle of preprogrammed operation. The automatic cycle consists of four modes in sequence, idling mode, Real Time Data, Memory Read Out and Telemetry Store Normal. The idling mode is the same as Real Time Data, but with the data output and transmitter control output inhibited. The modes shall have periods and sequence as follows:

| | | |
|---|---|---|
| 1. | Idling | 256 seconds |
| 2. | Real Time Data | 192 seconds |
| 3. | Memory Read Out | 512 seconds |
| 4. | Telemetry Store Normal | 6144 seconds |
| | | 7104 |

The subsatellite will remain in the Automatic Cycle Mode until an alternate mode command is received or until an undervoltage condition occurs.

9.19 Spare

9.20 Spare

9.21 Spare

9.22 Spare

B 10.0 TRANSMITTER INHIBIT FEATURE

In the event of a receiver or decoder failure in the automatic or Real Time Data mode, a transmitter inhibit is armed and actuated by the most significant bit (msb) of the elapsed time clock. The inhibit circuit is armed by a low-to-high transition of the msb and actuated by the next high-to-low transition after arming. When armed or inhibited, the circuit is cleared by any valid command. The inhibit will occur in a period of 6 to 18 days from receipt of the last valid command. Thus to guarantee that the inhibit will not occur, a valid command must be sent within every 6 day time interval.

TRW
SYSTEMS GROUP

ONE SPACE PARK • REDONDO BEACH, CALIFORNIA

CODE IDENT 11982

TITLE

# PARTICLES AND FIELDS SUBSATELLITE

# MEASUREMENT LIST

NAS 9-10800
Exh. A, Par. 4.6.4

DATE 29 January 1971

NO. 16763-40B

SUPERSEDING: 16763-40A
24 Sept. 1970

PREPARED BY: J B Gardner/ELM
J. B. Gardner

APPROVAL SIGNATURES:

E L Baines 7/9/70
DATE
E. L. Baines
Data Handling APM

Darius Hall 10-9-70
DATE
Darius Hall
MSC Contracting Officer

T. N. Pedersen 7/9/70
DATE
T. H. Pedersen
P&F Program Manager

J H Johnson 9/25/70
DATE

DATE

DATE

SYSTEMS 1391 REV. 3-67

TRW
SYSTEMS GROUP
ONE SPACE PARK • REDONDO BEACH, CALIFORNIA

# REVISION RECORD

Measurement List

| REV | DATE | AUTHORIZATION | CHANGE | PAGES AFFECTED |
|---|---|---|---|---|
| Basic | 9 July 70 | Contract NAS9-10800 | | |
| A | 8 Sept 70 | CDR direction and subsequent agreement with Mr. J. Johnson/MSC Experiment Manager. | Changes:<br>(1) Measurement S15B, High Voltage Monitor - deleted, Channel Code 192A5 is now a spare.<br>(2) Title of Measurement D07B changed<br>(3) Composite List of Measurements added for reference.<br>(4) Information added to measurement List and manner of presentation changed for clarity. | All |
| | 8 Sept 70 | E L Baines<br>E.L. Baines | | |
| | 9/10/70 | T N Pedersen<br>T.H. Pedersen | | |
| | 24 Sept 70 | MSC direction at Sept Management Review | 1) Incorporation of MSC's changes | 4,5,6, 9, 18,23 |
| | | E/B E. L. Baines<br>T/P T. H. Pedersen | | |
| B | 29 Jan 71 | ECP-013 | Changes:<br>(1) Use spare channel 192A5 for a zero gamma reference voltage.<br>(2) Use spare channel 2A2 for an ADC calibration voltage.<br>(3) Correction of transposition error (page 14, W19-f0-b1, line2)<br>(4) Added clarification of the floating point accumulator word. | Cover,ii, iii,4,5, 10,14,22<br>14<br>7,8, 10-16, 19-21 |
| | 1/29 | H.J.Horn | | |
| | 2/2/71 | S.R.Mayo | | |
| | 2/4/71 | T.H.Pedersen | | |
| SCN-1 | 15 Jul 71 | MSC Direction | Changes:<br>(1) Update to reference Calibration Report details<br>(2) Minor correction | 2,9,10,14 15,17,18,19<br>iii |
| | | H. Horn<br>B. L. Smith<br>T. Pedersen<br>A. Hartsfield(MSC) | | |
| | 7/27/71 | BC341/T184-71/L90 (MSC) | | |

| NAME AND ADDRESS<br>TRW Systems<br>One Space Park<br>Redondo Beach, Calif. 90278 | SPECIFICATION CHANGE NOTICE<br>☐ PRELIMINARY ☒ FINAL | PAGE 1 OF 9<br>DATE 7/27/71 |
|---|---|---|

| CONTRACT NUMBER | ECP NO. | SCN NO. | REVISION |
|---|---|---|---|
| NAS9-10800 | NA | 1 | NC |

| EXPERIMENT NUMBER | SPECIFICATION NUMBER, TITLE AND DATE |
|---|---|
| S164, S173, S174 | 16763-40B; P&F Subsatellite Measurement List |

| APPROVAL AUTHORITY | FILE OPPOSITE SPECIFICATION |
|---|---|
| MSC TWX #BC341/T184-71/L90 of 7/27 | PAGE NO. iii |

SPECIFICATION CHANGE

FORWARD, Page iii:

Last sentence is: .."transportation", should be "....transposition"

159

# FOREWORD

Provided herein is the P & F Subsatellite Telemetry Measurement List and Format. Included are a summary list of measurements, a single page data format table and a detailed table of measurement data. This detailed table includes such information as measurement accuracy, range, units, description, channel code, sampling interval, and work location for each measurement.

This document has been prepared in accordance with Contract NAS9-10800, Exhibit A, Paragraph 4.6.4, and Exhibit C Document Table item 40.

A Revision A incorporates the changes identified during the Critical Design Review (CDR) of July 14 and 15, and of subsequent agreements with the NASA/MSC Experiment Manager. Revision A also incorporates the changes from MSC and PI review of the first version of Revision A as identified at the September Management Review.

B Revision B incorporates changes of ECP-013 which consist of use of two spare telemetry channels to obtain valuable data from orbit, inclusion of additional clarifying information, plus correction of a transportation error.

# PARTICLES AND FIELDS SUBSATELLITE
# MEASUREMENT LIST

## 1. SCOPE

Provided herein is the Measurement List of the Particles and Fields Subsatellite. This document includes the list of measurements, the data format, and other pertinent information necessary for the reduction and analysis of the telemetered data.

## 2. COMPOSITE LIST OF MEASUREMENTS

Table 1 presents a composite list of measurements. Included are the measurement number, the measurement title, the channel code, and the main frame word location. Measurements which have the same word number are either subcommutated or are single bit bi-level measurements which form part of an 8 bit word. Detailed locations are obtained from the measurement list, Table 2.

## 3. MEASUREMENT LIST

The measurement list is presented as Table 2 and includes the format location, measurement table, measurement number, channel code, the sample interval in each mode, a measurement description, the units, maximum and minimum values, nominal accuracy and comments including scale factors, accumulation times and other relevant information.

### 3.1 Presentation

The measurement list is presented in blocks of 8 bit words in the order that they appear in the main frame. At the expense of duplication, super-commutated measurements are listed at each word position that they appear. Subcommutated measurements are listed contiguous with the first appearing subcommutated word.

#### A. Format Location

The format may be considered to be a 32 column by 8 row matrix with a word number designating the column and a frame number designating the row within the matrix. Each element of the matrix is an 8 bit word. When each bit is a separate measurement the bit is so identified. A main frame is considered as one 32 word sequence (row).

| NAME AND ADDRESS<br>TRW Systems<br>One Space Park<br>Redondo Beach, Calif.<br>90278 | SPECIFICATION CHANGE NOTICE<br>☐ PRELIMINARY ☒ FINAL | PAGE 2 OF 9<br>DATE 7/27/71 |
|---|---|---|

| CONTRACT NUMBER | ECP NO. | SCN NO. | REVISION |
|---|---|---|---|
| NAS9-10800 | NA | 1 | NC |

| EXPERIMENT NUMBER | SPECIFICATION NUMBER, TITLE AND DATE |
|---|---|
| S164, S173, S174 | 16763-40B; P&F Subsatellite Measurement List |

| APPROVAL AUTHORITY | FILE OPPOSITE SPECIFICATION |
|---|---|
| MSC TWX #BC341/T184-71/L90 of 7/27 | PAGE NO. 2 |

SPECIFICATION CHANGE

Page 2, Paragraph G. Comments.

Add the following sentence:

Detailed information concerning telemetry calibration data is contained in the individual Subsatellite Telemetry Calibration Report documents, No. 16763-30.

# 4. DATA FORMAT

## 4.1 Definitions

### A. Measurement Identification

The first letter denotes the subsystem wherein the measurement originates.

D - Data Handling
C - Communications
E - Electrical Power
S - Scientific Instrumentation
T - Sun Sensor

The next two characters are discrete numbers listed sequentially within each subsystem.

The last letter indicates the telemetry format as follows:

D - Dump data format only
R - Real time data format only
B - Both formats

### B. Channel Code

The first number is the normal data dump format sample interval in seconds. The letters define the channel type:

A - Analog (0-5VDC)
DP - Digital, parallel
DS - Digital, serial

The last number is the channel code number.

The dash number indicates the bit location for parallel digital words less than 8 bits in length.

4.2 Data Format - The Data Format is presented in Table 3.

TABLE I. COMPOSITE LIST OF MEASUREMENTS

| Meas. No. | Measurement Title | Channel Code | Main Frame Word Number | |
|---|---|---|---|---|
| **Data System Measurements** | | | | |
| D01B | Sync Word 1 | 2DP1 | W1 | |
| D02B | Sync Word 2 | 2DP2 | W2 | |
| D03B | Sync Word 3 | 2DP3-1234 | W3 | |
| D04B | Subsatellite I.D. | 2DP4-5 | W4 | |
| D05B | Data Format (R/T or Dump) | 2DP4-6 | W4 | |
| D06B | Auto or Manual Mode | 2DP4-7 | W4 | |
| D07B | Calibration (ON or OFF) | 2DP4-8 | W4 | |
| D08B | Elapsed Time, Coarse | 192DS1 | W10 | |
| D09B | Elapsed Time, Fine | 192DS2 | W26 | |
| D10B | Frame Count | 2DP3-5678 | W3 | |
| D11B | Bit Rate | 192DP1-4 | W10 | A |
| D12B | 2.56V Calibration Voltage | 2A2 | W18 | |
| **Command System Measurements** | | | | |
| C01B | Command Validity | 2DP4-1234 | W4 | |
| C02B | Receiver Signal Present | 2DP5-1 | W19 | |
| C03B | Receiver Loop Stress | 2A1 | W17 | |
| **Science Measurements** | | | | |
| S01D | Magnetometer Transverse Mag. ($B_{TM}$) | 24A1 | W6 | |
| S02D | Magnetometer Time Delay ($T_M$) | 24DS5 | W22 | |
| S03R | Magnetometer Transverse Out ($B_T$) | 24A1 | W6, W22 | |
| S04B | Magnetometer Parallel Out ($B_P$) | 24A2 | W7 | |
| S05B | Magnetometer Range I.D. ($R_t$) | 192DP1-1 | W10 | |
| S06B | C1 Detector Count | 12DS1 | W9, W25 | |
| S07B | C2 Detector Count | 24DS4 | W15 | |
| S08B | C3 Detector Count | 24DS6 | W23 | |
| S09B | C4 Detector Count | 24DS10 | W31 | |
| S10B | C5 Detector Sector I Count | 24DS1 | W5 | |
| S11B | C5 Detector Sector II Count | 24DS3 | W13 | |
| S12B | C5 Detector Sector III Count | 24DS7 | W21 | |
| S13B | C5 Detector Sector IV Count | 24DS9 | W29 | |
| S14B | Curved Plate Voltage Monitor | 192A8 | W26 | |
| S15B | Zero Gamma Reference | 192A5 | W10 | |
| S16B | Open Telescope, Channel 1-4 Count | 4DS1 | W(8,12,16,24,28,32 | |
| S17B | Shielded Telescope, Chan. 1-4 Count | 4DS1 | W(8,12,16,24,28,32 | |
| S18B | Open Telescope, Channel 2 Count | 24DS2 | W11 | |
| S19B | Shielded Telescope, Channel 2 Count | 24DS2 | W11 | |
| S20B | Open Telescope, Channel 3 Count | 48DS1 | W14 | |
| S21B | Shielded Telescope, Channel 3 Count | 48DS1 | W14 | |
| S22B | Open Telescope, Channel 4 Count | 48DS3 | W14 | |
| S23B | Shielded Telescope, Channel 4 Count | 48DS3 | W14 | |
| S24B | Open Telescope, Channel 5 Count | 48DS2 | W30 | |
| S25B | Shielded Telescope, Channel 5 Count | 48DS2 | W30 | |
| S26B | Open Telescope, Channel 6 Count | 48DS4 | W30 | |
| S27B | Shielded Telescope, Channel 6 Count | 48DS4 | W30 | |
| S28B | Telescope I.D. (Open or Shielded) | 192DP1-2 | W10 | |

| Meas. No. | Measurement Title | Channel Code | Main Frame Word Number |
|---|---|---|---|
| S29B | Open Telescope Det. Temp. | 192A9 | W10 |
| S30B | Shielded Tele. Det. Temp. | 192A10 | W26 |
| S31B | Magnetometer Range ($R_p$) | 192DP1-3 | W10 |
| S32B | PHA Threshold | 192DP1-6 | W10 |
| S33B | Spare | 192DP1-7 | W10 |
| S34B | Magnetometer Temperature | 192A1 | W10 |
| Sun Sensor Measurements | | | |
| T01B | Sun Pulse Delay | 24DS8 | W27 |
| T02B | Spin Count | 192DS4 | W26 |
| T03B | Sun Elevation Angle | 192DS3 | W10 |
| T04B | Sector Period | 192DS5 | W26 |
| T05B | Sun Sensor Polarity | 192DP1-5 | W10 |
| Electrical Power Measurements | | | |
| E02B | Solar Array Current | 192A2 | W26 |
| E03B | Battery Voltage | 192A3 | W10 |
| E04B | Battery Current | 192A4 | W26 |
| E05B | Battery Temperature | 192A7 | W10 |
| E06B | Low Voltage Monitor | 192A6 | W26 |
| E08B | Undervolt. Protection IN/OUT | 2DP5-2 | W19 |

TABLE 2 (16 Pages). PARTICLES AND FIELDS SUBSATELLITE
MEASUREMENT LIST

| FORMAT LOCATION | MEASUREMENT TITLE | MEAS NO | CHAN CODE | SAMPLE INTERVAL RTD | SAMPLE INTERVAL MRO | SAMPLE INTERVAL TSN | SAMPLE INTERVAL TSF | MEASUREMENT DESCRIPTION | UNITS | MAX VALUE | MIN VALUE | ACCURACY | COMMENTS |
|---|---|---|---|---|---|---|---|---|---|---|---|---|---|
| W1-f0-b1 | Sync bit No 1 | D01B | 2DP1 | 2 | 2 | N/A | N/A | Fixed Bit Value 1 | N/A | N/A | N/A | N/A | Aerospace Data Systems Standard 20 Bit Sync Pattern |
| -b2 | Sync bit No 2 | | | | | | | Fixed Bit, Value 1 | | | | | |
| -b3 | Sync bit No 3 | | | | | | | Fixed Bit Value 1 | | | | | |
| -b4 | Sync bit No 4 | | | | | | | Fixed Bit Value 0 | | | | | |
| -b5 | Sync bit No 5 | | | | | | | Fixed Bit Value 1 | | | | | |
| -b6 | Sync bit No 6 | | | | | | | Fixed Bit Value 1 | | | | | |
| -b7 | Sync bit No 7 | | | | | | | Fixed Bit Value 0 | | | | | |
| -b8 | Sync bit No 8 | | | | | | | Fixed Bit Value 0 | | | | | |
| W2-f0-b1 | Sync bit No 9 | D02B | 2DP2 | 2 | 2 | N/A | N/A | Fixed Bit, Value 1 | N/A | N/A | N/A | N/A | |
| -b2 | Sync bit No 10 | | | | | | | Fixed Bit Value 1 | | | | | |
| -b3 | Sync bit No 11 | | | | | | | Fixed Bit, Value 1 | | | | | |
| -b4 | Sync bit No 12 | | | | | | | Fixed Bit, Value 0 | | | | | |
| -b5 | Sync bit No 13 | | | | | | | Fixed Bit, Value 0 | | | | | |
| -b6 | Sync bit No 14 | | | | | | | Fixed Bit, Value 0 | | | | | |
| -b7 | Sync bit No 15 | | | | | | | Fixed Bit Value 1 | | | | | |
| -b8 | Sync bit No 16 | | | | | | | Fixed Bit, Value 0 | | | | | |
| W3-f0-b1 | Sync bit No 17 | D03B | 2DP3-1 | 2 | 2 | N/A | N/A | Fixed Bit, Value 0 | N/A | N/A | N/A | N/A | 4 Bit frame counter. In MRO mode, counts frames read out from memory. |
| -b2 | Sync bit No 18 | | 2DP3-2 | | | | | Fixed Bit Value 0 | | | | | |
| -b3 | Sync bit No 19 | | 2DP3-3 | | | | | Fixed Bit, Value 0 | | | | | |
| -b4 | Sync bit No 20 | D03B | 2DP3-4 | | | | | Fixed Bit, Value 0 | | | | | |
| -b5 | Frame Count, Bit 1 | D10B | 2DP3-5 | | | | | 0 in F1 to F8, 1 in F9 to F16 | | | | | |
| -b6 | Frame Count, Bit 2 | | 2DP3-6 | | | | | 0 in F1 to F4 1 in F5 to F8 | | | | | |
| -b7 | Frame Count, Bit 3 | | 2DP3-7 | | | | | 0 in F1 to F2 1 in F3 to F4 | | | | | |
| -b8 | Frame Count, Bit 4 | | 2DP3-8 | | | | | 0 in F1, 1 in F2, 0 in F3, etc. | | | | | |
| W4-f0-b1 | Valid Command, Bit 1 | C01B | 2DP4-1 | 2 | 2 | N/A | N/A | Valid Command-1 No Command-0 | N/A | N/A | N/A | N/A | Held for 4 frames after command was received. |
| -b2 | Valid Command, Bit 2 | | 2DP4-2 | | | | | Valid Command-0, No Command-0 | | | | | |
| -b3 | Valid Command, Bit 3 | | 2DP4-3 | | | | | Valid Command-1, No Command-0 | | | | | |
| -b4 | Valid Command, Bit 4 | | 2DP4-4 | | | | | Valid Command-1, No Command-0 | | | | | |
| -b5 | Subsatellite ID Bit | D04B | 2DP4-5 | | | | | S/C #1 Bit=1 S/C #2 Bit=0 | | | | | |
| -b6 | Data Format(RTD or MRO) | D05B | 2DP4-6 | | | | | RTD Mode Bit=0, MRO mode, bit=1 | | | | | |
| -b7 | Automatic or Manual | D06B | 2DP4-7 | | | | | Auto.mode, Bit=1, Otherwise-0 | | | | | |
| -b8 | Calibrate ON/OFF Bit | D07B | 2DP4-8 | | | | | Calib. ON-1, Calib. OFF-0 | | | | | |

A

| ORIGINATOR | DATE | TITLE |
|---|---|---|
| | | |
| | | |
| MJO | | |

ENGINEERING SKETCH
TRW SPACE TECHNOLOGY LABORATORIES
SK
SHEET 1 OF 16

STL Form 5238 (Rev 12 63)

SK CHG LTR

TABLE 2. PARTICLES AND FIELDS SUBSATELLITE
MEASUREMENT LIST



| FORMAT LOCATION | MEASUREMENT TITLE | MEAS. NO. | CHAN. CODE | SAMPLE INTERVAL | | | | MEASUREMENT DESCRIPTION | UNITS | MAX VALUE | MIN VALUE | ACCURACY | COMMENTS |
|---|---|---|---|---|---|---|---|---|---|---|---|---|---|
| | | | | RTD | MRO | TSN | TSF | | | | | | |
| W5-f0-b0 | C5 Detector Sector I Count | S10B | 24DS1 | 2 | N/A | 24 | 12 | Accumulated count Sector I from C5 detector output | Counts | $2^{19}-1$ | 0 | ±3.1% | Accumulation time<br>TSN mode 0.5 sector period<br>TSF mode 0.25 sector period<br>RTD mode .50 seconds<br>Sector I is -45° to +45° of B field vector<br>MSB 0000 LLLL = 0 Counts<br>Magnitude Mantissa |
| W6-f0-b0 | Magnetometer Transverse Mag. ($B_{TM}$) - in MRO mode only | S01D | 24A1 | N/A | N/A | 24 | 12 | Transverse magnetometer magnitude dual range, 0-50γ and 0-200γ, range bit is W10-f3-b1 | Gamma | 200 | 0 | 2% | Magnitude measurement is in stored data format only |
| W6-f0-b0 | Magnetometer Transverse out ($B_T$)- in RTD mode only | S03R | 24A1 | 1 | N/A | N/A | N/A | Transverse magnetometer output, dual range, 0-50γ and 0-200γ, range bit is W10-f3-b1 | Gamma | ±200 | 0 | 2% | Direct sample of transverse output, sampled in real time mode only Bandwidth is -3db at 0.5 Hz |
| W7-f0-b0 | Magnetometer Parallel Out ($B_p$) | S04B | 24A2 | 2 | N/A | 24 | 12 | Parallel magnetometer output, dual range 0-50γ and 0-200γ range bit is W10-f3-b3 | Gamma | ±200 | 0 | 2% | Bandwidth is -3 db at .02 Hz in TSN and TSF modes, Bandwidth is -3db at 0.25 Hz in RTD mode. |

B

| ORIGINATOR | DATE | TITLE | ENGINEERING SKETCH |
|---|---|---|---|
| | | | TRW SPACE TECHNOLOGY LABORATORIES |
| | | | SK |
| MJO | | | SHEET 2 OF 16 |

STL Form 3318 Rev. 4/71

SK CHG LTR

TABLE 2 PARTICLES AND FIELDS SUBSATELLITE
MEASUREMENT LIST



| FORMAT LOCATION | MEASUREMENT TITLE | MEAS NO | CHAN CODE | SAMPLE INTERVAL | | | | MEASUREMENT DESCRIPTION | UNITS | MAX VALUE | MIN. VALUE | ACCURACY | COMMENTS |
|---|---|---|---|---|---|---|---|---|---|---|---|---|---|
| | | | | RTD | MRO | TSN | TSF | | | | | | |
| W8-f1-b0<br>·f4<br>·f5<br>·f8 | Shielded Telescope Ch. 1-4 | S17B | 4DS1 | 0.25 | N/A | 4 | 2 | Shielded telescope channels 1-4 output | Counts | $2^{19}-1$ | Zero | ±3.1% | Accumulation time equals sample interval<br>MSB 0000-1111 = 0 Counts<br>Mantissa<br>Magnitude |
| W8-f2-b0<br>f3<br>f6<br>f7 | Open Telescope Ch. 1-4 | S16B | 4DS1 | 0.25 | N/A | 4 | 2 | Open telescope channels 1-4 | Counts | $2^{19}-1$ | 0 | ±3.1% | Accumulation time equals sample interval<br>MSB 0000-1111 = 0 Counts<br>Mantissa<br>Magnitude |
| W9-f0-b0 | C1 Detector Count | S06B | 12DS1 | 1 | N/A | 12 | 6 | C1 Detector Counts | Counts | $2^{19}-1$ | 0 | ±3 1% | Accumulation Time<br>TSN mode: 2 x sector period<br>TSF mode: 1 x sector period<br>RTD mode: 1 second<br>MSB 0000-1111 = 0 Counts<br>Magnitude Mantissa |
| W10-f1-b0 | Elapsed Time, Coarse | D08B | 192DS1 | 16 | N/A | 192 | 96 | Binary count of $2^{12}$ second intervals | $2^{12}$ sec. | $2^{12}(2^8-1)$ Sec | 0 | 0.05% | Msb cycles in $2^{20}$ seconds (12 days, 3 hrs., 16 m, 16 s), non-resetting |

| ORIGINATOR | DATE | TITLE | ENGINEERING SKETCH |
|---|---|---|---|
| | | | TRW SPACE TECHNOLOGY LABORATORIES |
| | | | SK |
| MJO | | | SHEET 3 OF 16 |

| NAME AND ADDRESS<br>TRW Systems<br>One Space Park<br>Redondo Beach, Calif.<br>90278 | SPECIFICATION CHANGE NOTICE<br>☐ PRELIMINARY ☒ FINAL | PAGE 3 OF 9<br>DATE 7/27/71 |
|---|---|---|

| CONTRACT NUMBER | ECP NO. | SCN NO. | REVISION |
|---|---|---|---|
| NAS9-10800 | NA | 1 | NC |

| EXPERIMENT NUMBER | SPECIFICATION NUMBER, TITLE AND DATE |
|---|---|
| S164, S173, S174 | 16763-40B; P&F Subsatellite Measurement List |

| APPROVAL AUTHORITY | FILE OPPOSITE SPECIFICATION |
|---|---|
| MSC TWX #BC341/T184-71/L90 of 7/27 | PAGE NO. 9 |

SPECIFICATION CHANGE

Page 9

1) Measurement No. T03B: Change comment to read;

"See Calibration Report for each subsatellite for interpretation of data."

2) Measurement No. S34B and 3) Measurement No. E03B: Change comment to read:

"See Calibration Report for each subsatellite for exact telemetry calibration range."

SK CHG LTR



TABLE 2 PARTICLES AND FIELDS SUBSATELLITE
MEASUREMENT LIST

| FORMAT LOCATION | MEASUREMENT TITLE | MEAS NO | CHAN CODE | SAMPLE INTERVAL RTD | MPO | TSN | TSF | MEASUREMENT DESCRIPTION | UNITS | MAX VALUE | MIN. VALUE | ACCURACY | COMMENTS |
|---|---|---|---|---|---|---|---|---|---|---|---|---|---|
| W10-f2-b0 | Sun Elevation Angle | T03B | 192DS3 | 16 | N/A | 192 | 96 | Elevation of sun above equatorial plane of satellite | Degrees | 36° | -36° | ± .2° | Angle = (t/T - 1 5/360) T] 960° where t = [(binary count)/1024] ·0.48 ms T = Spin period P = Polarity (+1 or -1) Polarity bit appears on W10-f3-b5 |
| W10-f3-b1 | $B_t$ Magn. Range ($R_t$) | S05B | 192DP1-1 | 16 | N/A | 192 | 96 | Range of transverse Magnet. | N/A | 1 | 0 | N/A | 0-50γ range, 1-200 γ range |
| -b2 | Telescope Identifier | S28R | 192DP1-2 | 16 | N/A | 192 | 96 | Level of Telescope Select | N/A | 1 | 0 | N/A | 0- Open, 1 - Shielded |
| -b3 | Bp Magn. Range ($R_p$) | S31B | 192DP1-3 | 16 | N/A | 192 | 96 | Range of Parallel Magnet. | N/A | 1 | 0 | N/A | 0-50γ range, 1-200γ range |
| -b4 | Bit Rate | D11B | 192DP1-4 | 16 | N/A | 192 | 96 | Bit rate of stored data | N/A | 1 | 0 | N/A | 0-8 bps (TSN), 1-16 bps (TSF) |
| -b5 | Sun Sensor Polarity | T05B | 192DP1-5 | 16 | N/A | 192 | 96 | Sun in upper/lower hemisphere | N/A | 1 | 0 | N/A | 0 - Upper, 1 - lower |
| -b6 | PHA Threshold Hi/Lo | S32B | 192DP1-6 | 16 | N/A | 192 | 96 | Threshold level of PHA | N/A | 1 | 0 | N/A | 0 - Low, 1 - High |
| -b7 | Spare | | 192DP1-7 | 16 | N/A | 192 | 96 | | | | | | |
| -b8 | Spare | | 192DP1-8 | 16 | N/A | 192 | 96 | | | | | | |
| W10-f4-b0 | Magnetometer Temp. | S34B | 192A1 | 16 | N/A | 192 | 96 | Temperature at magnetometer sensor | °C | -18 | +50 | ±1°C | See Calibration Report |
| W10-f5-b | Battery/Solar Array Volts | E03B | 192A3 | 16 | N/A | 192 | 96 | Battery & Solar Array Voltage | Volts | 17.92 | 0 | 2% | Scale Factor: 7 mV per bit |

A

A

| ORIGINATOR | DATE | TITLE |
|---|---|---|
| | | |
| | | |
| MJO | | |

ENGINEERING SKETCH
TRW SPACE TECHNOLOGY LABORATORIES
SK
SHEET 4 OF 16

STL Form 5218 (Rev. 12-81)

| NAME AND ADDRESS<br>TRW Systems<br>One Space Park<br>Redondo Beach, Calif.<br>90278 | SPECIFICATION CHANGE NOTICE<br>☐ PRELIMINARY ☒ FINAL | PAGE 4 OF 9<br>DATE 7/27/71 |
|---|---|---|

| CONTRACT NUMBER | ECP NO. | SCN NO. | REVISION |
|---|---|---|---|
| NAS9-10800 | NA | 1 | NC |

| EXPERIMENT NUMBER | SPECIFICATION NUMBER, TITLE AND DATE |
|---|---|
| S164, S173, S174 | 16763-40B; P&F Subsatellite Measurement List |

| APPROVAL AUTHORITY | FILE OPPOSITE SPECIFICATION PAGE NO. 10 |
|---|---|
| MSC TWX #BC341/T184-71/L90 of 7/27 | |

SPECIFICATION CHANGE
Page 10

1) Measurement No. S15B: Change comment to read:

"Output to be used for Zero Gamma reference value. See Calibration Report for each subsatellite for exact nominal value."

2) & 3) Measurement No.s E05B and S29B: Change comments to read:

"See Calibration Report for each subsatellite for exact telemetry calibration range."

SK CMG LTR

TABLE 2. PARTICLES AND FIELDS SUBSATELLITE
MEASUREMENT LIST



| FORMAT LOCATION | MEASUREMENT TITLE | MEAS. NO. | CHAN. CODE | SAMPLE INTERVAL | | | | MEASUREMENT DESCRIPTION | UNITS | MAX. VALUE | MIN. VALUE | ACCURACY | COMMENTS |
|---|---|---|---|---|---|---|---|---|---|---|---|---|---|
| | | | | RTD | MPO | TSN | TSF | | | | | | |
| W10-f6-b0 | Zero Gamma Reference Voltage | S15B | 192A5 | 16 | N/A | 192 | 96 | Analog voltage representing the zero gamma output of the magnetometer | Volts | 2.600 | 2 400 | ±0.010 | Output to be used for Zero Gamma reference value |
| W10-f7-b0 | Battery Temperature | E05B | 192A7 | 16 | N/A | 192 | 96 | Temperature of Satellite Batt. | °F | +118° | -10° | ± 2% | Scale Factor: 0.5°F per bit |
| W10-f8-b0 | Open Telescope Temp. | S29B | 192A9 | 16 | N/A | 192 | 96 | Detector temperature of open solid state telescope | °C | -40 | +40 | ± 1° | See Calibration Report |
| W11-f1-b0 -f5 | Shielded Telescope Channel 2 | S19B | 24DS2 | 2 | N/A | 24 | 12 | Shielded Telescope, Chan 2 | Counts | $2^{19}-1$ | 0 | ±3.1% | Accumulation Times are:<br>TSN mode - 24 seconds<br>TSF mode - 12 seconds<br>RTD mode - 2 seconds<br>MSB 0000-1111 = 0 Counts<br>Mantissa<br>Magnitude |

B

B

| ORIGINATOR | DATE | TITLE | ENGINEERING SKETCH |
|---|---|---|---|
| | | | TRW SPACE TECHNOLOGY LABORATORIES |
| | | | SK |
| MJO | | | SHEET 5 OF 16 |

STL Form 5218 -Rev

TABLE 2

| FORMAT LOCATION | MEASUREMENT TITLE | MEAS. NO. | CODE | SAMPLE INTERVAL | | | | MEASUREMENT DESCRIPTION | UNITS | MAX. VALUE | MIN. VALUE | ACCURACY | COMMENTS | |
|---|---|---|---|---|---|---|---|---|---|---|---|---|---|---|
| | | | | RTD | MRO | TSN | TSF | | | | | | | |
| W11-f2-b0 -f6 | Open Telescope Channel 2 | S18B | 24DS2 | 6 | N/A | 72 | 36 | Open Telescope, Chan. 2 | Counts | $2^{19}-1$ | 0 | $\pm$3.1% | Accumulation Times are:<br>TSN mode - 24 seconds<br>TSF mode - 12 seconds<br>RTD mode - 2 seconds<br>MSB 0000-1111 = 0 Counts<br>Magnitude └ Mantissa | B |
| W11-f3-b0 -f7 | Open Telescope Channel 2 | S18B | 24DS2 | 2 | N/A | 24 | 12 | Open Telescope, Chan 2 | Counts | $2^{19}-1$ | 0 | $\pm$3.1% | Accumulation Times are<br>TSN mode - 24 seconds<br>TSF mode - 12 seconds<br>RTD mode - 2 seconds<br>MSB 0000-1111 = 0 Counts<br>Magnitude └ Mantissa | B |
| W11-f4-b0 -f8 | Shielded Telescope Channel 2 | S19B | 24DS2 | 6 | N/A | 72 | 36 | Shielded Telescope, Chan. 2 | Counts | $2^{19}-1$ | 0 | $\pm$3.1% | Accumulation Times are:<br>TSN mode - 24 seconds<br>TSF mode - 12 seconds<br>RTD mode - 2 seconds<br>MSB 0000-1111 = 0 Counts<br>Magnitude └ Mantissa | B |
| W12-f1-b0 f2 f5 f6 | Open Telescope Channels 1-4 | S16B | 4DS1 | 0.5 | N/A | 4 | 2 | Open Telescope, Channels 1-4 | Counts | $2^{19}-1$ | 0 | $\pm$ 3.1% | Accumulation time equals sample interval<br>MSB 0000-1111 = 0 Counts<br>Mantissa<br>Magnitude | B |

| ORIGINATOR | DATE | TITLE | ENGINEERING SKETCH |
|---|---|---|---|
| | | | TRW SPACE TECHNOLOGY LABORATORIES |
| | | | SK |
| MJO | | | SHEET 6 OF 16 |

STL Form 5218 Rev

TABLE 2

| FORMAT LOCATION | MEASUREMENT TITLE | MEAS. NO. | CHAN. CODE | SAMPLE INTERVAL RTD | SAMPLE INTERVAL MRO | SAMPLE INTERVAL TSN | SAMPLE INTERVAL TSF | MEASUREMENT DESCRIPTION | UNITS | MAX. VALUE | MIN. VALUE | ACCURACY | COMMENTS | |
|---|---|---|---|---|---|---|---|---|---|---|---|---|---|---|
| W12-f3-b0<br>f4<br>f7<br>-f8 | Shielded Telescope Channels 1-4 | S17B | 4DS1 | 0.5 | N/A | 4 | 2 | Shielded Telescope, Chan. 1-4 | Counts | $2^{19}-1$ | 0 | ±3.1% | Accumulation time equals sample interval<br>MSB 0000-1111 = 0 Counts<br>Mantissa<br>Magnitude | B |
| W13-f0-b0 | $C_5$ Detector Sector II Count | S11B | 24DS3 | 0.5 | N/A | 24 | 12 | C5 Detector, Sector II | Counts | $2^{19}-1$ | 0 | ±3.1% | Accumulation time:<br>TSN mode 0.5 sector period<br>TSF mode 0.25 sector period<br>RTD mode 50 seconds<br>Sector II is -45° to -90° and +45° to +90° of B field vector.<br>MSB 0000-1111 = 0 Counts<br>Magnitude — Mantissa | B |
| W14-f1-b0<br>-f5 | Shielded Telescope Channel 3 | S21B | 48DS1 | 8 | N/A | 96 | 48 | Shielded Telescope, Chan. 3 | Counts | $2^{19}-1$ | 0 | ±3.1% | Accumulation times are:<br>TSN mode: 48 seconds<br>TSF mode: 24 seconds<br>RTD mode: 4 seconds<br>MSB 0000-1111 = 0 Counts<br>Magnitude — Mantissa | B |
| W14-f2-b0<br>f6 | Shielded Telescope Channel 4 | S23B | 48DS3 | 8 | N/A | 96 | 48 | Shielded Telescope, Chan. 4 | Counts | $2^{19}-1$ | 0 | ±3.1% | Accumulation times are:<br>TSN mode: 48 seconds<br>TSF mode: 24 seconds<br>RTD mode: 4 seconds<br>MSB 0000-1111 = 0 Counts<br>Magnitude — Mantissa | B |

| ORIGINATOR | DATE | TITLE | ENGINEERING SKETCH |
|---|---|---|---|
| | | | TRW SPACE TECHNOLOGY LABORATORIES |
| | | | SK |
| MJO | | | SHEET 7 OF 16 |

TABLE 2

| FORMAT LOCATION | MEASUREMENT TITLE | MEAS. NO. | CHAN CODE | SAMPLE INTERVAL | | | | MEASUREMENT DESCRIPTION | UNITS | MAX VALUE | MIN. VALUE | ACCURACY | COMMENTS | |
|---|---|---|---|---|---|---|---|---|---|---|---|---|---|---|
| | | | | RTD | MPO | TSN | TSF | | | | | | | |
| W14-f3-b0 -f7 | Open Telescope Channel 3 | S20B | 48DS1 | 8 | N/A | 96 | 48 | Open Telescope, Chan 3 | Counts | $2^{19}-1$ | 0 | ±3.1% | Accumulation Times are<br>TSN mode 48 seconds<br>TSF mode 24 seconds<br>RTD mode 4 seconds<br>MSB 0000-1111 = 0 Counts<br>Magnitude └ Mantissa | B |
| W14-f4-b0 -f8 | Open Telescope Channel 4 | S22B | 48DS3 | 8 | N/A | 96 | 48 | Open Telescope, Chan. 4 | Counts | $2^{19}-1$ | 0 | ±3.1% | Accumulation Times are<br>TSN mode 48 seconds<br>TSF mode 24 seconds<br>RTD mode 4 seconds<br>MSB 0000-1111 = 0 Counts<br>Mantissa<br>Magnitude | B |
| W15-f0-b0 | C2 Detector Count | S07B | 24DS4 | 2 | N/A | 24 | 12 | C2 Detector Count | Counts | $2^{19}-1$ | 0 | ±3.1% | Accumulation Times are<br>TSN mode 4 x sector period<br>TSF mode 2 x sector period<br>RTD mode 2 seconds<br>MSB 0000-1111 = 0 Counts<br>Mantissa<br>Magnitude | B |
| W16-f1-b0 -f2 -f5 -f6 | Open Telescope Channels 1-4 | S16B | 4DS1 | 25 | N/A | 4 | 2 | Open Telescope, Chan. 1-4 | Counts | $2^{19}-1$ | 0 | ±3.1% | Accumulation time equals sample interval<br>MSB 0000-1111 = 0 Counts<br>Mantissa<br>Magnitude | B |

| ORIGINATOR | DATE | TITLE |
|---|---|---|
| | | |
| | | |
| MJO | | |

ENGINEERING SKETCH
TRW SPACE TECHNOLOGY LABORATORIES
SK
SHEET 8 OF 16

STL Form 5218 Rev. 12/83

| NAME AND ADDRESS<br>TRW Systems<br>One Space Park<br>Redondo Beach, Calif.<br>90278 | SPECIFICATION CHANGE NOTICE<br>☐ PRELIMINARY ☒ FINAL | PAGE 5 OF 9<br>DATE 7/27/71 |
|---|---|---|

| CONTRACT NUMBER | ECP NO. | SCN NO. | REVISION |
|---|---|---|---|
| NAS9-10800 | NA | 1 | NC |

| EXPERIMENT NUMBER | SPECIFICATION NUMBER, TITLE AND DATE |
|---|---|
| S164, S173, S174 | 16763-40B; P&F Subsatellite Measurement List |

| APPROVAL AUTHORITY | FILE OPPOSITE SPECIFICATION |
|---|---|
| MSC TWX #BC341/T184-71/L90 of 7/27 | PAGE NO. 14 |

SPECIFICATION CHANGE

Page 14

1) Measurement No. C03B: Change comment to read:

"Deviation from center frequency is nominally 1KHz/count. See Calibration Report for each subsatellite for exact telemetry calibration range."

2) Measurement No. D12B: Change comment to read:

"See Calibration Report for each subsatellite for exact nominal value."

TABLE 2

| FORMAT LOCATION | MEASUREMENT TITLE | MEAS. NO. | CHAN. CODE | SAMPLE INTERVAL RTD | MRO | TSN | TSF | MEASUREMENT DESCRIPTION | UNITS | Max VALUE | MIN. VALUE | ACCURACY | COMMENTS |
|---|---|---|---|---|---|---|---|---|---|---|---|---|---|
| W16-f3-b0<br>-f4<br>-f7<br>-f8 | Shielded Telescope Channels 1-4 | S17B | 4DS1 | 25 | N/A | 4 | 2 | Shielded Telescope, Chan. 1-4 | Counts | $2^{19}-1$ | 0 | ±3 1% | Accumulation time equals sample interval<br>MSB 0000-1111 = 0 Counts<br>Mantissa<br>Magnitude |
| W17-f0-b0 | Receiver Loop Stress | C03B | 2A1 | 2 | 2 | N/A | N/A | Indicates deviation of locked frequency from center freq. | Hz | +150Hz | -150Hz | ±2% | Center Frequency - 2.5V (binary counts = 128)<br>Deviation from C.F - 50 KHz per volt nominal (1 KHz per bit) |
| W18-f0-b0 | 2.56V Calibration Voltage | D12B | 2A2 | 2 | 2 | N/A | N/A | Analog voltage quantitatively indicating performance of the analog-to-digital converter (ADC) | Volts | 2.570 | 2.550 | ±1% | |
| W19-f0-b1<br>-b2<br>-b3<br>-b4<br>-b5<br>-b6<br>-b7<br>-b8 | Receiver Sig. Present<br>UV Protection IN/OUT | C02B<br>E08B | 2DP5-1<br>2DP5-2 | 2<br>2 | 2<br>2 | N/A<br>N/A | N/A<br>N/A | Indicates lock-up of receiver<br>Command Verification | N/A<br>N/A | 1<br>1 | 0<br>0 | N/A<br>N/A | 0 - Rcvr not locked, 1 - Recvr locked<br>0 - UVP in, 1 - UVP out |

| ORIGINATOR | DATE | TITLE |
|---|---|---|
| | | |
| | | |
| MJO | | |

ENGINEERING SKETCH
TRW SPACE TECHNOLOGY LABORATORIES
SK
SHEET 9 OF 16

STL Form 5218 (Rev 12 63)

| NAME AND ADDRESS<br>TRW Systems<br>One Space Park<br>Redondo Beach, Calif. 90278 | SPECIFICATION CHANGE NOTICE<br>☐ PRELIMINARY ☒ FINAL | PAGE 6 OF 9<br>DATE 7/27/71 |
|---|---|---|

| CONTRACT NUMBER | ECP NO. | SCN NO. | REVISION |
|---|---|---|---|
| NAS9-10800 | NA | 1 | NC |

| EXPERIMENT NUMBER | SPECIFICATION NUMBER, TITLE AND DATE |
|---|---|
| S164, S173, S174 | 16763-40B; P&F Subsatellite Measurement List |

| APPROVAL AUTHORITY | FILE OPPOSITE SPECIFICATION |
|---|---|
| MSC TWX #BC341/T184-71/L90 of 7/27 | PAGE NO. 15 |

SPECIFICATION CHANGE
Page 15

1) Measurement No S02D: Change comment to read:

$$T_m = \frac{\text{(binary count)}}{32} + 0.0156$$

2) Measurement No. S03R; Change comment to read:

"In RTD mode only. Same as W6-f0-b0. See Calibration Report for each subsatellite for exact telemetry calibration range."

TABLE 2

| FORMAT LOCATION | MEASUREMENT TITLE | MEAS NO. | CHAN CODE | SAMPLE INTERVAL | | | | MEASUREMENT DESCRIPTION | UNITS | MAX VALUE | MIN VALUE | ACCURACY | COMMENTS |
|---|---|---|---|---|---|---|---|---|---|---|---|---|---|
| | | | | RTD | MRO | TSN | TSF | | | | | | |
| W20-f0-b1<br>-b2<br>-b3<br>-b4<br>-b5<br>-b6<br>-b7<br>-b8 | Spare | | 2DP6-1 | 2 | 2 | N/A | N/A | | | | | | |
| W21-f0-b0 | C5 Detector Sector III Count | S12B | 24DS7 | 2 | N/A | 24 | 12 | C5 Detector, Sector III counts | Counts | $2^{19}-1$ | 0 | ±3 1% | Accumulation time<br>TSN mode 0.5 sector period<br>TSF mode 0 25 sector period<br>RTD mode 50 seconds<br>Sector III is -90° to 135° and +90° to +135° of B field vector<br>MSB 0000-1111 = 0 Counts<br>Magnitude — Mantissa |
| W22-f0-b0 | Magn Time Delay ($T_M$) (in MRO mode only) | S02D | 24DS5 | N/A | N/A | 24 | 12 | Time delay of magnetometer zero crossing pulse reference to frame start | 31.2 ms | 8 sec | 0 sec | ±15.6ms | Tm = (0.0312) x (binary count)+.0155<br>In TSN or TSF modes only |
| W22-f0-b0 | Magnetometer Transverse Out ($B_T$) - in RTD mode only. | S03R | 24A1 | 2 | N/A | N/A | N/A | Transverse Magnetometer output, dual range, 0-50γ and 0-200 range bit is W10-f3-b0 | Gamma | +200 | -200 | ± 1% | In RTD mode only Same as W6-f0-b0. |

B

| ORIGINATOR | DATE | TITLE | ENGINEERING SKETCH |
|---|---|---|---|
| | | | TRW SPACE TECHNOLOGY LABORATORIES |
| | | | SK |
| MJO | | | SHEET 10 OF 16 |

TABLE 2 PARTICLES AND FIELDS SUBSATELLITE
MEASUREMENT LIST

| FORMAT LOCATION | MEASUREMENT TITLE | MEAS NO | CHAN. CODE | SAMPLE INTERVAL RTD | MRO | TSN | TSF | MEASUREMENT DESCRIPTION | UNITS | MAX VALUE | MIN. VALUE | ACCURACY | COMMENTS |
|---|---|---|---|---|---|---|---|---|---|---|---|---|---|
| W23-f0-b0 | C3 Detector Count | S08B | 24DS6 | 2 | N/A | 24 | 12 | C3 Accumulated Count | Counts | $2^{19}-1$ | 0 | ± 3.1% | Accumulation Time:<br>TSN mode: 4 x sector period<br>TSF mode: 2 x sector period<br>RTD mode: 2 seconds<br>MSB 0000-1111 = 0 Counts<br>Magnitude └ Mantissa |
| W24-f1-b0<br>-f2<br>-f5<br>-f6 | Open Telescope Channels 1-4 | S16B | 4DS1 | 25 | N/A | 4 | 2 | Open Telescope, Chan. 1-4 | Counts | $2^{19}-1$ | 0 | ± 3.1% | Accumulation time equals sample interval<br>MSB 0000-1111 = 0 Counts<br>Mantissa<br>Magnitude |
| W24-f3-b0<br>-f4<br>-f7<br>-f8 | Shielded Telescope Channels 1-4 | S17B | 4DS1 | 25 | N/A | 4 | 2 | Shielded Telescope, Chan. 1-4 | Counts | $2^{19}-1$ | 0 | ± 3.1% | Accumulation time equals sample interval.<br>MSB 0000-1111 = 0 Counts<br>Mantissa<br>Magnitude |
| W25-f0-b0 | C1 Detector Count | S06B | 12DS1 | 1 | N/A | 12 | 6 | C1 Accumulated Counts | Counts | $2^{19}-1$ | 0 | ± 3.1% | Accumulation Time:<br>TSN mode: 2 x sector period<br>TSF mode: 1 x sector period<br>RTD mode: 1 second<br>MSB 0000-1111 = 0 Counts<br>Mantissa<br>Magnitude |

B B B B

| NAME AND ADDRESS<br>TRW Systems<br>One Space Park<br>Redondo Beach, Calif. 90278 | SPECIFICATION CHANGE NOTICE<br>☐ PRELIMINARY ☒ FINAL | PAGE 7 OF 9<br>DATE 7/27/71 |
|---|---|---|

| CONTRACT NUMBER | ECP NO. | SCN NO. | REVISION |
|---|---|---|---|
| NAS9-10800 | NA | 1 | NC |

| EXPERIMENT NUMBER | SPECIFICATION NUMBER, TITLE AND DATE |
|---|---|
| S164, S173, S174 | 16763-40B; P&F Subsatellite Measurement List |

| APPROVAL AUTHORITY | FILE OPPOSITE SPECIFICATION |
|---|---|
| MSC TWX #BC341/T184-71/L90 of 7/27 | PAGE NO. 17 |

SPECIFICATION CHANGE

Page 17

Measurement No. E02B: Change comments to read:

See Calibration Report for each S/S for exact TLM calibration range.

TABLE 2. PARTICLES AND FIELDS SUBSATELLITE
MEASUREMENT LIST

| FORMAT LOCATION | MEASUREMENT TITLE | MEAS. NO. | CHAN. CODE | SAMPLE INTERVAL | | | | MEASUREMENT DESCRIPTION | UNITS | MAX VALUE | MIN. VALUE | ACCURACY | COMMENTS |
|---|---|---|---|---|---|---|---|---|---|---|---|---|---|
| | | | | RTD | MRO | TSN | TSF | | | | | | |
| W26-f1-b0 | Elapsed Time, Fine | D09B | 192DS2 | 16 | N/A | 192 | 96 | Binary count of $2^4$ second intervals | $2^4$ sec | $2^4(2^8-1)$ Sec | 0 | 0.05% | 8 bit counter counts units of 16 second intervals, thus LSB changes state every 16 seconds. |
| W26-f2-b0 | Spin Count | T02B | 192DS4 | 16 | N/A | 192 | 96 | Count of sun pulses and magnetometer pulses | revs | 256 | 0 | | Non-resetting counter, counts sun pulses in sunlight and magnetometer pulses in eclipse. Sun presence logic level output selects magnetometer pulses in eclipse. |
| W26-f3-b0 | Sector Period | T04B | 192DS5 | 16 | N/A | 192 | 96 | Period of Spin | sec | 8 | 0 | ±15.6ms | Measured spin period that is used in retaining and accumulation control. Updated every 8 frames. Period = (.0312)(binary count) |
| W26-f4-b0 | Solar Array Current | E02B | 192A2 | 16 | N/A | 192 | 96 | Output current of solar array | Amps | 2.048 | 0 | ±2% | Scale Factor: 8 mA per bit |

| ORIGINATOR | DATE | TITLE |
|---|---|---|
| | | |
| | | |
| MJO | | |

ENGINEERING SKETCH
TRW SPACE TECHNOLOGY LABORATORIES

SK
SHEET 12 OF 16

STL Form 5218 (Rev. 12-83)

| NAME AND ADDRESS<br>TRW Systems<br>One Space Park<br>Redondo Beach, Calif.<br>90278 | SPECIFICATION CHANGE NOTICE<br>☐ PRELIMINARY ☒ FINAL | PAGE 8 OF 9<br>DATE 7/27/71 |
|---|---|---|

| CONTRACT NUMBER | ECP NO. | SCN NO. | REVISION |
|---|---|---|---|
| NAS9-10800 | NA | 1 | NC |

| EXPERIMENT NUMBER | SPECIFICATION NUMBER, TITLE AND DATE |
|---|---|
| S164, S173, S174 | 16763-40B; P&F Subsatellite Measurement List |

| APPROVAL AUTHORITY | FILE OPPOSITE SPECIFICATION |
|---|---|
| MSC TWX #BC341/T184-71/L90 of 7/27 | PAGE NO. 18 |

SPECIFICATION CHANGE

Page 18

1) Measurement No. E04B · Change comment to read:

"See Calibration Report for each S/S for exact TLM calibration range."

2) Measurement No. E06B Change comments to read:

"Scale Factor: 20 mV per bit. See Calibration Report for each S/S for exact nominal value".

3) Measurement No. S14B Change comments to read:

"Scale Factor: 20 mV per bit. See Calibration Report for each S/S for exact nominal value".

4) Measurement No. S30B Change comments to read:

"See Calibration Report for each S/S for exact TLM calibration range."

TABLE 2. PARTICLES AND FIELDS SUBSATELLITE
MEASUREMENT LIST

| FORMAT LOCATION | MEASUREMENT TITLE | MEAS NO. | CHAN. CODE | SAMPLE INTERVAL | | | | MEASUREMENT DESCRIPTION | UNITS | MAX VALUE | MIN. VALUE | ACCURACY | COMMENTS |
|---|---|---|---|---|---|---|---|---|---|---|---|---|---|
| | | | | RTD | MRO | TSN | TSF | | | | | | |
| W26-f5-b0 | Battery Current | E04B | 192A4 | 16 | N/A | 192 | 96 | Positive or negative battery current | Amps | +1.92 | -1 92 | 2% | Scale Factor: 15 mA per bit |
| W26-f6-b0 | Low Voltage Monitor | E06B | 192A6 | 16 | N/A | 192 | 96 | +5 Volt Monitor | Volts | 5 12 | 0 | 2% | Scale Factor: 20 mV per bit |
| W26-f7-b0 | Curved Plate Volt Monitor | S14B | 192A8 | 16 | N/A | 192 | 96 | 5.0 Volt Monitor proportional to HV | Volts | 5 12 | 0 | 2% | Scale Factor: 20 mV per bit |
| W26-f8-b0 | Shielded Telescope Temperature | S30B | 192A10 | 16 | N/A | 192 | 96 | Detector Temperature | °C | -40 | +40 | 2% | See Calibration Report |

A

| NAME AND ADDRESS<br>TRW Systems<br>One Space Park<br>Redondo Beach, Calif.<br>90278 | SPECIFICATION CHANGE NOTICE<br>☐ PRELIMINARY ☒ FINAL | PAGE 9 OF 9<br>DATE 7/27/71 |
|---|---|---|

| CONTRACT NUMBER | ECP NO. | SCN NO. | REVISION |
|---|---|---|---|
| NAS9-10800 | NA | 1 | N C |

| EXPERIMENT NUMBER | SPECIFICATION NUMBER, TITLE AND DATE |
|---|---|
| S164, S173, S174 | 16763-40B; P&F Subsatellite Measurement List |

| APPROVAL AUTHORITY | FILE OPPOSITE SPECIFICATION |
|---|---|
| MSC TWX #BC341/T184-71/L90 of 7/27 | PAGE NO. 19 |

SPECIFICATION CHANGE

Page 19

1) Measurement No. T01B Change comment to read:

$$T_s = \frac{\text{Binary Counts}}{32} + .0156$$

185

TABLE 2. PARTICLES AND FIELDS SUBSATELLITE
MEASUREMENT LIST

| FORMAT LOCATION | MEASUREMENT TITLE | MEAS. NO. | CHAN. CODE | SAMPLE INTERVAL RTD | SAMPLE INTERVAL MPO | SAMPLE INTERVAL TSN | SAMPLE INTERVAL TSF | MEASUREMENT DESCRIPTION | UNITS | MAX. VALUE | MIN. VALUE | ACCURACY | COMMENTS |
|---|---|---|---|---|---|---|---|---|---|---|---|---|---|
| W27-f0-b0 | Sun Pulse Delay | T01B | 24DS8 | 2 | N/A | 24 | 12 | Time delay of sun pulse from frame start | sec | 8 sec | 0 | ±15.6ms | $T_s$ = ( 0312) (binary count) + 0.0155 |
| W28-f1-b0 -f2 -f5 -f6 | Open Telescope Channels 1-4 | S16B | 4DS1 | 0.5 | N/A | 4 | 2 | Open Telescope, Chan 1-4 | Counts | $2^{19}-1$ | 0 | ± 3 1% | Accumulation time equals sample interval. MSB 0000-1111 = 0 Counts (Mantissa / Magnitude) B |
| W28-f3-b0 .f4 .f7 -f8 | Shielded Telescope Channels 1-4 | S17B | 4DS1 | 0.5 | N/A | 4 | 2 | Shielded Telescope, Chan. 1-4 | Counts | $2^{19}-1$ | 0 | ± 3 1% | Accumulation time equals sample interval. MSB 0000-1111 = 0 Counts (Mantissa / Magnitude) B |
| W29-f0-b0 | C5 Detector Sector IV Count | S13B | 24DS9 | 0.5 | N/A | 24 | 2 | C5 Detector, Sector IV | Counts | $2^{19}-1$ | 0 | ± 3 1% | Accumulation time: TSN mode 0.5 sector period; TSF mode 0.25 sector period; RTD mode 50 seconds. Sector IV is +135° to -135° from B field vector. MSB 0000-1111 = 0 Counts (Magnitude / Mantissa) B |

| ORIGINATOR | DATE | TITLE |
|---|---|---|
| | | |
| | | |
| MJO | | |

ENGINEERING SKETCH
TRW SPACE TECHNOLOGY LABORATORIES
SK
SHEET 14 OF 16

TABLE 2 PARTICLES AND FIELDS SUBSATELLITE
MEASUREMENT LIST

| FORMAT LOCATION | MEASUREMENT TITLE | MEAS. NO. | CHAN CODE | SAMPLE INTERVAL | | | | MEASUREMENT DESCRIPTION | UNITS | MAX VALUE | MIN VALUE | ACCURACY | COMMENTS |
|---|---|---|---|---|---|---|---|---|---|---|---|---|---|
| | | | | RTD | MRO | TSN | TSF | | | | | | |
| W30-f1-b0 -f5 | Shielded Telescope Channel 5 | S25B | 48DS2 | 8 | N/A | 96 | 48 | Shielded Telescope Chan 5 | Counts | $2^{19}-1$ | 0 | ± 3.1% | Accumulation Time: TSN mode 48 seconds TSF mode 24 seconds RTD mode 4 seconds MSB 0000-1111 = 0 Counts Magnitude └ Mantissa |
| W30-f2-b0 -f6 | Shielded Telescope Channel 6 | S27B | 48DS4 | 8 | N/A | 96 | 48 | Shielded Telescope Chan. 6 | Counts | $2^{19}-1$ | 0 | ± 3.1% | Accumulation Time TSN mode 48 seconds TSF mode 24 seconds RTD mode 4 seconds MSB 0000-1111 = 0 Counts Magnitude └ Mantissa |
| W30-f3-b0 -f7 | Open Telescope Channel 5 | S24B | 48DS2 | 8 | N/A | 96 | 48 | Open Telescope, Chan. 5 | Counts | $2^{19}-1$ | 0 | ± 3.1% | Accumulation Time TSN mode 48 seconds TSF mode 24 seconds RTD mode 4 seconds MSB 0000-1111 = 0 Counts Magnitude └ Mantissa |
| W30-f4-b0 -f8 | Open Telescope Channel 6 | S26B | 48DS4 | 8 | N/A | 96 | 48 | Open Telescope, Chan. 6 | Counts | $2^{19}-1$ | 0 | ± 3.1% | Accumulation Time: TSN mode 48 seconds TSF mode 24 seconds RTD mode 4 seconds MSB 0000-1111 = 0 Counts Magnitude └ Mantissa |

B B B B

SK CHG LTR

TABLE 2. PARTICLES AND FIELDS SUBSATELLITE
MEASUREMENT LIST



| FORMAT LOCATION | MEASUREMENT TITLE | MEAS. NO. | CHAN CODE | SAMPLE INTERVAL | | | | MEASUREMENT DESCRIPTION | UNITS | MAX. VALUE | MIN. VALUE | ACCURACY | COMMENTS |
|---|---|---|---|---|---|---|---|---|---|---|---|---|---|
| | | | | RTD | MRO | TSN | TSF | | | | | | |
| W31-f0-b0 | C4 Detector Count | S09B | 24DS10 | 2 | N/A | 24 | 12 | C4 Detector Counts | Counts | $2^{19}-1$ | 0 | ± 3.1% | Accumulation Time:<br>TSN mode: 4 x sector period<br>TSF mode: 2 x sector period<br>RTD mode: 2 seconds<br>MSB 0000-1111 = 0 Counts<br>Mantissa<br>Magnitude |
| W32-f1-b0<br>-f2<br>-f5<br>-f6 | Open Telescope Channels 1-4 | S16B | 4DS1 | 25 | N/A | 4 | 2 | Open Telescope, Chan. 1-4 | Counts | $2^{19}-1$ | 0 | ± 3.1% | Accumulation time equals sample interval<br>MSB 0000-1111 = 0 Counts<br>Mantissa<br>Magnitude |
| W32-f3-b0<br>-f4<br>-f7<br>-f8 | Shielded Telescope Channels 1-4 | S17B | 4DS1 | 25 | N/A | 4 | 2 | Shielded Telescope, Chan. 1-4 | Counts | $2^{19}-1$ | 0 | ± 3.1% | Accumulation time equals sample interval<br>MSB 0000-1111 = 0 Counts<br>Mantissa<br>Magnitude |
| | | | | | | | | | | | | | |

| ORIGINATOR | DATE | TITLE |
|---|---|---|
| | | |
| | | |
| MJO | | |

ENGINEERING SKETCH
TRW SPACE TECHNOLOGY LABORATORIES

SK

SHEET 16 OF 16

STL Form 5238 (Rev. 12-83)

TABLE 3. SUBSATELLITE DOWNLINK ATA FORMAT (16 WORDS/SEC) (Page 1 of 2)

1 word = 8 bits, 1 frame = 32 words (2 secs), 1 data cycle = 8 frames (16 secs).

*Words 6 and 22 are 24A1 (S03R) in Real Time Mode ( ) = Stored Format Word No.

| W D. | 1 | 2 | 3 | 4 | 5(1) | 6(2) | 7(3) | 8(4) | 9(5) | 10(6) | 11(7) | 12(8) | 13(9) | 14(10) | 15(11) | 16(12 |
|---|---|---|---|---|---|---|---|---|---|---|---|---|---|---|---|---|
| 1 | 2DP1 D01B | 2DP2 D02B | 2DP3 Note 4 | 2DP4 Note 1 | 24DS1 S10B | 24A1* S01D | 24A2 S04B | 4DS1 S17B | 12DS1 S06B | 192DS1 D08B | 24DS2 S19B | 4DS1 S16B | 24DS3 S11B | 48DS1 S21B | 24DS4 S07B | 4DS1 S16B |
| | 2A1 C03B | 2A2 D12B | 2DP5 Note 2 | 2DP6 Note 5 | 24DS7 S12B | 24DS5* S02D | 24DS6 C08B | 4DS1 S16B | 12DS1 S06B | 192DS2 D09B | 24DS8 T01B | 4DS1 S16B | 24DS9 S13B | 48DS2 S25B | 24DS10 S09B | 4DS1 S16B |
| 2 | 2DP1 D01B | 2DP2 D02B | 2DP3 Note 4 | 2DP4 Note 1 | 24DS1 S10B | 24A1 S01D | 24A2 S04B | 4DS1 S16B | 12DS1 S06B | 192DS3 T03B | 24DS2 S19B | 4DS1 S16B | 24DS3 S11B | 48DS3 S23B | 24DS4 S07B | 4DS1 S16B |
| | 2A1 C03B | 2A2 D12B | 2DP5 Note 2 | 2DP6 Note 5 | 24DS7 S12B | 24DS5 S02D | 24DS6 S08B | 4DS1 S16B | 12DS1 S06B | 192DS4 T02B | 24DS8 T01B | 4DS1 S16B | 24DS9 S13B | 48DS4 S27B | 24DS10 S09B | 4DS1 S16B |
| 3 | 2DP1 D01B | 2DP2 D02B | 2DP3 Note 4 | 2DP4 Note 1 | 24DS1 S10B | 24A1 S01D | 24A2 S04B | 4DS1 S16B | 12DS1 S06B | 192DP1 Note 3 | 24DS2 S19B | 4DS1 S17B | 24DS3 S11B | 48DS1 S20B | 24DS4 S07B | 4DS1 S17B |
| | 2A1 C03B | 2A2 D12B | 2DP5 Note 2 | 2DP6 Note 5 | 24DS7 S12B | 24DS5 S02D | 24DS6 S08B | 4DS1 S17B | 12DS7 S06B | 192LS5 T04B | 24DS3 T01B | 4DS1 S17B | 24DS9 S13B | 48DS2 S24B | 24DS10 S09B | 4DS1 S17B |
| 4 | 2DP1 D01B | 2DP2 D02B | 2DP3 Note 4 | 2DP4 Note 1 | 24DS1 S10B | 24A1 S01D | 24A2 S04B | 4DS1 S17B | 12DS1 S06B | 192A1 S34B | 24DS2 S19B | 4DS1 S17B | 24DS3 S11B | 48DS3 S22B | 24DS4 S07B | 4DS1 S17B |
| | 2A1 C03B | 2A2 D12B | 2DP5 Note 2 | 2DP6 Note 5 | 24DS7 S12B | 24DS5 S02D | 24DS6 S08B | 4DS1 S17B | 12DS1 S06B | 192A2 E02B | 24DS3 T01B | 4DS1 S17B | 24DS9 S13B | 48DS4 S26B | 24DS10 S09B | 4DS1 S17B |
| 5 | 2DP1 D01B | 2DP2 D02B | 2DP3 Note 4 | 2DP4 Note 1 | 24DS1 S10B | 24A1 S01D | 24A2 S04B | 4DS1 S17B | 12DS1 S06B | 192A3 E03B | 24DS2 S19B | 4DS1 S16B | 24DS3 S11B | 48DS1 S21B | 24DS4 S07B | 4DS1 S16B |
| | 2A1 C03B | 2A2 D12B | 2DP5 Note 2 | 2DP6 Note 5 | 24DS7 S12B | 24DS5 S02D | 24DS6 S08B | 4DS1 S16B | 12DS1 S06B | 192A4 E04B | 24DS8 T01B | 4DS1 S16B | 24DS9 S13B | 48DS2 S25B | 24DS10 S09B | 4DS1 S16B |
| 6 | 2DP1 D01B | 2DP2 D02B | 2DP3 Note 4 | 2DP4 Note 1 | 24DS1 S10B | 24A1 S01D | 24A2 S04B | 4DS1 S16B | 12DS1 S06B | 192A5 S15B | 24DS2 S18B | 4DS1 S16B | 24DS3 S11B | 48DS3 S23B | 24DS4 S07B | 4DS1 S16B |
| | 2A1 C03B | 2A2 D12B | 2DP5 Note 2 | 2DP6 Note 5 | 24DS7 S12B | 24DS5 S02D | 24DS6 S08B | 4DS1 S16B | 12DS1 S06B | 192A6 E06B | 24DS8 T01B | 4DS1 S16B | 24DS9 S13B | 48DS4 S27B | 24DS10 S09B | 4DS1 S16B |
| 7 | 2DP1 D01B | 2DP2 D02B | 2DP3 Note 4 | 2DP4 Note 1 | 24DS1 S10B | 24A1 S01D | 24A2 S04B | 4DS1 S16B | 12DS1 S06B | 192A7 E05B | 24DS2 S18B | 4DS1 S17B | 24DS3 S11B | 48DS1 S20B | 24DS4 S07B | 4DS1 S17B |
| | 2A1 C03B | 2A2 D12B | 2DP5 Note 2 | 2DP6 Note 5 | 24DS7 S12B | 24DS5 S02D | 24DS6 S08B | 4DS1 S17B | 12DS1 S06B | 192A8 S14B | 24DS3 T01B | 4DS1 S17B | 24DS9 S13B | 48DS2 S24B | 24DS10 S09B | 4DS1 S17B |
| 8 | 2DP1 D01B | 2DP2 D02B | 2DP3 Note 4 | 2DP4 Note 1 | 24DS1 S10B | 24A1 S01D | 24A2 S04B | 4DS1 S17B | 12DS1 S06B | 192A9 S29B | 24DS2 S19B | 4DS1 S17B | 24DS3 S11B | 48DS3 S22B | 24DS4 S07B | 4DS1 S17B |
| | 2A1 C03B | 2A2 D12B | 2DP5 Note 2 | 2DP6 Note 5 | 24DS7 S12B | 24DS5 S02D | 24DS6 S08B | 4DS1 S17B | 12DS1 S06B | 192A10 S30B | 24DS8 T01B | 4DS1 S17B | 24DS9 S13B | 48DS4 S26B | 24DS10 S09B | 4DS1 S17B |